DOKUZ EYLÜL UNIVERSITY

GRADUATE SCHOOL OF NATURAL AND APPLIED SCIENCES

STRUCTURAL ANALYSIS OF REINFORCED CONCRETE BEAMS MADE OF ULTRA-HIGH PERFORMANCE CONCRETE

by

Ayodele AKIN-ADAMU

July, 2023

İZMİR

STRUCTURAL ANALYSIS OF REINFORCED CONCRETE BEAMS MADE OF ULTRA-HIGH PERFORMANCE CONCRETE

A Thesis Submitted to the
Graduate School of Natural and Applied Sciences of Dokuz Eylül University
In Partial Fulfillment of the Requirements for the Degree of Master of Science in Civil Engineering, Structural Program

by

Ayodele AKIN-ADAMU

July, 2023

İZMİR

M.Sc. THESIS EXAMINATION RESULT FORM

We have read the thesis entitled **"STRUCTURAL ANALYSIS OF REINFORCED CONCRETE BEAMS MADE OF ULTRA-HIGH PERFORMANCE CONCRETE"** completed by **AYODELE AKIN-ADAMU** under the supervision of **ASSOC. PROF. DR. ÇAĞLAR YALÇINKAYA** and **ASSOC. PROF. DR. ONUR MERTER,** we certify that in our opinion it is fully adequate, in scope and quality, as a thesis for the degree of Master of Science.

Assoc. Prof. Dr. Çağlar YALÇINKAYA	Assoc. Prof. Dr. Onur MERTER
Supervisor	Co-Supervisor
Prof. Dr. Halit YAZICI	Assoc. Prof. Dr. Taner UÇAR
Jury Member	Jury Member

Assist. Prof. Dr. M. Alper ÇANKAYA

Jury Member

Prof. Dr. Okan FISTIKOĞLU

Director

Graduate School of Natural and Applied Sciences

ACKNOWLEDGEMENT

First, I thank God for giving me the courage and knowledge that was needed to finish this M.Sc. thesis. Secondly, I would like to show my appreciation to my parents and younger sister for all the financial support and advice concerning my academic pursuits. Thirdly, I would like to thank the Türkiye Scholarship for providing me with the opportunity to study at Dokuz Eylul University. Fourth, I would like to express my gratitude to my two project supervisors, Assoc. Prof. Dr. Çağlar YALÇINKAYA and Assoc. Prof. Dr. Onur MERTER, for providing me with adequate guidance for the completion of my project thesis. Also, I would like to express my gratitude to ANSYS for providing students with a free copy of their Finite Element application. My thesis would not exist without the help of ANSYS. Again, I would like to appreciate some lecturers at Dokuz Eylul University who provided references for my doctoral program application abroad. Prof. Egemen Teomete, Prof. Çağlar Yalçınkaya, Prof. Binnur Goren Kiral and Prof Ali Gül are among them. Lastly, I would like to give thanks to the YouTuber, Dr. Brock Hedegaard at the University of Minnesota Duluth, for introducing me to the Menetrey Willams, Drucker Prager, and the Microplane concrete models for predicting the mechanical behavior of concrete in general.

Ayodele AKIN-ADAMU

STRUCTURAL ANALYSIS OF REINFORCED CONCRETE BEAMS MADE OF ULTRA-HIGH PERFORMANCE CONCRETE

ABSTRACT

The Microplane and Menetrey Willam concrete models are formulated on the research work of Bazant and Gambarova, and Menetrey Willams in the nineties respectively. These models are used in this thesis to predict how reinforced Ultra-High Performance Concrete (UHPC) beams will behave when subjected to flexural and shear dominant loadings. The numerical models are available in ANSYS, and they can simulate UHPC's extraordinary mechanical properties, such as high compression and tension strength, strain hardening, and softening behavior in compression and tension. In this research, four UHPC beams with dimensions of 180 wide by 270 deep by 4000 mm long with tensile reinforcements at the bottom were studied using the two cementitious composite models mentioned above with the ANSYS software. The beams were investigated under flexural four-point loading and shear three-point loading with the ANSYS program. A quarter-geometric section model of the full beam was considered for the four-point loading to take advantage of symmetry in the longitudinal and transverse directions of the beam. For the three-point loading, the full geometry model of the beam was considered only because of the lack of symmetry. The results from the ANSYS finite element software were validated with experimental data obtained in a previous article to show its capacity to predict the bending and shear behavior of reinforced UHPC beams. The comparisons of the results of both material models show that they can simulate the behavior of UHPC beams by using experimental load-deflection plots of the beam specimens and force-strain plots of the longitudinal tensile reinforcements in the sample beams.

Keywords: Ultra-high performance concrete, ANSYS, MENETREY WILLAMS Concrete Model, Microplane concrete model, DRUCKER PRAGER concrete model, UHPC Beams, finite element analysis.

ULTRA YÜKSEK PERFORMANSLI BETONDAN İMAL EDİLEN BETONARME KİRİŞLERİN YAPISAL ANALİZİ

ÖZ

Microplane ve Menetrey Willam beton modelleri sırasıyla Bazant ve Gambarova'nın ve Menetrey Willams'ın doksanlı yıllardaki araştırma çalışmaları üzerine formüle edilmiştir. ANSYS'de bulunan bu sayısal modeller, ultra yüksek performanslı betonun (UYPB) yüksek basınç ve çekme dayanımını, çekmede deformasyon sertleşmesi etkisini, donatılı UYPB kirişlerin basınç ve çekme altında yumuşama özellikleri gibi üstün mekanik özelliklerini açıklar. Bu çalışmada, 180 mm genişliğinde, 270 mm derinliğinde ve 4000 mm uzunluğundaki dört adet çekme donatılı UYPB kiriş, yukarıda belirtilen beton modelleri kullanılarak ANSYS yazılımı ile incelenmiştir. Kirişler ANSYS programı ile eğilmede dört noktalı yükleme ve kesmede üç noktalı yükleme altında incelenmiştir. Kirişin uzunlamasına ve enine doğrultularındaki simetriden yararlanmak üzere dört noktalı yükleme için tam kirişin çeyrek geometrik kesit modeli değerlendirilmiştir. Üç noktalı yükleme için, simetri olmaması nedeniyle kirişin tam geometrik modeli dikkate alınmıştır. ANSYS sonlu elemanlar yazılımından elde edilen sonuçlar, donatılandırılmış UYPB kirişlerin eğilme ve kesme davranışını tahmin etme kapasitesini göstermek için önceki bir makalede elde edilen deneysel verilerle doğrulanmıştır. Karşılaştırmalar, ANSYS yazılımında oluşturulan beton modellerin, ön yükleme aşamasından betonun ezilmesine veya çatlak lokalizasyon modlarına kadar tüm yükleme aralığında UYPB kirişlerinin tepkisini yakalayabildiğini göstermektedir.

Anahtar Kelimeler: Ultra yüksek performanslı beton, ANSYS, MENETREY WILLAMS beton modeli, mikrodüzlem beton modeli, DRUCKER PRAGER beton modeli, UYBP kirişler, sonlu elemanlar analizi.

CONTENTS

Page

M.SC. THESIS EXAMINATION RESULT FORM……..……ii
ACKNOWLEDGEMENT ii
ABSTRACT iv
ÖZ v
LIST OF FIGURES viii
LIST OF TABLES xiii

CHAPTER ONE – INTRODUCTION 1

1.1 Background of study 1
1.2 Aim and objective of research 4

CHAPTER TWO – LITERATURE REVIEW 5

2.1 UHPC characterization 5
2.1.1 Uni-axial compressive stress-strain curve of UHPC 5
2.1.2 Uni-axial tensile stress-strain curve of UHPC 6
2.2 3D-finite element analysis 7
2.2.1 Preprocessing phase 9
2.2.2 Solution phase 10
2.2.3 Implicit and Explicit Time Integration 11
2.2.4 Postprocessing phase 13
2.2.5 Verification and validation 13
2.3 Microplane model 14
2.3.1 Coupled damage plasticity microplane model parameters 15
2.3.2 Identification of CDP microplane model parameters……..... 17
2.4 Menetrey-Willam Model 18
2.4.1 Loading surface function……..……19
2.4.2 Formulation of hardening/softening behaviour ……...20

CHAPTER THREE – DESIGN METHODOLOGY **19**

3.1 Test Specimen 21
3.2 Test setup 22
3.3 Material Characterization 23
3.3.1 UHPC mix design 25
3.4 Material representation of UHPC in ANSYS 25
3.4.1 Coupled damage-plasticity microplane model 25
3.4.2 Menetrey Willam model 29
3.5 Material representation of reforcing steel in ANSYS 30
3.6 Geometry model of reinforced UHPC beams in ANSYS 32
3.6.1 Geometry model of U-B3 reinforced UHPC beam on ANSYS 32
3.6.2 Geometry model of U-B5 reinforced UHPC beam on ANSYS 34
3.6.3 Geometry model of U-B4 reinforced UHPC beam on ANSYS 36
3.6.4 Geometry model of U-B6 reinforced UHPC beam on ANSYS 36
3.7 ANSYS finite element procedures for the analysis problem 37

CHAPTER FOUR – RESULTS AND DISSCUSSION **39**

4.1 Presentation of beam U-B5 ANSYS results with experimental data 41
4.2 Presentation of beam U-B6 ANSYS results with experimental data 56
4.3 Presentation of beam U-B3 ANSYS results with experimental data 64
4.4 Presentation of beam U-B4 ANSYS results with experimental data 78

CHAPTER FIVE – SUMMARY AND CONCLUSIONS **86**

5.1 Conclusions 86

REFERENCES **88**

LIST OF FIGURES

Pages

Figure 2.1 Sketch of UHPC compression stress/strain diagram with strain softening post-yield behavior (Valente, Alves & Pacheco, 2020)..... 5
Figure 2.2 Sketch of UHPC tension stress/strain diagram with strain softening post yield behavior (Solhmirzaei & Kodur, 2021) 6
Figure 2.3 Another sketch of UHPC tension stress/strain diagram with strain softening post-yield behavior (Graybeal & Russell, 2013) 7
Figure 2.4 Basic 3D finite element types (Binnur, 2022) 8
Figure 2.5 A finite element solution plot 11
Figure 2.6 Stable and unstable solution illustration 13
Figure 2.7 Smooth 3-surface microplane cap yield function (ANSYS, 2022) 15
Figure 2.8 Linear softening in compression and tension (ANSYS, 2022) 20
Figure 2.9 Exponential softening in compression and tension (ANSYS, 2022) 20
Figure 3.1 Cross-sectional dimensions (in mm) and reinforcement details of the tested beams 21
Figure 3.2 Flexural Loading (Beams U-B3 & U-B5) 22
Figure 3.3 Shear loading (beams U-B4 & U-B6) 23
Figure 3.4 Uniaxial stress-strain response for UHPC (a) Compressive, (b) Tensile (Solhmirzaei & Kodur, 2017) 24
Figure 3.5 Stress-strain response of steel reinforcement (Solhmirzaei & Kodur, 2017) 24
Figure 3.6 Coupled damage-plasticity microplane parameters (Mechanical APDL Code)..... 26
Figure 3.7 Uniaxial cyclic compression and tension test cubes on ANSYS 27
Figure 3.8 Uniaxial cyclic tension test on ANSYS..... 27
Figure 3.9 Combined Microplane model calibration data and experimental data for UHPC in compression 28
Figure 3.10 Uniaxial cyclic tensile test on ANSYS..... 28
Figure 3.11 Combined Microplane model calibration data and experimental data for UHPC in tension 29
Figure 3.12 Tensile stress-strain curve model of reinforcing steel on ANSYS..... 31

Figure 3.13 Combined tensile stress-strain curves of reinforcing steel 31
Figure 3.14 3D quarter geometry model of U-B3 in mm 33
Figure 3.15 Quarter geometry model of U-B3 in mm 33
Figure 3.16 3D full geometry model of U-B3 in mm 33
Figure 3.17 Quarter geometry model of U-B3 in mm 34
Figure 3.18 3D quarter geometry model of U-B5 in mm 34
Figure 3.19 Quarter geometry model of U-B5 in mm 35
Figure 3.20 3D full geometry model of U-B5 in mm 35
Figure 3.21 Quarter geometry model of U-B5 in mm 35
Figure 3.22 3D full geometry model of U-B4 36
Figure 3.23 Full geometry model of U-B4 in mm 36
Figure 3.24 3D full geometry model of U-B6 in mm 37
Figure 3.25 Full geometry model of U-B6 in mm 37
Figure 4.1 Total applied load vs midspan deflection of U-B5, (a) Full geometric U-B5, (b) Combined plot of Microplane model and experimental data from Solhmirzaei & Kodur's study (2017)..... 42
Figure 4.2 Load strain response at mid-span of rebars of U-B5, combined experimental plot and ANSYS microplane model plot 43
Figure 4.3 U-B5 deflection color plot at failure load. (a) Full geometric microplane model plot, (b) Quarter geometric microplane model plot, (c) Quarter geometric Menetrey Willam model plot……...…45
Figure 4.4 Total applied load vs midspan deflection of U-B5. (a) Quarter geometry, (b) Quarter geometric ANSYS microplane, and Mentray Willam model plots combined with experimental test data..... 46
Figure 4.5 Total strain color plot for tensile reinforcements at failure load in mm/mm. (a) Full geometric ANSYS microplane, (b) Quarter geometric ANSYS microplane, (b) quarter geometric ANSYS Mentrey Willam..... 47
Figure 4.6 Equivalent von-Mises stress color plot for tensile reinforcements at failure load in MPa. (a) Full geometric ANSYS microplane, (b) Quarter geometric ANSYS microplane (b) Quarter geometric ANSYS Mentrey Willam 49

Figure 4.7 Coupled damage-plasticity microplane damage Output, (a) Experimental crack pattern, (Solhmirzaei & Kodur, 2017) (b) Total damage TOTA, (c) Tensile damage TENS 50
Figure 4.8 Coupled damage-plasticity microplane damage output, (a) Transformed compressive damage COMP, (b) Split weight factor (RW) 51
Figure 4.9 Equivalent von-Mises stress color plot for U-B5 at failure load in MPa. (a) Full geometric ANSYS microplane, (b) Quarter geometric ANSYS microplane (b) quarter geometric ANSYS Mentrey Willam. 53
Figure 4.10 Plastic strain color plot for U-B5 at failure load in MPa. (a) Full geometric ANSYS microplane, (b) Quarter geometric ANSYS microplane (b) Quarter geometric ANSYS Mentrey Willam. 54
Figure 4.11 Equivalent von-Mises stress color plot for U-B5 at failure load in MPa. (a) Full geometric ANSYS microplane, (b) Quarter geometric ANSYS microplane (b) Quarter geometric ANSYS Mentrey Willam. 55
Figure 4.12 Total applied load vs midspan deflection of U-B6, (a) Full geometry (b) Combined plot of experimental and full geometric ANSYS microplane model plot 57
Figure 4.13 Load strain response of rebars in U-B6, ANSYS microplane model plot 58
Figure 4.14 U-B6 deflection color plot at failure load, full geometric microplane model plot. 58
Figure 4.15 Total strain color plot for tensile reinforcements at failure load in mm/mm, full geometric ANSYS microplane 59
Figure 4.16 Equivalent von-Mises stress color plot for tensile reinforcements at failure load in MPa, full geometric ANSYS microplane (U-B6) 59
Figure 4.17 Coupled damage-plasticity microplane damage output – U-B6, (a) Experimental crack pattern, (Solhmirzaei & Kodur, 2017), (b) Transformed total damage TOTA, (c) Transformed tensile damage TENS 61
Figure 4.18 Coupled damage-plasticity microplane damage output, (a) Transformed compressive damage COMP, (b) Split weight factor RW. 62
Figure 4.19 Normal stress color plot for U-B6 at failure load in MPa, full geometric ANSYS microplane 62

Figure 4.20 Plastic strain color plot for U-B5 at failure load in MPa, full geometric ANSYS microplane 63
Figure 4.21 Equivalent von-Mises stress color plot for U-B6 at failure load in MPa, full geometric ANSYS microplane..... 63
Figure 4.22 Total applied load vs midspan deflection of U-B3, (a) U-B3 full geometry model, (b) Full geometic ANSYS microplane model plot. 65
Figure 4.23 Load strain response at mid-span of rebars of U-B3, combined experimental and ANSYS microplane model plot 66
Figure 4.24 U-B3 deflection color plot at failure load. (a) Full geometric microplane model plot, (b) Quarter geometric microplane model plot, (c) Quarter geometric Menetrey Willam model plot. 67
Figure 4.25 Total applied load vs midspan deflection of U-B3. (a) Quarter geometry on ANSYS (b) Quarter geometric ANSYS Microplane and Menetrey Willam model plot. 69
Figure 4.26 Total strain color plot for tensile reinforcements at failure load in mm/mm for U-B3. (a) Full geometric ANSYS microplane, (b) Quarter geometric ANSYS microplane, (b) Quarter geometric ANSYS Mentrey Willam.. 70
Figure 4.27 Equivalent von-Mises stress color plot for tensile reinforcements at failure load in MPa for U-B3. (a) Full geometric ANSYS microplane, (b) Quarter geometric ANSYS microplane (b) Quarter geometric ANSYS Mentrey Willam. 71
Figure 4.28 Coupled damage-plasticity microplane damage output for U-B3, (a) Transformed total damage TOTA, (b) Transformed tensile damage TENS 72
Figure 4.29 Coupled damage-plasticity microplane damage output for U-B3, (a) Transformed compressive damage COMP, (b) Split weight factor RW 73
Figure 4.30 Equivalent von-Mises stress color plot for U-B3 at failure load in MPa. (a) Full geometric ANSYS microplane, (b) Quarter geometric ANSYS microplane (b) Quarter geometric ANSYS Menetrey Willam 75
Figure 4.31 Plastic strain color plot for U-B3 at failure load in MPa. (a) Full geometric ANSYS microplane, (b) Quarter geometric ANSYS microplane (b) Quarter geometric ANSYS Mentrey Willam..... 76

Figure 4.32 Equivalent von-Mises stress color plot for U-B3 at failure load in MPa. (a) Full geometric ANSYS microplane, (b) Quarter geometric ANSYS microplane (b) Quarter geometric ANSYS Menetrey Willam 77
Figure 4.33 Total applied load vs midspan deflection of U-B4, (a) U-B4 full geometry model, (b) Combined experimental and full geometric ANSYS microplane model plots..... 79
Figure 4.34 Load strain response of rebars in U-B4, ANSYS microplane model plot. 80
Figure 4.35 U-B4 deflection color plot at failure load. full geometric microplane model plot. 80
Figure 4.36 Total strain color plot for tensile reinforcements at failure load in mm/mm, full geometric ANSYS microplane..... 81
Figure 4.37 Equivalent von-Mises stress color plot for tensile reinforcements at failure load in MPa, full geometric ANSYS microplane (U-B4)..... 81
Figure 4.38 Coupled damage-plasticity microplane damage output – U-B4, (a) Transformed total damage TOTA, (b) Transformed tensile damage TENS 82
Figure 4.39 Coupled damage-plasticity microplane damage output, (a) Transformed compression damage COMP, (b) Split weight factor RW..... 83
Figure 4.40 Normal stress color plot for U-B4 at failure load in MPa, full geometric ANSYS microplane 84
Figure 4.41 Plastic strain color plot for U-B4 at failure load in MPa, full geometric ANSYS microplane 84
Figure 4.42 Equivalent von-Mises stress color plot for U-B4 at failure load in MPa, full geometric ANSYS microplane..... 85

LIST OF TABLES

Pages

Table 2.1 Characteristics of implicit and explicit time integration..... 12
Table 2.2 Parameters of the coupled damage microplane model 16
Table 3.1 Density and Uni-axial compression and tension parameters of the flexural and shear test Solhmirzaei & Kodur (2017) 23
Table 3.2 Menetrey Willam UHPC parameters on ANSYS..... 30
Table 3.3 Reinforcement steel material model on ANSYS 31
Table 4.1 Tabular presentation of key thesis results. 40

CHAPTER ONE
INTRODUCTION

1.1 Background of the study

The appearance of digital computers and developments in structural analysis have changed dramatically during the last three to four decades. Argyris (1969) asserts that the strong relationship between structural theories and computers contributed significantly to the creation of large-scale finite element software packages that have a variety of uses in a variety of engineering sciences domains. Aside from the ANSYS software program, other finite element software programs that can be used in the numerical study of structural components include ABAQUS, ADINA, DIANA, NASTRAN, MARC, MSC-DYTRAN, SAP200, etc. However, ANSYS is the best program because of its huge library of free online courses and the fact that it is made freely available to students with little or no restrictions.

Ultrahigh-Performance Concrete (UHPC) has been researched as a structural material and has been in use in the construction industry for 3–4 decades now in many developed countries like the USA, China, Canada, France, Sweden, etc. Seldom has UHPC been used in developing and underdeveloped countries because of a lack of technical understanding of its mechanical properties and the huge cost of production. Generally, they are mostly used in the construction of bridge components such as decks, girders, piers, and bridge foundations. Due to the significant improvement in the material properties of normal (conventional) concrete in the last 4 decades through carefully designed material selection (using particle packing theory) and the use of fiber material as its constituent material, UHPC was invented.

Structures can be built with less material and weight because of UHPC's high compressive strength, which ranges from 200 to 250 MPa. The compression and tension behaviors of UHPC differ greatly from traditional concrete, so this will necessitate a change in the way structures would be defined with this material. El-Helou & Graybeal (2022) carried out intensive research work on the flexural behavior of UHPC by testing an 18.9 m span girder containing 26 pre-tension strands to failure.

El-Helou & Graybeal (2022) examined the flexural behavior of a girder by using a 4-point load test setup. A flexural design framework was formulated to predict the flexural behavior of beams based on observations from their study and prior research by other authors. A localized crack failure is usually formed in reinforced UHPC beams because of its superior compressive and post cracking tensile strength and the short bond length of its discrete fiber contents. During beam loading the steel fibers are stretched and they help to bridge crack formation before rupture of the tensile longitudinal reinforcement is seen (El-Helou & Graybeal, 2022). Straight steel fibers were used with a length and diameter dimension of 13 mm and 0.2 mm respectively. The minimum tensile strength of the fibers was 2,600 MPa.

Yoo, Banthia, & Yoon (2017) studied the bending of reinforced UHPC beams that failed by compression crushing rather than by the common crack localization failure. Their research work sought to develop a design approach that might fully utilize the high compressive strength of UHPC. (El-Helou & Graybeal, 2022) suggested that an oversimplified and dangerous results can be obtained when the tensile strength of UHPC is completely ignored. It may result in wrong prediction of failure modes of UHPC beams and inaccurate ductility estimation for the UHPC beams. The use of structural finite element software which considers constitutive models like the microplane model and Menetrey-Willam model can be used to overcome this shortcoming.

Since UHPC structural materials are very expensive, some researchers have considered partial replacement of the top section of traditional reinforced concrete beams with UHPC layers. They argued that this partial replacement at the compression zone of the beam can improve the flexural capacity and increase the ductility of this composite beam. Dahish & Bekri, 2022 investigated this idea by experimentation and by carrying out finite element analysis with ABAQUS. They found out that the optimum layer thickness for partial replacement at the top of the beam is about one-fifth of the total height of the composite beam for a tensile reinforcement ratio of up to 3%.

Ahmad et al. (2023) also investigated the possibility of strengthening normal reinforced concrete beams with different levels of pre-damage by providing UHPC layers in thickness of 30 mm at the tension region of these beams. The UHPC layers were placed at the bottom tensile face of the experimented normal reinforced beams, 2 side faces, and a combination of bottom and 2 side faces of the beams. Ahmad et al. (2023) investigated specimen beams by comparing the cracking load capacities of all the beams to a control beam that was not strengthened by using UHPC. It was found that beams with 3 sides strengthened show higher cracking load over other strengthening configurations for all degrees of pre-damage.

During the loading regime of beams made from UHPC, microcracks are always formed, which leads to the degradation of the elastic stiffness of this material. These microcracks eventually result in strain softening, which is seen in both the compression and tension properties of UHPC. (Bazant, & Gambarova, 1984) explained that the elastic stiffness degradation, the appearance of microcracks in any structural material during loading, violates the basic hypothesis of the theory of plasticity, usually expressed as Drucker's stability postulate. They also stated that these microcracks complicate analysis because the elastic stiffness becomes anisotropic. The cracks introduces nonlinearity in the mechanical performance of the structural material.

The microplane model is a model that can describe material behavior through stress-strain laws on several individual planes. It can capture the oriented nature of damage such as tensile cracking, friction, slip, compression splitting, and orientation of fiber reinforcements. The microplane model that is available in the ANSYS program is based on the research of (Bazant & Byung, 1985) and (Bazant & Gambarova, 1984). The microplane model is best suited for engineering materials consisting of various aggregate compositions with differing properties. For instance, concrete has fine and coarse rock aggregates that are embedded in a weak matrix of cement can be given as an example of this engineering materials. The microplane model has been extensively used to simulate concrete materials using finite element techniques, however, it has not been utilized extensively to simulate UHPC materials.

The Menetrey-Willam model is another material model that can be used for simulating the behavior of bonded aggregates such as concrete. The Menetrey-Willam constitutive model is based on the Willam-Warnke yield surface Menetrey (1994) and Willam (1975). This model is used for the description of concrete failure under triaxial conditions. It describes the overload and ultimate load analysis of three-dimensional concrete structures. This thesis is focused on creating a step-by-step procedure for capturing flexural and shear behavior (responses) of UHPC beams at first cracking, yielding of reinforcement, the response at the development of a localized crack, and compression failure using the ANSYS finite element program. This flexural step-by-step procedure is founded on the use of a concrete plasticity-damage microplane model and the Menetrey-Willam models that can capture the elastic, plastic, and damage behavior of concrete and is proposed for beams made with UHPC and reinforced with conventional steel reinforcing bars. The ANSYS program is used to define the geometry beam models (3D solid model) and material model characterization for UHPC and reinforcing steel and it is also used to carry out finite element analysis based on the concept of 3D stress and strain of a solid body. The experimental results of the load-deflection curve, compression stress-strain curve, and tension stress-strain curve are validated and visualized in the ANSYS program. Color plots that illustrate damage in the test beams are also plotted from the ANSYS program.

1.2 Aim and objective of this research

The aims and objectives of this research work include the following:

1. Prediction of the flexural and shear capacity of 4m span reinforced UHPC beams with ANSYS finite element program.
2. Validation of the microplane model and Menetrey-Willams model by comparing ANSYS finite element results with experimental (load-deflection curve) and (tensile and compressive stress-strain curve) for UHPC beams.
3. Visualization of the damage after loading UHPC beams to failure.

CHAPTER TWO
LITERATURE REVIEW

The theoretical background of UHPC characterization, 3D-Finite Element Analysis, Microplane Concrete Model, and Menetray-Willam Concrete Model are discussed in this section.

2.1 UHPC characterization

UHPC's mechanical and durability properties are many times better than conventional concrete because of the use of fibers and its high particle packing density. The fibers can either be made of steel or Poly vinyl alcohol (PVA) materials. The mechanical properties of UHPC are discussed below.

2.1.1 Uni-axial compressive stress-strain curve for UHPC

The compression mechanical properties of UHPC are explained in Figure 2.1. It shows the elastic, hardening, and softening properties of UHPC in compression depending on the fiber content provided.

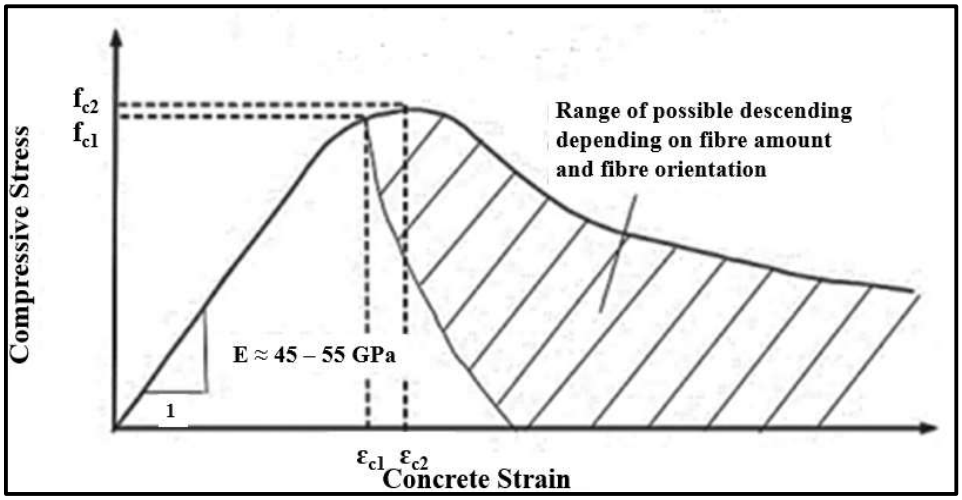


Figure 2.1 Sketch of UHPC compression stress-strain diagram with strain softening post-yield behavior (Valente, Alves & Pacheco, 2020)

The compression stress-strain curve shown in Figure 2.1 is used to describe the behavior of UHPC with or without fiber reinforcements (Valente, Alves & Pacheco, 2020). UHPC shows a linear elastic behavior until about 75 to 80 % of the ultimate compressive strength. There is a small portion of strain hardening just after the elastic region of the curve. At this path, there is a continued increase in strain with increasing stress value. However, this occurs at a reduced slope (elastic stiffness). The region beyond the ultimate yield limit, (ε_{c2}, f_{c2}) is termed the strain-softening region. At the strain-softening region, the UHPC material becomes permanently deformed and does not recover from strain. For non-fiber UHPC with coarse aggregate (rock), the strain length between yield point and failure is shorter as shown in Figure 2.1 compared to fiber UHPC made only with fine aggregate (sand), thus showing the non-fiber UHPC with coarse aggregate is more brittle. This complex mechanical behaviour leads to nonlinearity in the material.

2.1.2 Uni-axial tensile stress-strain curve of UHPC

Figure 2.2 explained the tension behavior of UHPC made with and without fiber reinforcement. As shown in Figure 2.2, the tension behavior of UHPC without fibers is described by the blue curve alone (Solhmirzaei & Kodur, 2021).

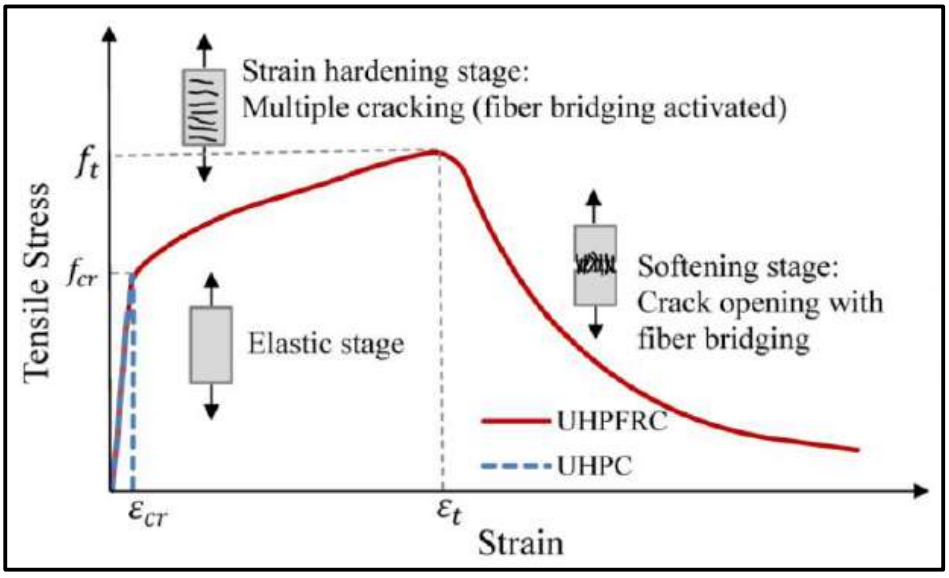


Figure 2.2 Sketch of general UHPC tension stress-strain diagram with strain softening post-yield behavior (Solhmirzaei & Kodur, 2021)

It shows that UHPC without fibers is very brittle and does not exhibit strain hardening and strain softening behavior after cracking compared with fiber reinforced UHPC that showed strain hardening (multiple cracking) and strain softening (crack opening) behaviors. Figure 2.2 idealizes the tension behavior of fiber-reinforced concrete into I, II, and III respectively for the elastic, strain-hardening, and softening stages. (Solhmirzaei & Kodur, 2021). This tension behavior depicted above leads to material nonlinearity.

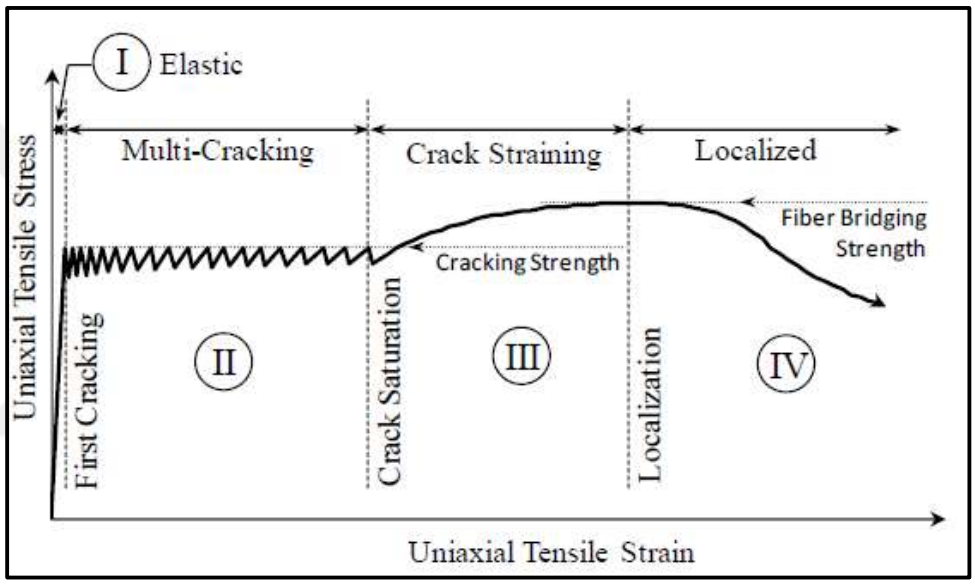


Figure 2.3 Another sketch of UHPC tension stress-strain diagram with strain softening post-yield behavior (Graybeal & Russell, 2013)

(Graybeal & Russell, 2013) idealized the tension behavior of fiber UHPC into 4 stages: elastic, multi-cracking, crack straining, and localized stages. The difference between this tension model in Figure 2.3 and Figure 2.2 is that the softening branch of Figure 2.2 is divided into 2 stages in Figure 2.3 as crack straining and localized stages. Stage 3 (Crack straining) of Figure 2.3 denotes the widening of microcracks, and stage 4 (Localized stage) represents the fiber pull-out phase from the UHPC matrix.

2.2 3D-finite element analysis

Solid bodies can be modeled by using 3D finite elements. The type and quantity of finite element required depend on the complexity of the shape of the solid body. The

different color of the mechanical component in Figure 2.4 shows that different finite element types and quantities are used to model its parts.

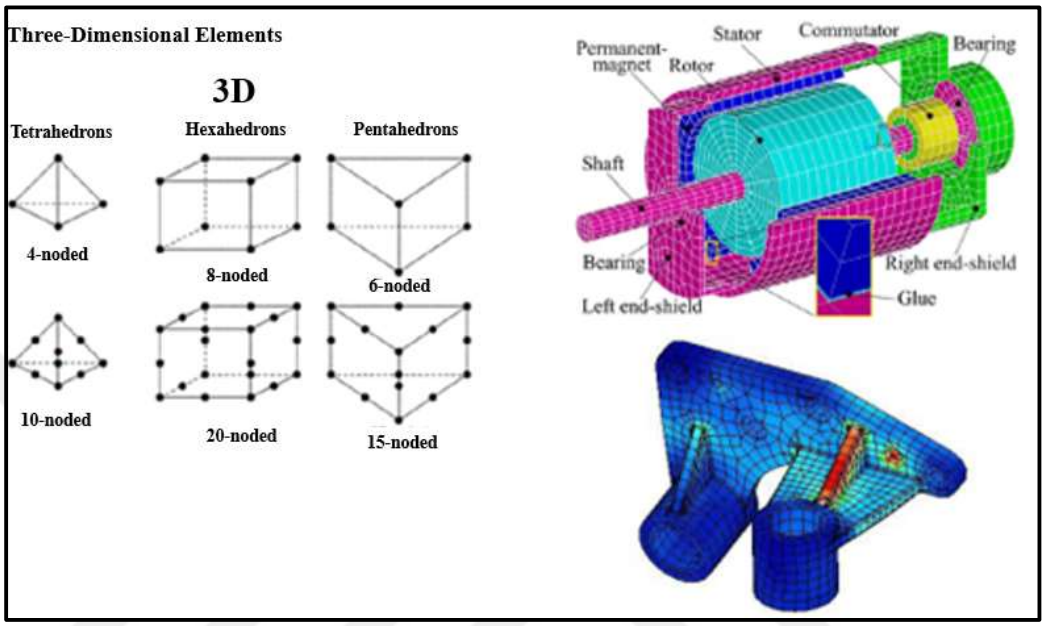


Figure 2.4 Basic 3D finite element types (Binnur, 2022)

Solid mechanics problems can be analyzed by using a finite element procedure. In this procedure, a complex region defining a continuum like the machine parts shown in Figure 2.4 is discretized into simple geometric shapes called finite elements. These finite elements can be defined as either 1D, 2D, or 3D finite elements. Also, beam analysis problems can be modeled either using 1D, 2D, or 3D elements. The choice of finite elements depends on the complexity of the problem. The linear elastic isotropic constitutive material law is generally applied to either the 1D, 2D, or 3D finite element problems, However, large deformation and material nonlinearity invalidates the use of this constitutive material law.

Solving more complex finite element analysis problems that do not obey Hooke's elastic law, other constitutive material models are adopted to predict the behavior of these structural components. For example, the adoption of just the elastic isotropic law for concrete or UHPC material cannot predict its behavior because these materials are composite materials, and microcracks are developed in the materials during loading effects. These factors can either lead to strain hardening or strain softening behavior

in the stress-strain relationship, which deviates from the theory of Hooke's law. Binnur (2022) classified the finite element method of analysis into 3 phases: the preprocessing phase, solution phase, and postprocessing phase.

2.2.1 Preprocessing phase

The preprocessing phase includes the following basic steps:

1. Creation and discretization of the solution domain into finite elements; subdivision of the structural problem into nodes and elements.
2. Assumption of a shape function to represent an element's physical behavior, i.e., a continuous function is assumed to represent an element's approximate behavior (solution).
3. Development of equations for each element.
4. Assembling of the equations of each element to present the entire problem and construction of the global stiffness matrix.
5. Application of boundary conditions, initial conditions, and loading (Binnur, 2022).

Step 1 involves discretizing the structural solution domain into 1D, 2D, or 3D finite elements. The 1D finite elements are line elements that can be used to depict the behavior of bars in tension, compression, torsion, truss structural problems, beam problems, and frame problems. 1D finite elements with 2 nodes (start and end) are linear elements, while 1D finite elements with 3 nodes are term quadratic elements. For a static structural problem, each node can be defined with a minimum of 1 degree of freedom and a maximum of 3 degrees of freedom.

The 2D finite elements are plane elements that can be used to describe the behavior of shells and plates. This element can also be used to solve structural beam problems. Examples of these 2D finite elements include the Constant Strain Triangles (CST), 4-node quadrilaterals (linear element), 8-node quadrilaterals (quadratic element), and 6-node triangles (quadratic element). Each node is usually defined with 2 degrees of freedom.

The 3D finite elements are shown in Figure 2.4. They include tetrahedral elements (tetrahedrons), block/brick elements (hexahedrons), and pentahedral elements. As shown in Figure 2.4, the tetrahedral elements may be defined with 4 or 10 nodes: block/brick elements with 8 and 20 nodes, and the pentahedral with 6 and 15 nodes for linear and quadratic elements, respectively.

Step 2 is the phase where the constitutive models/laws are incorporated into the finite element analysis. For an elastic/isotopic material, the constitutive model is Hooke's law.

$$\sigma = K \times \varepsilon \tag{2.1}$$

Step 3 involves the formulation of an equation for the calculation of the local stiffness matrix of each finite element.

Step 4 involves the systematic assembly of the local stiffness matrix of each element into a single matrix called the global stiffness matrix.

Step 5 in solid mechanics involves specifying the structural support, settlement, initial crack, and loading effects on the structure for the finite element mathematical model.

2.2.2 Solution phase

In this phase, a set of linear or nonlinear algebraic equations are solved simultaneously to obtain displacement nodal results (Binnur, 2022). For a 3D structural problem, these results are displacements u, v, and w along the 3 degrees of freedom at each node of the finite elements. Based on stability and accuracy considerations the implicit time integration method is used in this study for analysis. The implicit time integration is very stable and assures stability of the numerical solution. The UHPC beams that will be analyzed are quasi-static in nature, so the implicit time integration method is used.

2.2.3 Implicit and Explicit Time Integration

The time integration algorithms used by finite element programs are very important consideration in the solution of finite element problems because using a wrong time-step integration method may lead to wrong results or require unrealistic computation costs. Engineers and scientists should be capable of choosing the right time integration methods for solving the ordinary differential equations for finite element solutions. The considerations for selecting the appropriate time integration method may be based on their accuracy, stability, and computational characteristics for the specific problem. There are 2 types of time integration in finite element analysis. We have the Implicit and explicit time integration method.

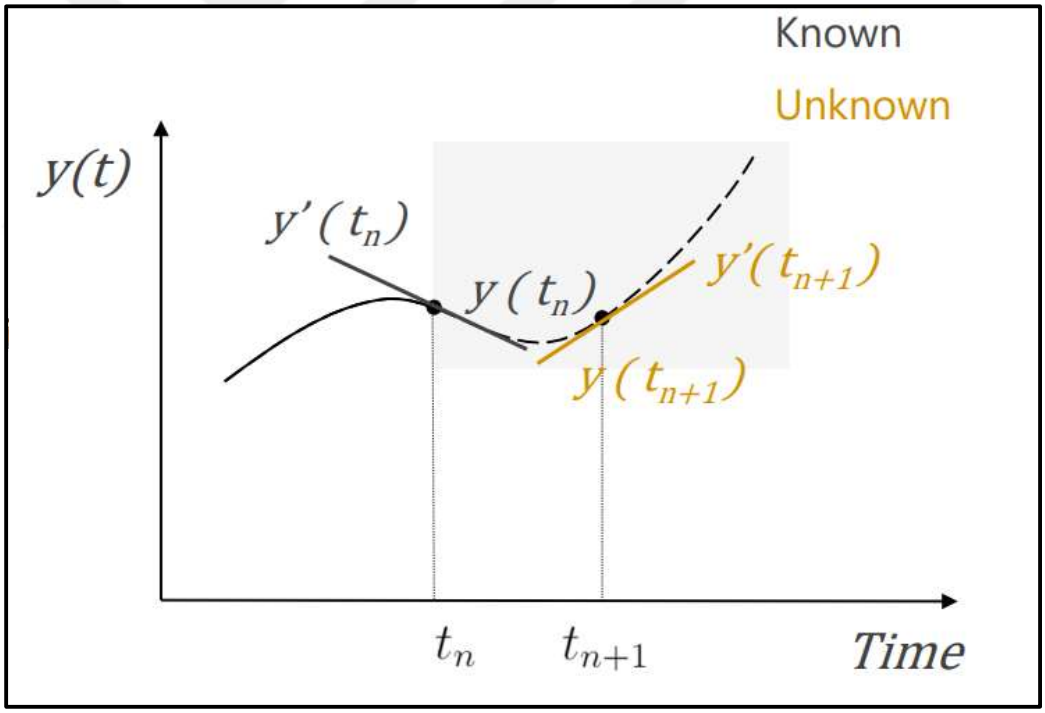


Figure 2.5 A finite element solution plot

Figure 2.5 below shows a 1D finite element solution y(t) plotted with respect to time on the x-axis. Two time points are shown on this curve at t_n and t_{n+1}. The slope at each point is given as $y'(t_n)$ and $y'(t_{n+1})$ respectively. Assuming $y(t_n)$ and $y'(t_n)$ are known quantities and $y(t_{n+1})$ and $y'(t_{n+1})$ are unknown as illustrated in Figure 2.5.

Implicit time integration technique uses the slope at the unknown step $y'(t_{n+1})$ to find the next solution. The next solution is shown by equation (2.2) for the implicit time integration.

$$y(t_{n+1}) = y(t_n) + \Delta t \times y'(t_{n+1}) \tag{2.2}$$

In equation (2.2), because $y'(t_{n+1})$ is unknown, $y(t_{n+1})$ cannot be computed directly. Thus, this method is called implicit time integration.

Explicit time integration uses the slope at the known step $y'(t_n)$ to compute the next solution. The explicit time integration equation is shown by equation (2.3). This solution can be computed easily because the slope $y'(t_n)$ is known. Thus, this method is called explicit time integration.

$$y(t_{n+1}) = y(t_n) + \Delta t \times y'(t_n) \tag{2.3}$$

From the explanation above, it can be said that the implicit method requires extra computation effort to solve the equation for each time step. This can be hard to solve for practical problems. The explicit method seems to have no such issue. However, the explicit method can exhibit stability issues if the time-step is not wisely chosen. So, a smaller time step is usually required for the explicit method. In contrast, the implicit method is proven to be stable for a linear system. Because of the limitation of time-step size, explicit methods are not used in finite element dynamic problems of long duration. The characteristics of the 2 methods are summarized in Table 2.1 below.

Table 2.1 Characteristics of implicit and explicit time integration

	Explicit	**Implicit**
Stability	Depends on time-step size	Unconditionally stable
Time-step size	Very small	Large
Solving speed for one step	Fast	Slow

Stable and unstable solutions are depicted in Figure (2.6) for a cantilever beam problem impacted by a load at its end. The amplitude of the oscillation grows in time without bound, leading to an explosive numerical instability.

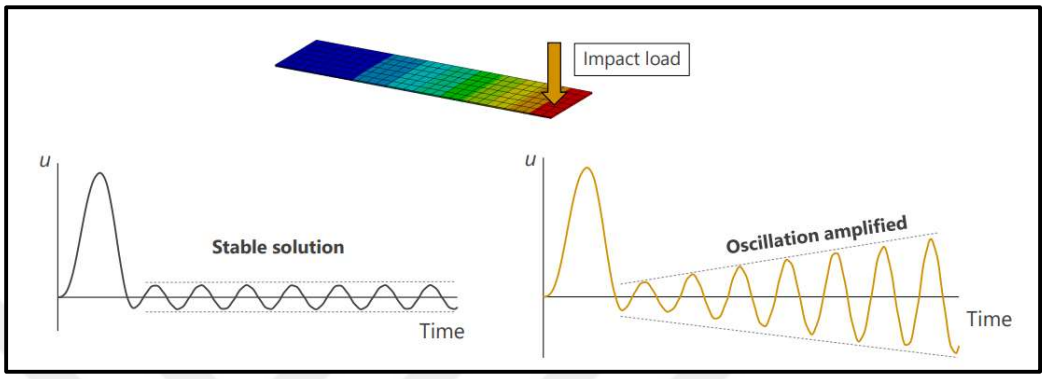


Figure 2.6 Sable and unstable solution illustration

2.2.4 Postprocessing phase

Other important information (results) for the structural problem is obtained based on the results of the displacement values at each node (Binnur, 2022). It may include strain, stress, reaction, bending moment, shear force, axial force results, etc.

2.2.5 Verification and validation

Since finite element analysis is not an exact analysis, i.e., the results most of the time are usually an approximation of the exact solution. There is a need to always check the validity of finite element results and perform mesh sensitivity analysis.

Rajesh (2021) verifications for validity include the following:

1. Check that the solution agrees with the mathematical model.
    - Are the boundary conditions on displacement and traction satisfied?
    - Is equilibrium satisfied? Do reactions balance the applied load?
2. Check that the numerical error is acceptable.
    - Are the finite element results reasonably independent of mesh?

3. Check the comparison with hand calculations for maximum displacement (Rajesh, 2021)

Rajesh (2021) used experimental data from the lab and digital image correlation technology for the validation of this structural analysis problem with the ANSYS program.

2.3 Microplane Model

The Microplane model is a nonlinear finite element material model that can be used to simulate structural materials made from aggregate materials such as sand, granite, and cement for concrete and UHPC. This model provides a mathematical description of structural response in any stress conditions such as compression, tension, torsion etc. This model helps to describe the material nonlinearity of cementitious structural materials.

Zreid and Kaliske (2018) provided an enhancement to the microplane model by considering damage and plasticity of any cementitious structural composites under loading conditions. This enchancement is called the Coupled damage-plasticity microplane model.

The coupled damage-plasticity microplane model is defined by a plot curve of the volumetric stress on the x-axis and the deviatoric stress state on the y-axis. The plot is called the smooth surface Drucker Prager cap yield function. The volumetric stress state is the stress state that causes changes in the volume of the body, while the deviatoric stress state is the stress state that leads to the change in the shape of a loaded structural body. This plot is shown in Figure 2.5 below.

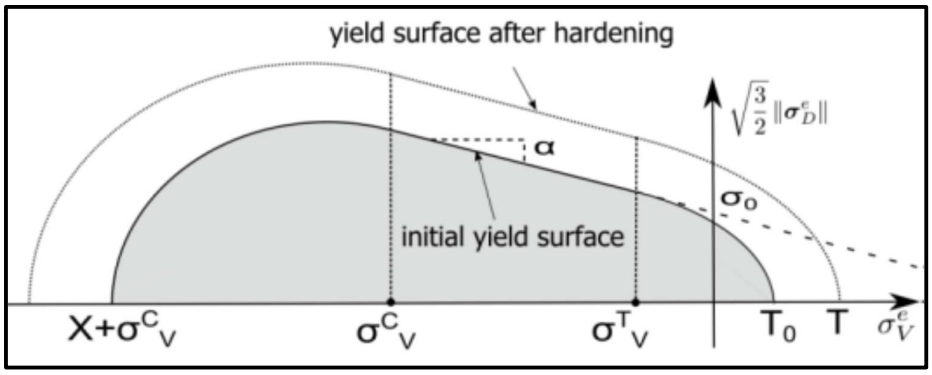


Figure 2.7 Smooth surface drucker-prager cap yield function (ANSYS, 2022)

In Figure 2.5, the initial yield of the loaded body is defined by 3 sections. The compression cap on the left of the plot, the tension cap at the right of the curve and a straight line connecting the 2 caps together (the drucker-prager yield line function). After the loaded body has yielded the initial yield surface in the plot expands outward to a new yield surface to define hardening and damage in the structural material.

2.3.1 Coupled damage platicity (CDP) microplane model parameters

There are 15 coupled damage plasticity microplane model parameters on ANSYS (2022) shown in Table 2.2.

Table 2.2 Parameters of the coupled damage microplane model

Parameter Type	Parameter Subtype	Parameter	Description
Elasticity	--	E	Modulus of elasticity
	--	v	Poisson's ratio
Plasticity	Drucker-Prager yield function	f_{uc}	Uni-axial compression strength
		f_{bc}	Bi-axial compression strength
		f_{ut}	Uni-axial tension strength
	Compressive cap	$\sigma_v{}^c$	Compressive cap and Drucker Prager yield function x coordinate intersection point.
		R	Evaluation ratio for the cap's major and minor axes
	Hardening	D	Material constant for hardening
		R_T	Hardening constant for tension cap
Damage	--	γ_{t0}, γ_{c0}	Damage thresholds for tension and compression
	--	β_t, β_c	Damage evolution constants for tension and compression
Non-local	--	c	Parameter for Non-local interaction range
	--	m	Parameter for over non-local averaging

The parameters for plasticity f_{uc}, f_{bc}, and f_{ut} are used as inputs that can be found experimentally for concrete. The biaxial and uniaxial stress is used to determine the friction coefficient α and initial yield stress σ_0 as shown in 2.4 and 2.5 (ANSYS, 2022):

$$\alpha = \frac{\sqrt{3}(f_{bc} - f_{uc})}{2f_{bc} - f_{uc}} \tag{2.4}$$

$$\sigma_0 = \left(\frac{1}{\sqrt{3}} - \frac{\alpha}{3}\right) f_{uc} \tag{2.5}$$

The x-coordinate intersection points of the tension cap and the Drucker-Prager yield function $\sigma_v{}^T$ is determined by the uniaxial variable, and the initial x-coordinate intersection point of the cap T_0 is evaluated below:

$$\sigma_v{}^T = -\frac{f_{uc}}{3} \tag{2.6}$$

$$T_0 = \frac{f_{ut}}{3} \tag{2.7}$$

2.3.2 Identification of CDP microplane model parameters

The CDP parameters can be identified by using engineering judgement and empirical formulas.

1. The parameters of elasticity, E and v can be determined by using stress-strain material curve, or by empirical formulas in the literature.

2. The strength parameters for plasticity, f_{uc}, f_{bc}, and f_{ut} is estimated by using empirical formulas or from experimental investigations (Jiang & Zhao, 2015):

$$f_{bc} = 1.15 f_{uc} \tag{2.8}$$

$$f_{ut} = 1.4 \left(\frac{f_{uc}}{10}\right)^{\frac{2}{3}} \tag{2.9}$$

The compressive cap parameters are identified from tri-axial experimental results. The $X_0 + \sigma_v{}^c$ is evaluated by the application of volumetric load until the yielding starts (ANSYS, 2022). $\sigma_v{}^c$ can also be estimated empirically as:

$$\sigma_v{}^c = -\frac{2}{3} f_{bc} \tag{2.10}$$

The parameter R is the ratio between the major axis and minor axis of the caps, and it is calculated as (ANSYS, 2022):

$$R = \frac{X_0}{f_1(\sigma_v^c)} \tag{2.11}$$

3. **Damage and Hardening:** Cyclic tests are needed to determine the damage and hardening parameters. These damage and hardening parameters are very similar because their interaction controls the unloading slope and softening. Uniaxial cyclic compression test is required to determine the parameters D, β_c, and γ_{c0}. Similarly, uniaxial cyclic tension test determines the parameters R_T, β_t, and γ_{t0}. Without uniaxial cyclic tension tests, $R_T = 1$ and $\beta_t = 1.5\beta_c$ can be assumed as starting values. The tension damage threshold γ_{t0} is often equated to zero because softening in tension starts almost immediately after the elastic limit (ANSYS, 2022).

4. **Nonlocal Parameters:** The over-nonlocal averaging parameter m is a numerical parameter, where $m > 1$ regularizes the solution. Typically, $m = 2.5$ (ANSYS, 2022).

2.4 Menetrey-Willam Model

The Menetrey-Willam constitutive model is derived on the Willam-Warnke yield surface and uses the concept of flow plasticity theory. This model is implemented in many finite element programs including in ANSYS program. The Menetrey-Willam model can describe mechanical properties of cement composites such as the compression strength, tensile strength, nonlinear strain hardening, strain softening and dilatation properties. The dilatancy of cementitious composite is usually described either as an angle or a coefficient. It describes the nonlinear volume increase due to the shear effect of the microstructure of a structural material. Many literatures investigated the dilatancy parameters with a test called the shear box test.

There are 3 main components of the Menetrey Willam model. These include:

- A loading surface function
- A formulation of hardening and softening behavior
- A function for plastic potential.

2.4.1 Loading surface function

The loading surface function is described by the mathematical expression shown in equation (2.12). This function is described by 3 main parameters shown in equation (2.13), equation (2.14) and equation (2.15). They are called the hydrostatic stress invariant ξ, deviatoric stress invariant ρ, and deviatoric polar angle θ, respectively. I1, J2 and J3 are also defined in equation (2.16), equation (2.17) and equation (2.18) and they are the three invariants of stress tensor that are also used to define the loading surface component.

$$F(\xi, \rho, \theta) = \frac{C_2}{C_3}\left[\sqrt{2}\,\xi + r\rho\right] + \rho^2 - \frac{1}{c_3} \tag{2.12}$$

$$\xi = \frac{1}{\sqrt{3}} I_1 \tag{2.13}$$

$$\rho = \sqrt{2J_2} \tag{2.14}$$

$$\cos 3\theta = \frac{3\sqrt{3}}{2}\frac{J_3}{\sqrt{J_2^3}} \tag{2.15}$$

$$I_1 = \sigma_1 + \sigma_2 + \sigma_3 \tag{2.16}$$

$$J_2 = \frac{1}{6}\left((\sigma_1 - \sigma_2)^2 + (\sigma_2 - \sigma_3)^2 + (\sigma_3 - \sigma_1)^2\right) \tag{2.17}$$

$$J_3 = \left(\sigma_1 - \frac{I_1}{3}\right)\left(\sigma_2 - \frac{I_1}{3}\right)\left(\sigma_3 - \frac{I_1}{3}\right) \tag{2.18}$$

2.4.2 Formulation of hardening/softening behavior

Cracking and crushing effects in cementitious structural materials are described with a strain-softening model shown in Figure 2.6 or Figure 2.7. Figure 2.6 describes softening of material in compression and tension by using a linear model, while Figure 2.7 describes softening behavior by using an exponential model.

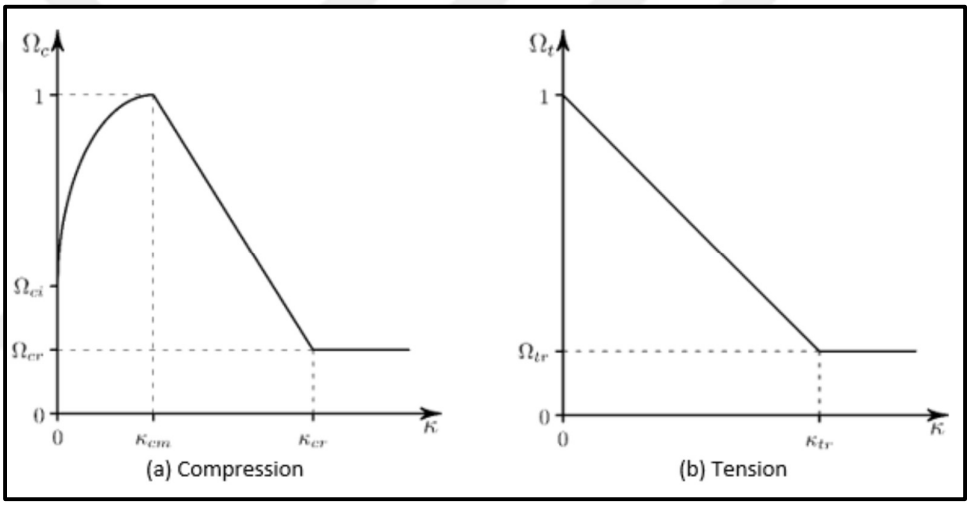


Figure 2.8 Linear softening in compression and tension (ANSYS, 2022).

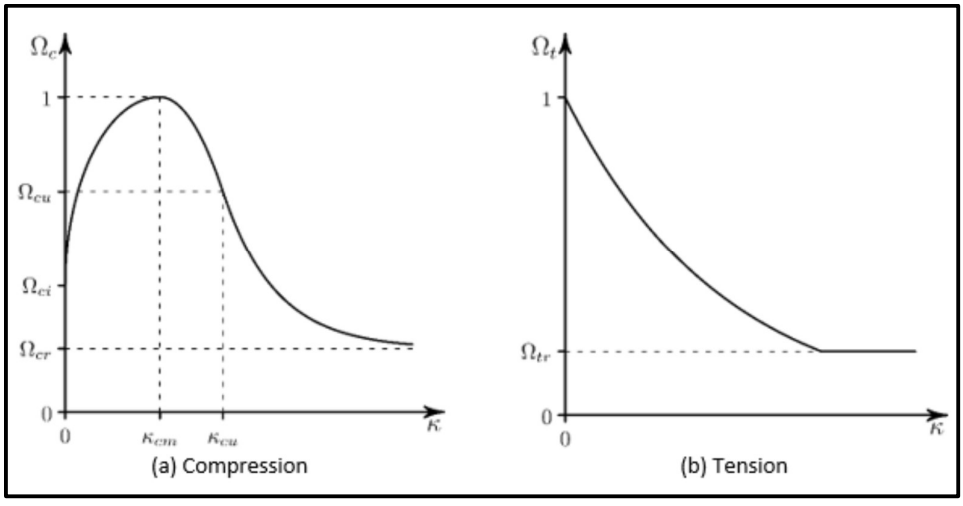


Figure 2.9 Exponential softening in compression and tension (ANSYS, 2022)

CHAPTER THREE
DESIGN METHODOLOGY

In this section, numerical models are built using ANSYS for tracking the structural behavior of reinforced UHPC beams under shear and flexural loads. The structural analysis was performed using a displacement control technique that increased the beam's load incrementally until failure occurred. The loading of the analyzed is displacement applied or controlled. The numerical techniques are described in depth below, including geometric models, discretization details, and material models.

3.1 Test Specimen

To conduct the numerical analysis described in this research, 4 reinforced rectangular section beams made with UHPC were tested under displacement-controlled loading in flexure and shear to failure. The cross-sectional dimensions and reinforcement details of the tested beams are shown in Figure 3.1

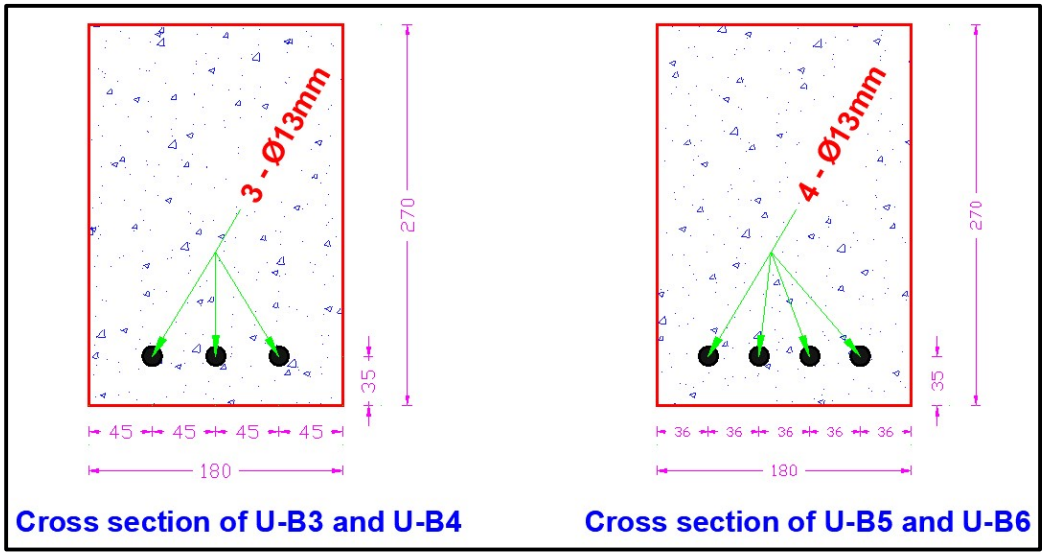


Figure 3.1 Cross-sectional dimensions (in mm) and reinforcement details of the tested beams

Beam sections U-B3 and U-B4, have 3 number of 13 mm diameter straight steel bars at the bottom layer, while UB5 and U-B6 contain 4 number of 13 mm diameter straight steel bars. The 13 mm diameter reinforcement is grade 700 MPa with a cross-

section area of 132.73 mm^2 and maximum ultimate strength of 700 MPa. The gross cross-sectional properties of the beams are an area of 4.86 x 10^4 mm^2 and a moment of inertia about the centroid (about the x-axis) of 2.95 x 10^8 mm^4. Also, a total displacement load of 105 mm is applied on the loading plates of U-B3 and U-B5. While a displacement load of 72 mm is applied on U-B4 and U-B6. The problems are solved by using an implicit time integration method and the displacement loads are specified with a minimum and maximum load step of 200 and 10,000 respectively.

3.2 Test setup

Beams U-B3 and U-B5 were tested under 2-point loads applied on the top face of the beams at 432 mm on either side of the mid-span as shown in Figure 3.2. The effective shear depth ratio of U-B3 and U-B5 is 5.95. This test setup is designed to simulate pure bending between points of load application. Beams U-B4 and U-B6 were subjected to a single point load applied on the top face of the beams at the distance of 610 mm from support (shear span) to examine the shear capacity as compared to the bending moment of the beams (see Figure 3.3) (Solhmirzaei & Kodur, 2017). The effective shear depth ratio of U-B4 and U-B6 is 2.6.

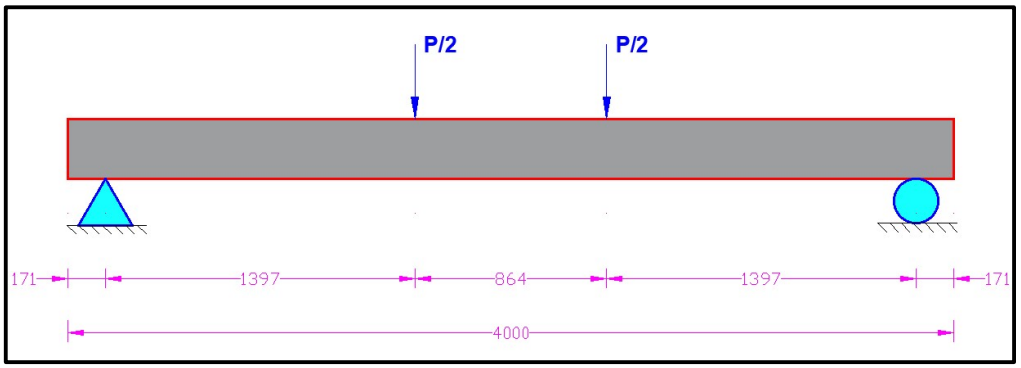


Figure 3.2 Flexural Loading (Beams U-B3 & U-B5)

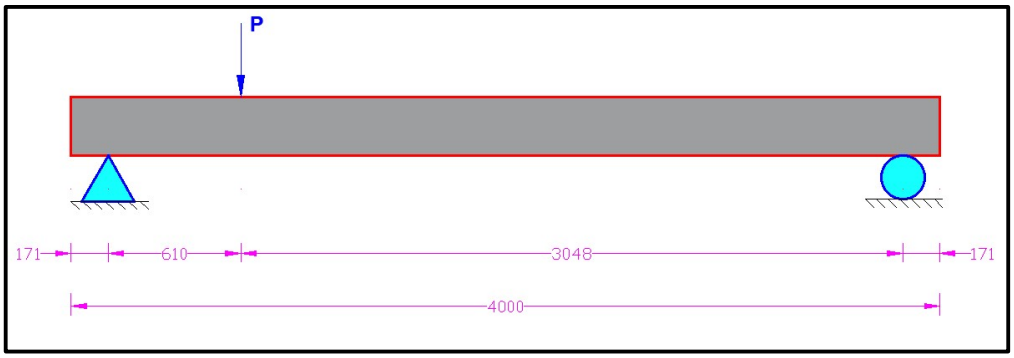


Figure 3.3 Shear loading (beams U-B4 & U-B6)

3.3 Material Characterization

The main objective of this study is to predict the flexural and shear response of the tested experimental beams utilizing the material model types on ANSYS software. The mechanical properties were obtained from tests on compression and tension specimens. These tests were used to assess the mechanical properties of UHPC such as density, poison ratio, compression parameters, tension properties, and biaxial compression parameters at the time of the test. The average results of the sample tests are shown in Table 3.1.

Table 3.1 Density and Uni-axial compression and tension parameters of the flexural and shear test Solhmirzaei & Kodur (2017)

Material	**Density** $\bar{w}_c[kg/m^3]$	**Poison ratio**	**Compression parameters**				**Tension parameters**			**Biaxial compression parameter**
			$E_c[MPa]$	$\bar{f}'_c[MPa]$	ε_p	ε_{uc}	f_t	ε_{cr}	ε_{ut}	$\bar{f}'_b[MPa]$
UHPC	2565	0.2	43970	193	0.0044	0.008	7.11	0.00016	0.0181	223.88

The experimental uniaxial stress-strain curves (compressive and tensile) for the UHPC are shown in Figure 3.4.

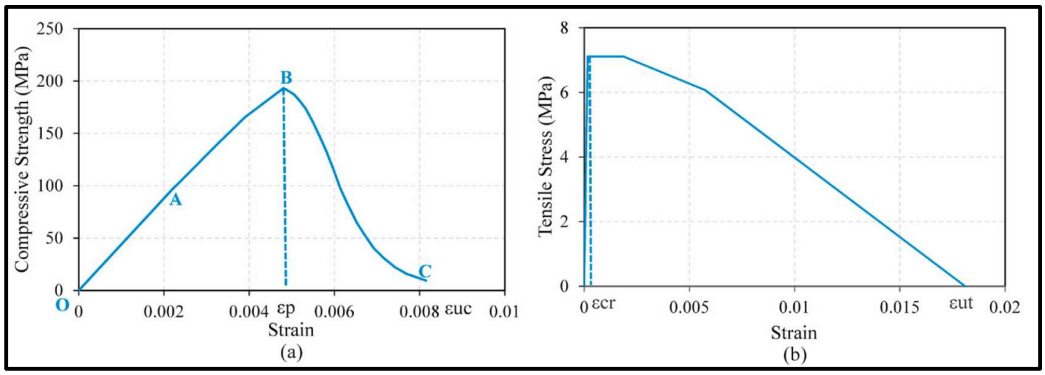


Figure 3.4 Uniaxial stress-strain response for UHPC (a) compressive, (b) tensile (Solhmirzaei & Kodur, 2017)

The experimental tensile longitudinal stress-strain curves for the steel reinforcements were determined experimentally and plotted in Figure 3.5.

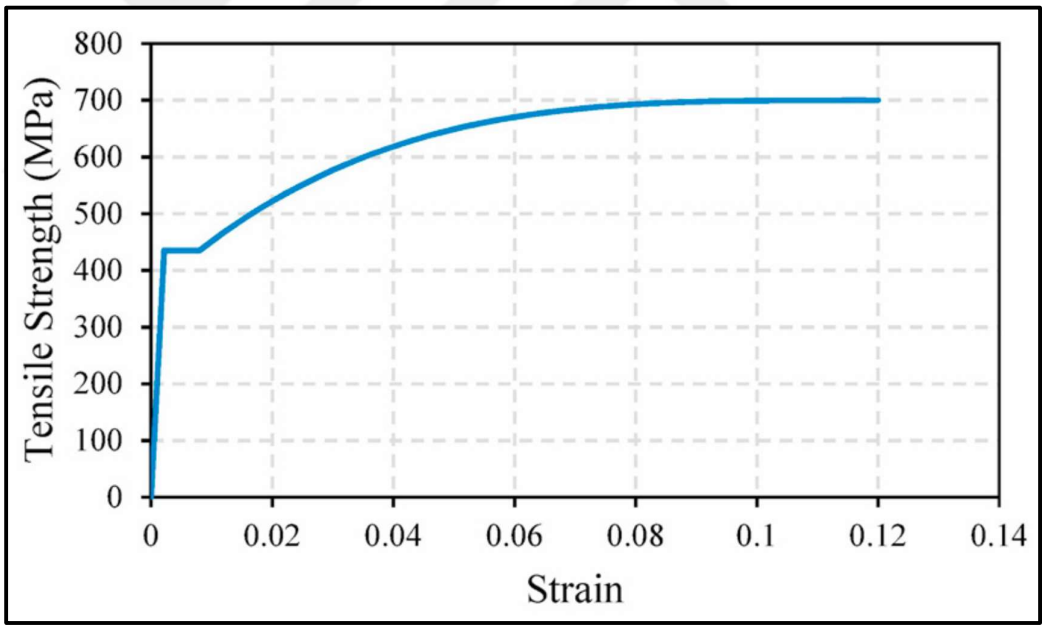


Figure 3.5 Stress-strain response of steel reinforcement (Solhmirzaei & Kodur, 2017)

The yield strength was assessed at 0.21% for the steel reinforcement. The steel test specimen had a density of 7850 kg/m^3, poison ratio of 0.3, an average yield strength f_y of 435 MPa, an average ultimate tensile strength f_u of 700 MPa, and an average rupture strain ε_u of 0.12. The strand's modulus of elasticity E_p was found to be 207 GPa. The strain data were determined until a Uni-axial strain of about 0.12.

3.3.1 UHPC mix design

Solhmirzaei & Kodur (2017) did not provide information on the type and quantity of UHPC constituent material used in the experiment. It is assumed that a propriety UHPC such as Ductal was used for the casting of the test specimen beams. The three main components of this propriety UHPC consists of Preblended powder consisting of (fine aggregate particles such as cement, silica fume, ground quartz and sand), Liquid admixtures and Steel fibers. From the mechanical properties of the UHPC highlighted in Table 3.1, it is assumed that the mix design consisted of 2,200 kg/m^3 of preblended powder, 170 kg/m^3 of water, 80 kg/m^3 of liquid admixture, and 160 kg/m^3 of straight steel fibers (2% volume). The steel fiber specification is 13 mm and 0.2 mm in length and diameter respectively and the reported manufactured minimum tensile strength of 2,650 MPa.

3.4 Material representation of UHPC in ANSYS

Two different material models are used to represent UHPC in the ANSYS software for this research. These include the following:

3.4.1 Coupled damage-plasticity microplane model

By using Mechanical APDL codes on ANSYS software, the following parameters shown below are defined in the ANSYS software after carrying out a uniaxial cyclic compression and tension test on ANSYS. These parameters are shown in Figure 3.6.

```
! This means these commands will be carried out during pre-processing
/PREP7

! Step 1: Define elastic properties of material
E = 43970           ! Young's Modulus, MPa
nu = 0.2            ! Poisson's Ratio, unitless

! Step 2: Define microplane model properties
!  - Approximations and typical ranges per intuition... your concrete may be different!
fc = 193             ! Uniaxial compressive strength, MPa
fb = 223.88             ! Biaxial compressive strength, MPa         (estimate as 1.15*fc if unknown)
ft = 7.11             ! Tensile strength, MPa                    (estimate as 0.1*fc if unknown)
Rt = 1              ! Tension cap hardening constant, unitless  (typically = 1)
D = 0.5e4           ! Compressive hardening constant, MPa^2     (typically between 1e4 and 50e4)
sigma_cv = -149.2533      ! Int. of comp. cap and DP yield, MPa       (always negative, approximately -2/3*fb or lower)
Rc = 2              ! Compression cap ratio constant, unitless  (typically = 2)
gamma_t = 1e-3         ! Tensile damage threshhold, unitless       (typically = 0)
gamma_c = 15e-5      ! Compressive damage threshhold, unitless   (typically between 1e-5 to 10e-5)
beta_t = 50       ! Tension damage evolution, unitless        (typically 1.5*beta_c)
beta_c = 30000       ! Compression damage evolution, unitless    (typically between 1000 and 10000)

! Step 3: Define nonlocal parameters c and m
c = 10000             ! Nonlocal range parameter, mm^2            (element size should be < 0.5*sqrt(c))
m = 2               ! Over-nonlocal parameter, unitless         (typically 1 to 3)


! Step 4: Select element type
element = 215       ! Element type number (Linear = 215, Quadratic = 216)

! Assign Elastic Properties
MP,EX,conc,E        ! Assign Young's Modulus
MP,NUXY,conc,nu     ! Assign Poisson's Ratio

! Assign microplane properties for coupled damaged-plasticity (MPLANE-DPC)
TB,MPLANE,conc,,,DPC
TBDATA,1,fc,fb,ft,Rt,D,sigma_cv
TBDATA,7,Rc,gamma_t,gamma_c,beta_t,beta_c

! Assign nonlocal properties to microplane model (MPLANE-NLOCAL)
TB,MPLANE,conc,,,NLOCAL
TBDATA,1,c,m

! Define coupled elements (this code assumes ITYPE = matid, which it should be in almost all cases)
itype = conc

et,itype,element
keyopt,itype,18,2     ! Element needs 2 nonlocal parameters for keyopt(18)

! Switch element type of those that are assigned Concrete
esel,s,mat,,conc
emodif,all,type,itype

! To check that everything worked out, print the element list
allsel
etlist,all

! Now proceed to the solution and output all results
/SOLU
```

Figure 3.6 Coupled damage-plasticity microplane parameters (Mechanical APDL Code)

Two cubes were modeled in the ANSYS software of size $1\ mm\ x\ 1\ mm\ x\ 1\ mm$. These cubes are restrained in 3 orthogonal directions by using the symmetry tool function on ANSYS software. According to Figure 3.4(a and b), using the maximum compression strain value in the figures, 0.008 mm compressive displacement load is applied to the face of one of the cubes, while a tension maximum strain value of 0.0181 mm is applied on the face of the second cube as displacement load. The two cubes modeled in the ANSYS software are shown below:

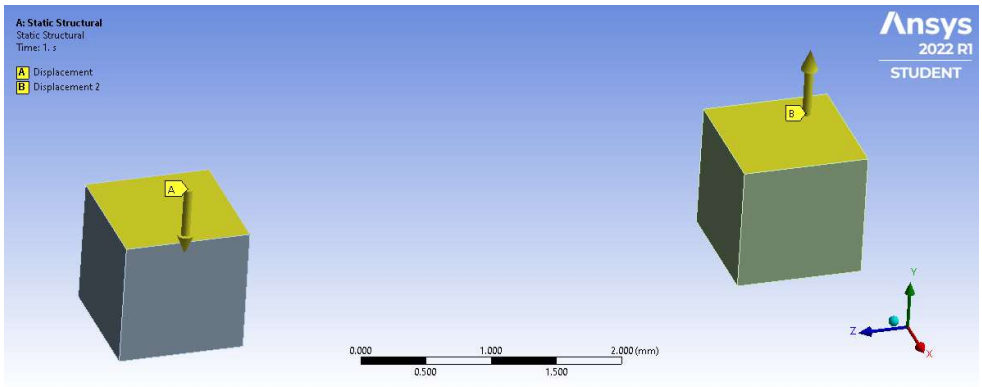


Figure 3.7 Uniaxial cyclic compression and tension test cubes on ANSYS

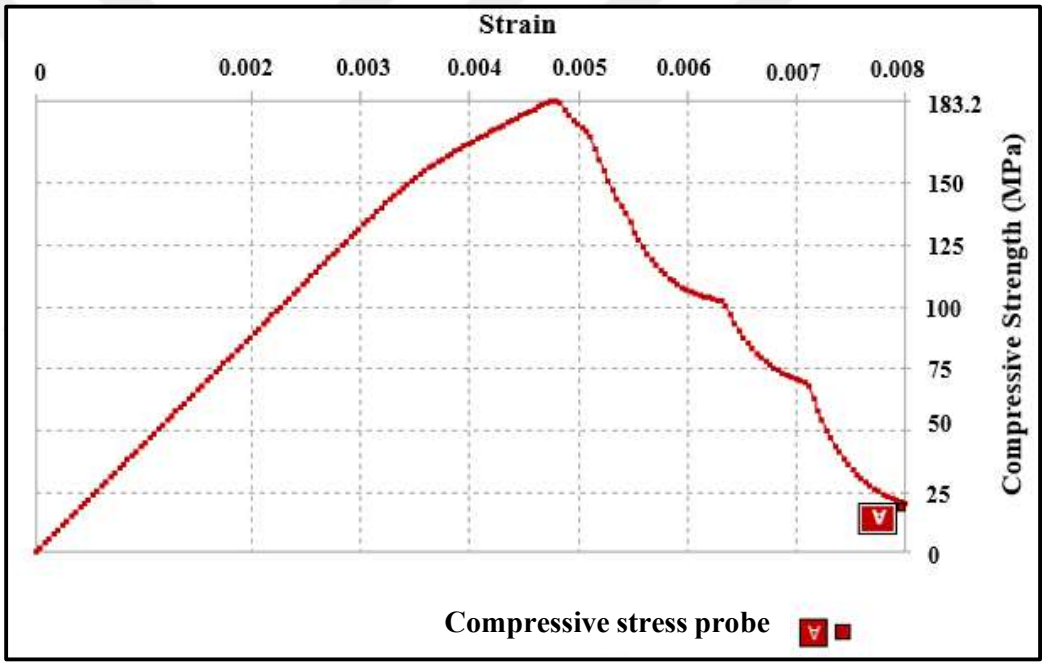


Figure 3.8 Uniaxial cyclic compressive test on ANSYS

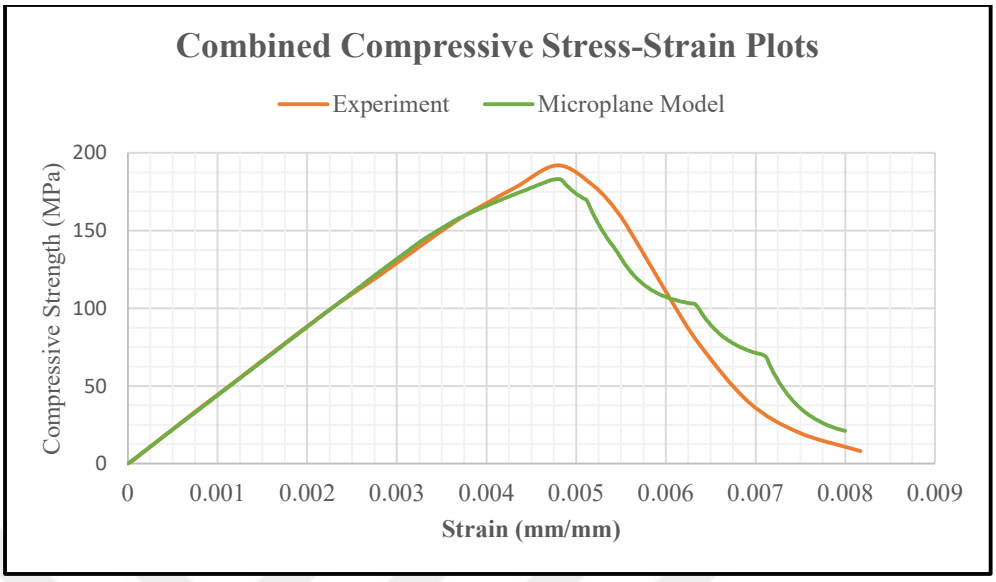


Figure 3.9 Combined Microplane model calibration data and experimental data for UHPC in compression

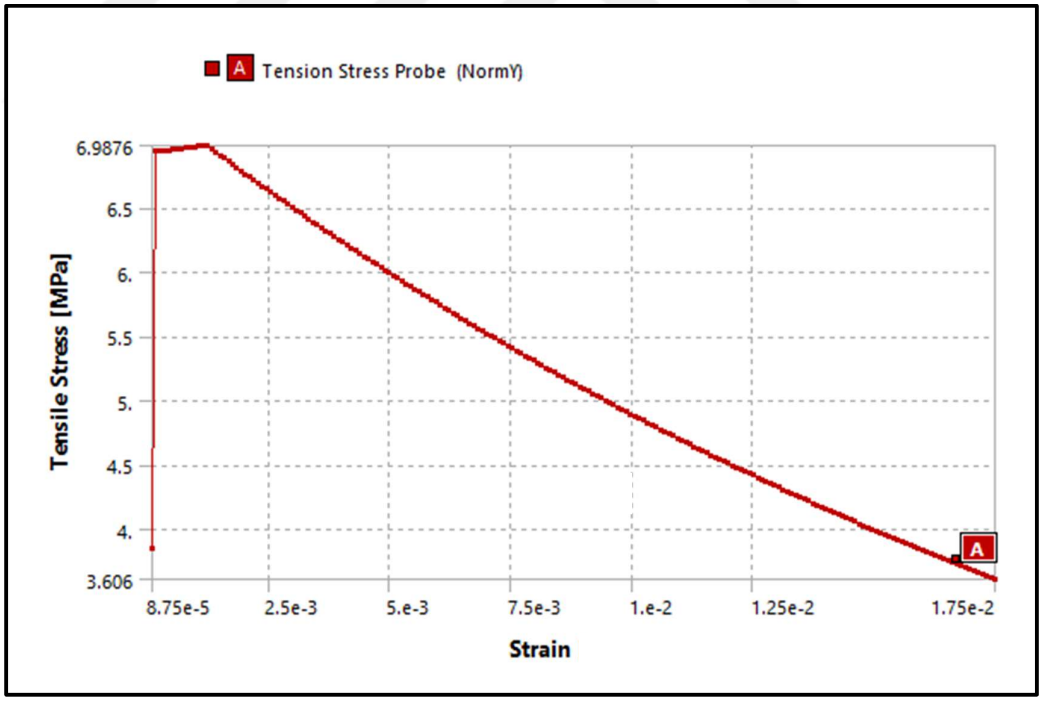


Figure 3.10 Uniaxial cyclic tensile test on ANSYS

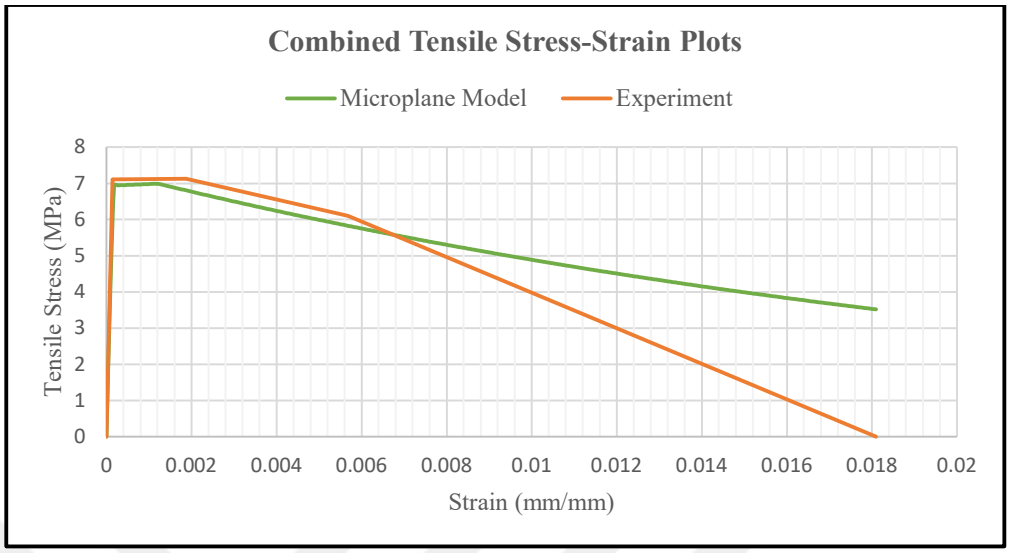


Figure 3.11 Combined Microplane model calibration data and experimental data for UHPC in tension

3.4.2 Menetrey Willam model

In the ANSYS engineering data section, the following Menetrey Willam parameters in Table 3.2 are defined with the following values to represent the structural UHPC material used in this research.

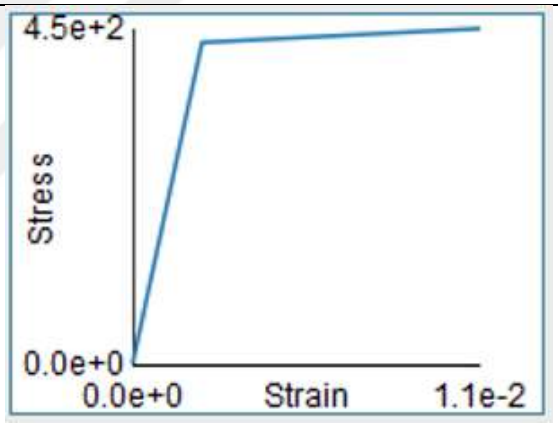
Table 3.2 Menetrey Willam UHPC parameters on ANSYS

UHPC	
Structural	
Isotropic Elasticity	
Derive from	Young's Modulus and Poisson's Ratio
Young's Modulus	43970 MPa
Poisson's Ratio	0.2
Bulk Modulus	24428 Mpa
Shear Modulus	18321 MPa
Menetrey-William	
Menetrey-William Base	
Uniaxial compressive Strength	193 MPa
Uniaxial Tensile Strength	7.11 MPa
Biaxial Compressive Strength	223.88 MPa
Dilatancy Angle	30 degrees
Softening	
Active Table	Linear
Uni-axial Compression Plastic Strain	0.0044
Ultimate Equivalent Compressive Plastic Strain	0.008
Percentage Stress at the Beginning of Non-linear Hardening	0.95
Remaining Compression Relative Stress	0.08
Plastic Tensile Strain Limit	0.02
Remaining Tensile Percentage Stress	0.2

3.5 Material representation of reinforcing steel in ANSYS

The tensile reinforcement used in the beam experimental test is represented on ANSYS as shown in Table 3.3 and Figure 3.12 as a bilinear isotropic hardening model with a slope of 207 GPa and 2,248 MPa respectively.

Table 3.3 Reinforcement steel material model on ANSYS

Reinforcing Steel	
Density	$7.85e^{-06}$ Kg/mm^2
Structural	
Isotropic Elasticity	
Derive from	Young's Modulus and Poisson's Ratio
Young's Modulus	$2.07e^{+05}$ MPa
Poisson's Ratio	0.3
Bulk Modulus	1.725e+05 MPa
Shear Modulus	79615 MPa
Bilinear Isotropic Hardening	

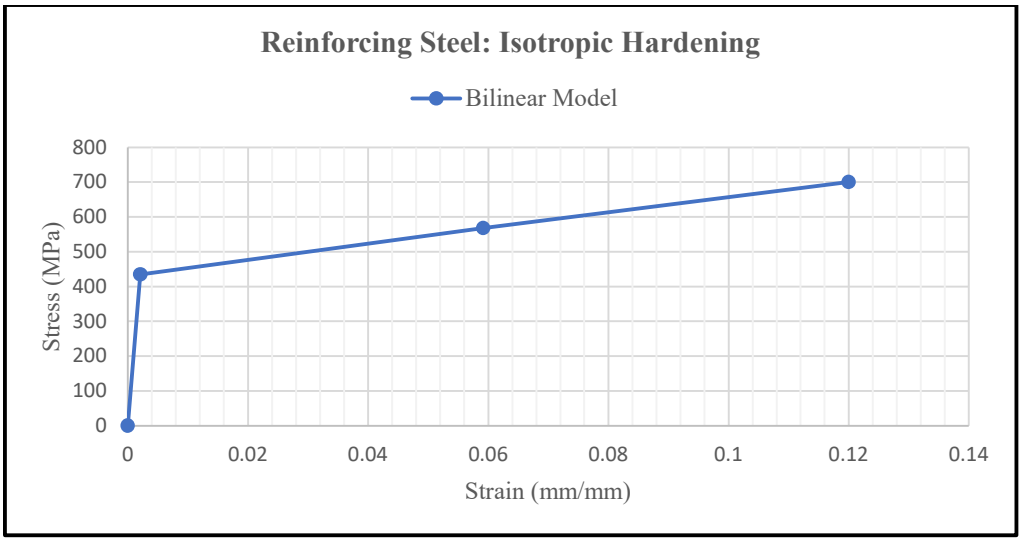


Figure 3.12 Tensile stress-strain curve model of reinforcing steel on ANSYS

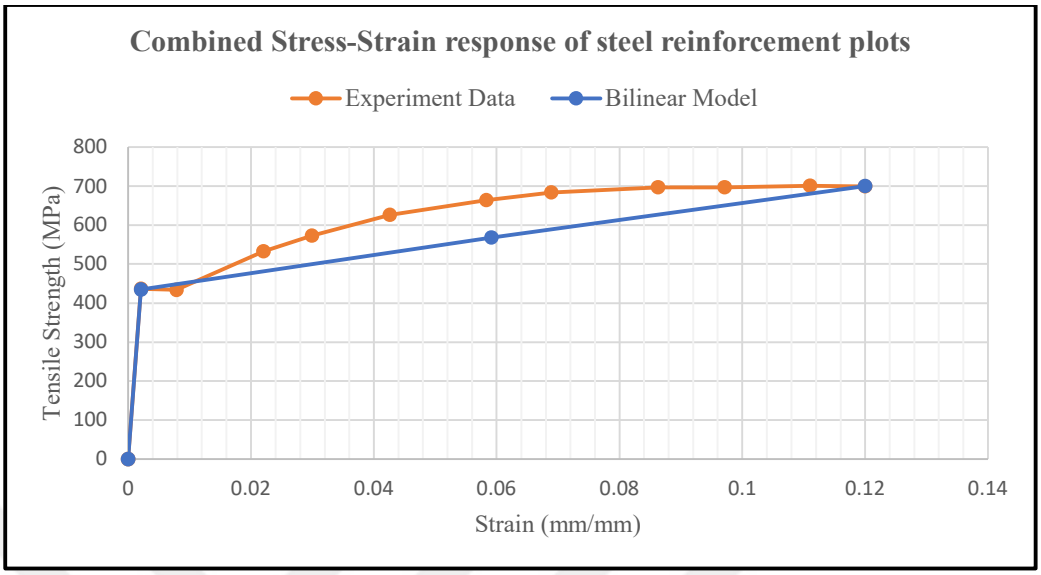


Figure 3.13 Combined tensile stress-strain curves of reinforcing steel

3.6 Geometry model of reinforced UHPC beams in ANSYS

Although the geometry of the 4 beams studied in this research is similar, different geometric techniques are used to define each of the beams.

3.6.1 Geometry model of U-B3 reinforced UHPC beam on ANSYS

U-B3 contains 3 tensile reinforcements at the bottom and a 4-point load system is applied on it. Since this beam is symmetric in geometry and loading in 2 directions a quarter model of the full geometry is used for numerical analysis as shown below in Figures 3.14 and 3.15. Also, the full geometry model of U-B3 is used for numerical analysis as shown in Figures 3.16 and 3.17.

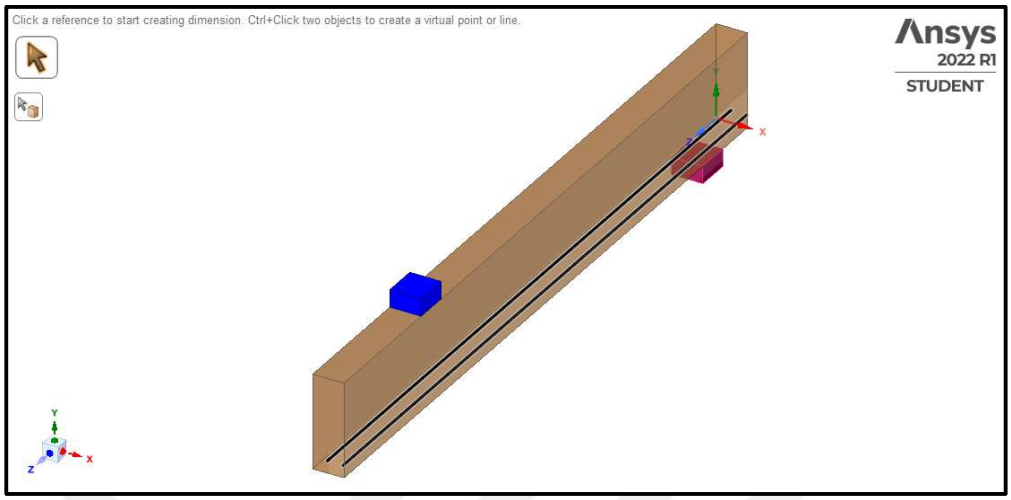


Figure 3.14 3D quarter geometry model of U-B3 in mm

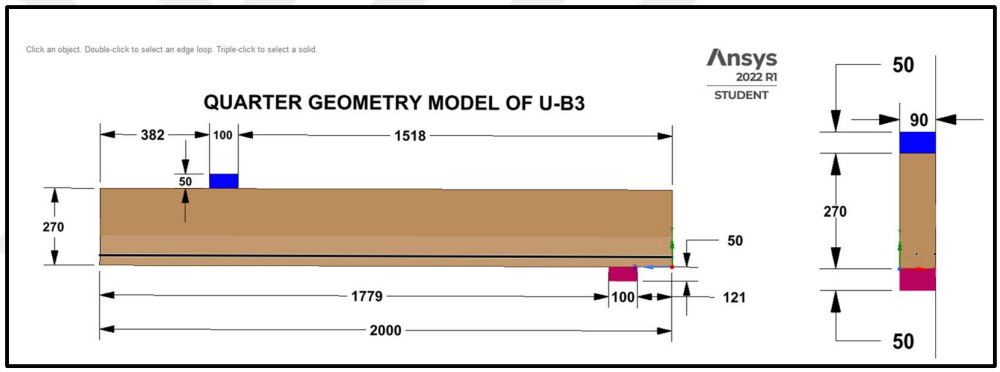


Figure 3.15 Quarter geometry model of U-B3 in mm

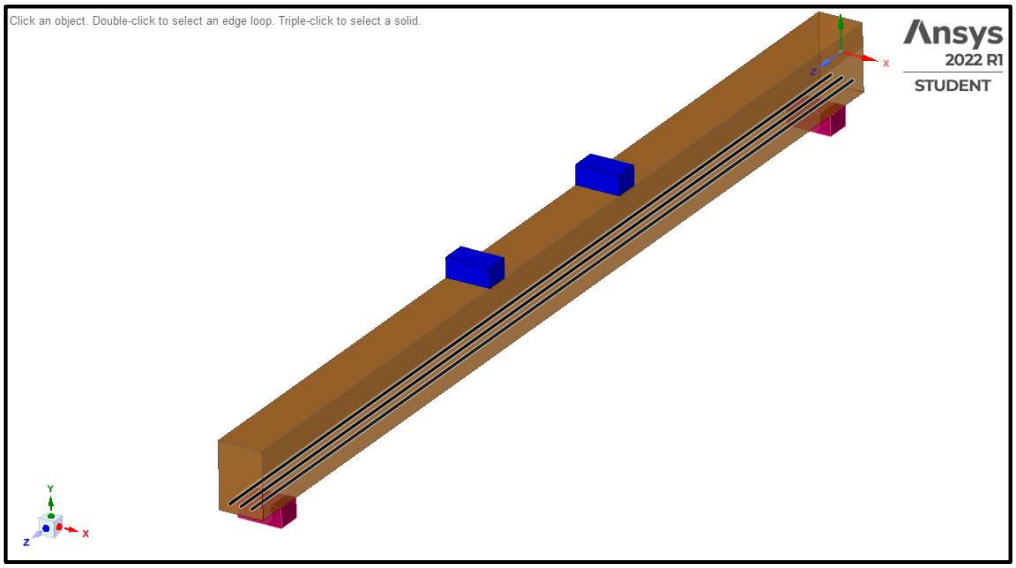


Figure 3.16 3D full geometry model of U-B3 in mm

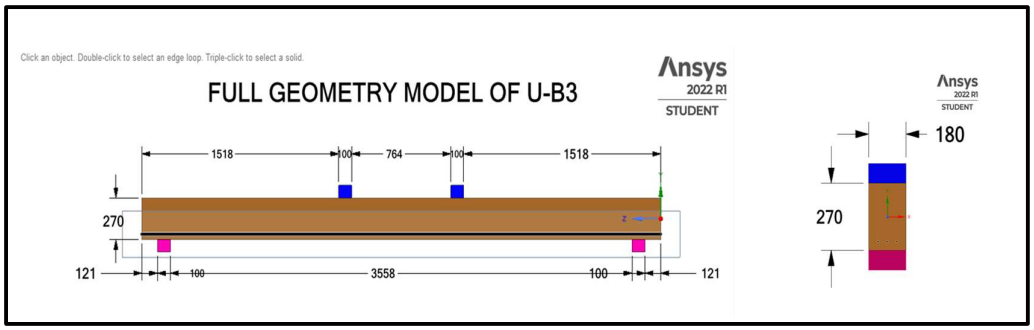


Figure 3.17 Quarter geometry model of U-B3 in mm

3.6.2 Geometry model of U-B5 reinforced UHPC beam on ANSYS

According to Figures 3.1 and 3.2, U-B5 contains 4 tensile reinforcements at the bottom, and a 4-point load system is applied on it. Since this beam is symmetric in geometry and loading in 2 directions a quarter model of the full geometry is used for numerical analysis as shown below in Figures 3.18 and 3.19. Also, the full geometry model of U-B5 is used for numerical analysis as shown in Figures 3.20 and 3.21.

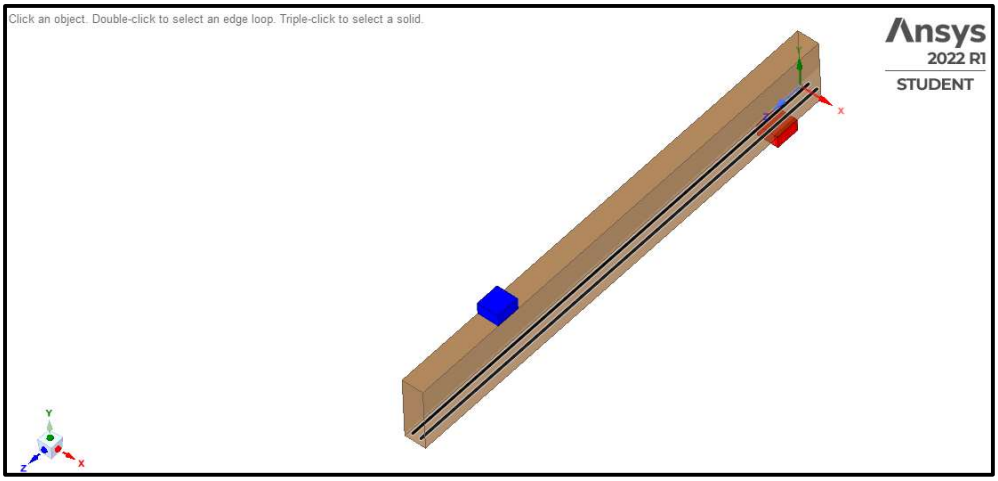


Figure 3.18 3D quarter geometry model of U-B5 in mm

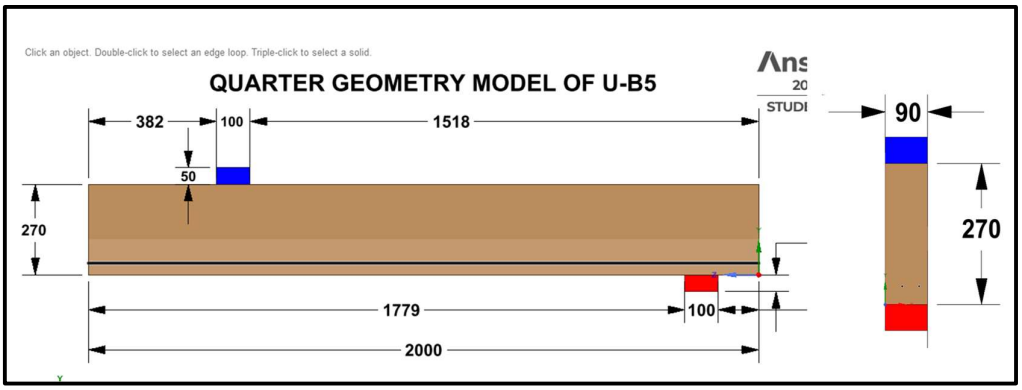


Figure 3.19 Quarter geometry model of U-B5 in mm

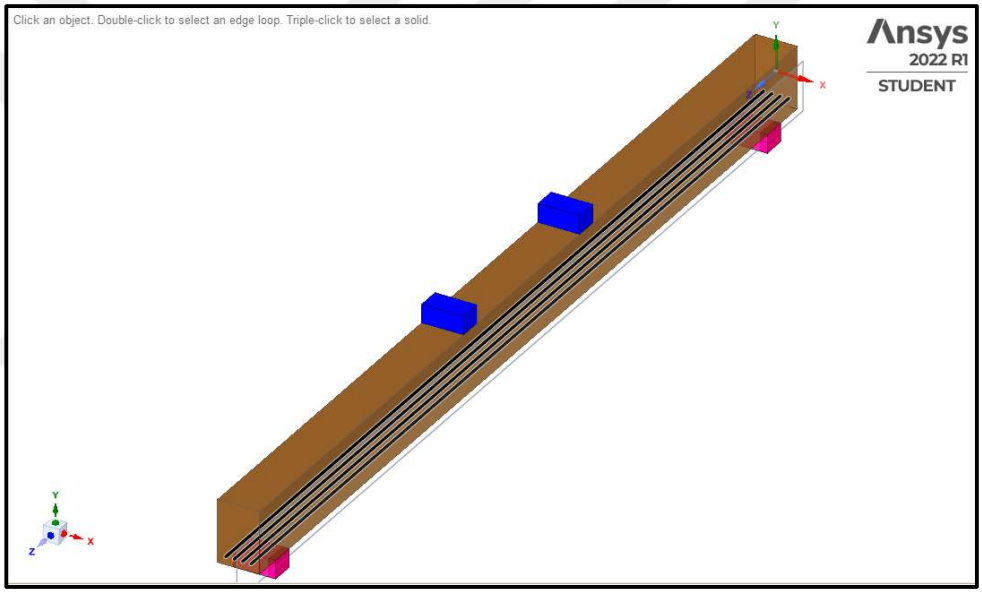


Figure 3.20 3D full geometry model of U-B5 in mm

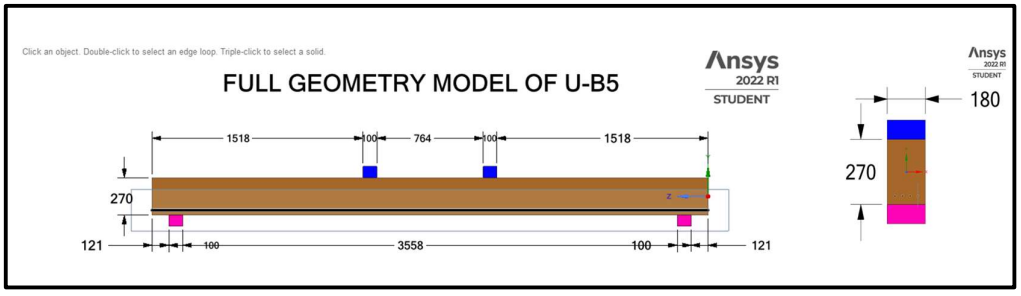


Figure 3.21 Quarter geometry model of U-B5 in mm

3.6.3 Geometry model of U-B4 reinforced UHPC beam on ANSYS

According to Figures 3.1 and 3.2, U-B4 contains 3 tensile reinforcements at the bottom, and a 3-point load system is applied on it. Since this beam is not symmetric in geometry and loading, the full geometry is used for numerical analysis as shown below in Figures 3.22 and 3.23:

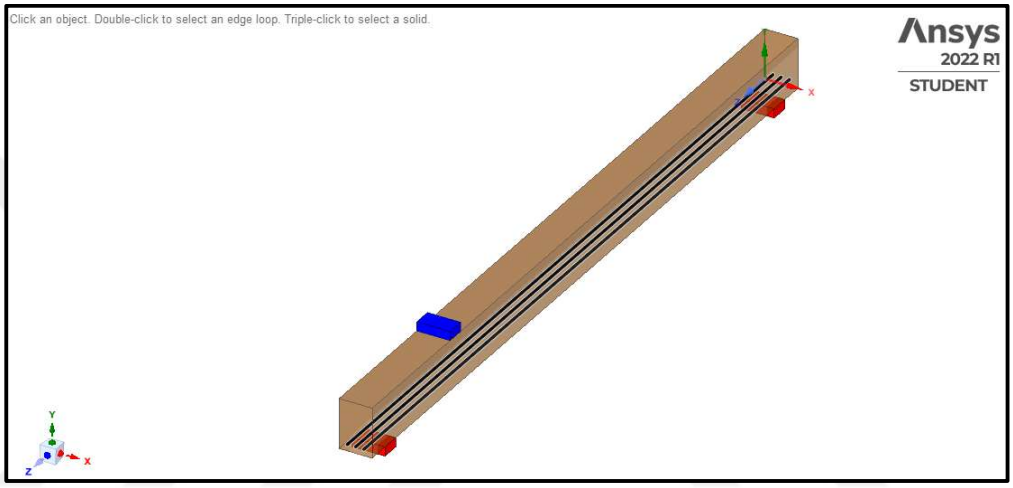


Figure 3.22 3D full geometry model of U-B4

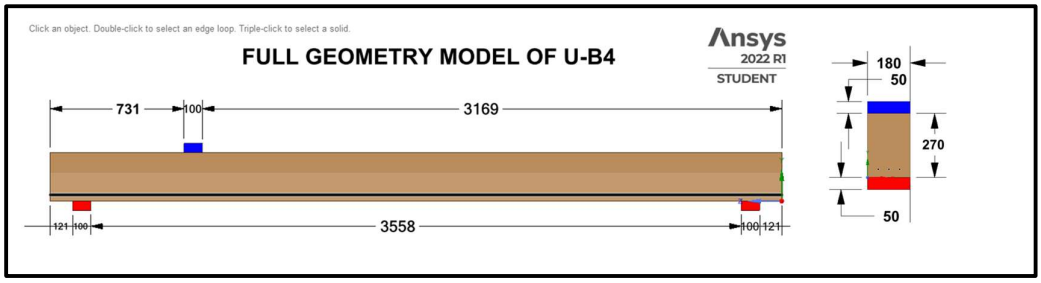


Figure 3.23 Full geometry model of U-B4 in mm

3.6.4 Geometry model of U-B6 reinforced UHPC beam on ANSYS

According to Figures 3.1 and 3.2, U-B6 contains 4 tensile reinforcements at the bottom, and a 3-point load system is applied on it. Since this beam is not symmetric in geometry and loading, the full geometry is used for numerical analysis as shown below in Figures 3.24 and 3.25:

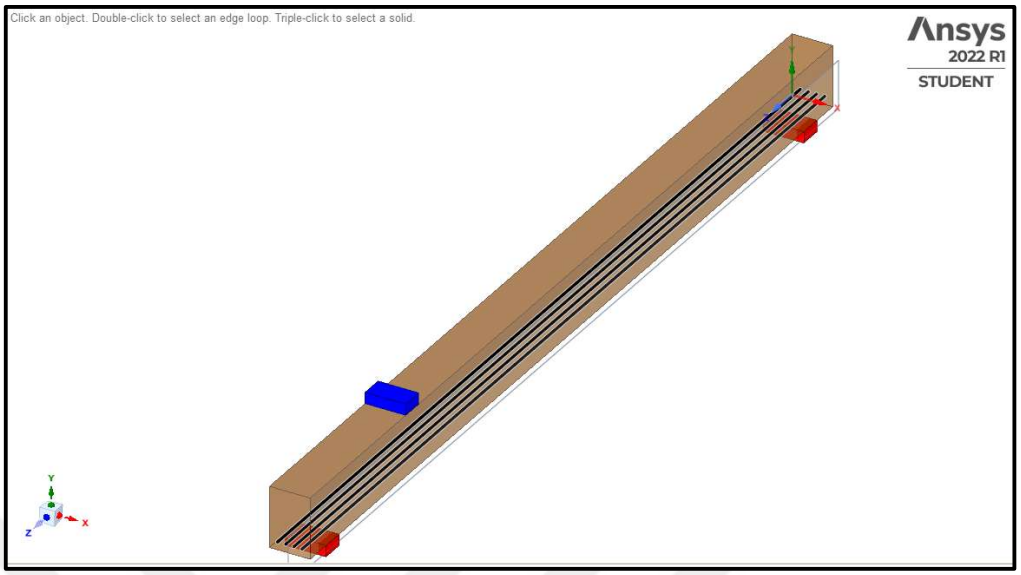


Figure 3.24 3D full geometry model of U-B6 in mm

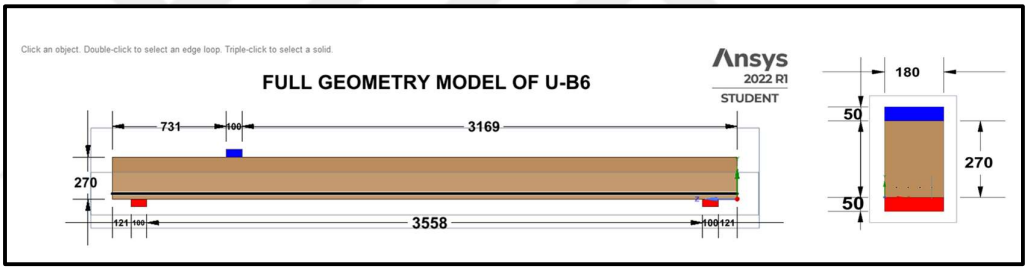


Figure 3.25 Full geometry model of U-B6 in mm

3.7 ANSYS finite element procedures for the analysis problem

2 Finite element methods based on different material model types are used for the structural analysis of the 4 reinforced UHPC beams mentioned in this research work.

These methods include:

1. Menetrey Willam method
2. Coupled Damage-Plasticity Microplane method

The step-by-step procedure for the finite element methods is listed below:

1. Definition of engineering material models in the engineering data tab on the static structural solver (ANSYS). These definitions include material models for

tensile reinforcement steel, support plates, loading plates, and UHPC. If the coupled damage-plasticity microplane method is used, a dummy material is defined for UHPC with an arbitrary value for the Young modulus, E and Poisson ratio, v initially. Later the UHPC material is defined by using mechanical APDL code.

2. Definition of the geometry model for the reinforced UHPC beams under the geometry tab of the static structural solver (ANSYS). This tab opens a 3D modeling environment to define the geometry of the beams (Spaceclaim).
3. Material assignments, boundary condition assignments, and finite element discretization are specified on the model tab of the static structural solver (ANSYS). This modal tab opens a window interface called “Mechanical” for the various assignments and discretization.
4. If the coupled damage-plasticity microplane method is used, ANSYS Mechanical APDL parameters are used to redefine the UHPC dummy material created in Step 1.
5. The solution is analyzed to show the result of deformation, stress, strain, different chart plot results, and damage color plot representation of the beams.

CHAPTER FOUR
RESULTS AND DISCUSSION

In this section, the numerical results of all the reinforced UHPC beams using ANSYS software are presented either in the form of color plots or charts, or tables. The results for the material numerical methods stated in Chapter 3 are reported for all test beams. For validation, the ANSYS findings are compared to experimental data. Important numerical results for the reinforced UHPC are presented in table 4.1 on the next page. Data images from the reference paper were digitized to combine the experimental and the finite element solutions for the sample beams.

Table 4.1 Tabular presentation of key thesis results Solhmirzaei & Kodur (2017)

Beam Type Label	ANSYS FE Results															
	Experimental Results			Microplane Material model									Menetrey William Model		
				Full Geometry Model						Quarter Geometry Model					
	Load Capacity (kN) (1)	Max Midspan deflection (mm) (2)	Total strain in longitudinal reinforcement (mm/mm)	Load Capacity (kN) (3)	Ratio (1)/(3)	Maximum deflection (mm) (4)	Ratio (2)/(4)	Total strain in longitudinal reinforcement (mm/mm)	Max Rebar tensile Stress (MPa)	Load Capacity (kN)	Maximum deflection (mm)	Max Rebar tensile Stress (MPa)	Load Capacity (kN)	Maximum deflection (mm)	Max Rebar tensile Stress (MPa)
U-B3	97.1	a	0.025	116.27	0.835	121.72	a	0.035311	509.57	120.33	122.24	511.14	98.512	132.19	635.33
U-B4	142.1	a	a	151.64	0.937	89.999	a	0.050354	543.47	b	b	b	b	b	b
U-B5	126.6	122	0.025	135.07	0.937	120.39	1.01	0.033968	506.64	140.15	121.15	508.32	115.82	121.73	606.36
U-B6	177.1	83	a	176.4	1.000	88.71	0.936	0.049332	541.17	b	b	b	b	b	b

[a]Data not reported

[b]ANSYS results not available because the loading is not symmetric on U-B4 and U-B6

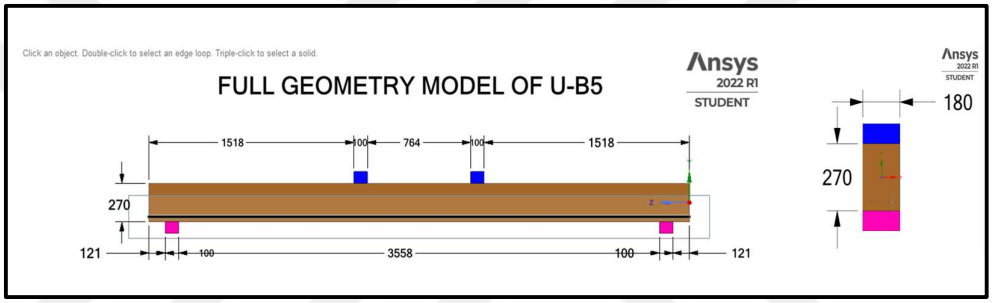
4.1 Presentation of beam U-B5 ANSYS results with experimental data

The midspan deflection at the bottom of the U-B5 beam is plotted against the total applied load (kN) on the two steel plates at the top of the beam in Figure 4.1. This reinforced UHPC beam U-B5, has a dimension of 180 mm x 270 mm x 4000 mm and consists of 4 tensile reinforcements at the bottom section of the beam as shown in Figure 4.1(a). The beam is analyzed using ANSYS by three methods. In the first method, the microplane material model is used to analyze the full geometry section of U-B5. In the second and third methods, a quarter geometry section is analyzed using the microplane material model and the Menetrey Willam model respectively. Also mesh sensitivity analysis is carried out for U-B5 for 45mm and 30mm mesh sizes by using the microplane material model. Due to high computation cost only 2 mesh sizes are considered.

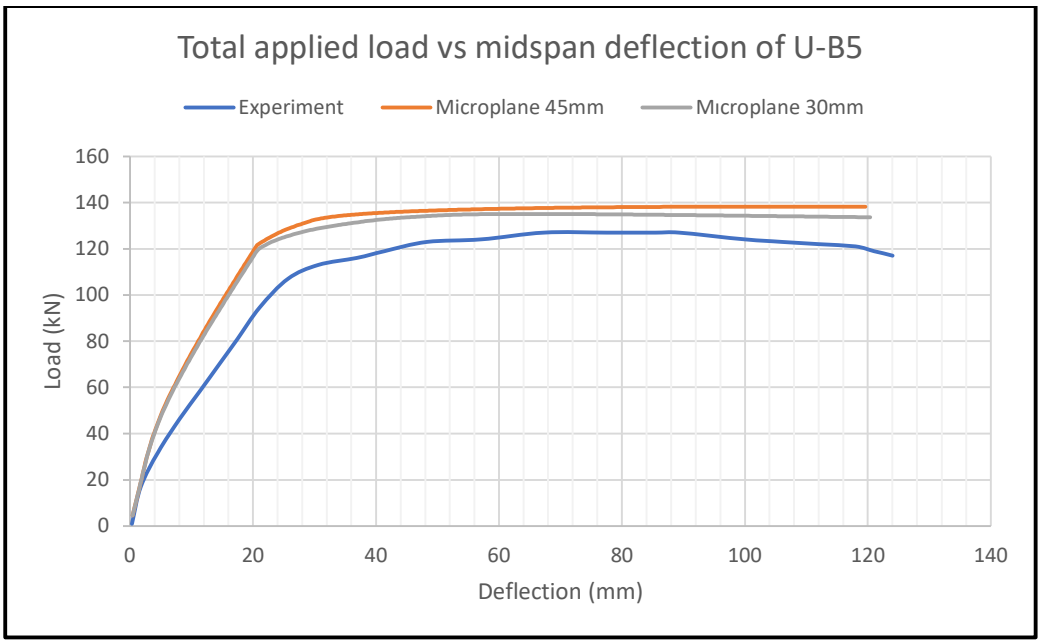
By discretizing the beam problem using a 45 and 30 mm hexagonal finite element meshes, U-B5 is numerically modeled on ANSYS. For the full and quarter geometry model structural analysis, the beam was tested using the 4-point load test to capture the flexural behavior of the beam. Equal displacement loading of $105mm$ was applied on the 2 steel plates at the top of the U-B5 beam. Displacement support specification of 0 mm in the x, y, and z direction was applied under one of the support steel plates to stimulate pinned support, while a displacement support specification of free, 0 mm, and free in the x, y, and z direction respectively were applied on the other steel plate support to stimulate roller support.

Figure 4.1b shows 3 plots for comparison. One of the curve plots is the experimental plot from the research work of Solhmirzaei & Kodur (2017). This plot recorded a maximum applied load and midspan deflection of 126.6 kN and 120 mm respectively. The other curve plots show the result plot of the full geometry structural analysis on ANSYS using the microplane model with 45mm and 30mm linear 3D finite element meshes. Under a 105 mm displacement loading at the top of the beam, a maximum applied load and midspan deflection of 138.24 kN and 119.62 mm are estimated for 45mm mesh, while a maximum applied load and midspan deflection of

135.07 kN and 120.39 mm are estimated for the 30mm mesh. Overall, the shapes of the load–deflection curve from ANSYS are very similar to the plot from the experimental research work. However, the microplane ANSYS result overestimates the capacity of U-B5 by about 6.7% and the result of the modeling is more rigid than in the experiment. This can be explained by the existence of microcracks and imperfections in the beam specimen which are not considered by the model. Overall, this shows the microplane model in ANSYS can be used to predict the flexure behavior of reinforced UHPC beams.



(a)



(b)

Figure 4.1 Total applied load vs midspan deflection of U-B5, (a) Full geometric U-B5, (b) Combined plot of Microplane modal and experimental data from Solhmirzaei & Kodur's study (2017)

Figure 4.2 is a combined experimental and microplane model plot of the total applied load (kN) on the 2 steel plates at the top of the U-B5 beam vs the total strain in the tensile reinforcement at the bottom section of the beam. 45 and 30mm finite element mesh results were also presented in Figure 4.2. Under a 105 mm displacement loading at the top of the beam, a total strain of 0.028848 is estimated for the microplane material model with 45 mm finite element mesh. While a total strain of 0.036671 is calculated by using 30mm mesh size. The results in Figure 4.2 show that the response of the rebars in this material model is stiffer than the experimental result. The difference in results is because a bilinear tensile stress-strain model is used to approximate the hardening behavior of the steel rebars and this is a bit different from the actual mechanical property of the reinforcement steel. Overall, the ANSYS plot in figure 4.2 matches well with the experimental plot.

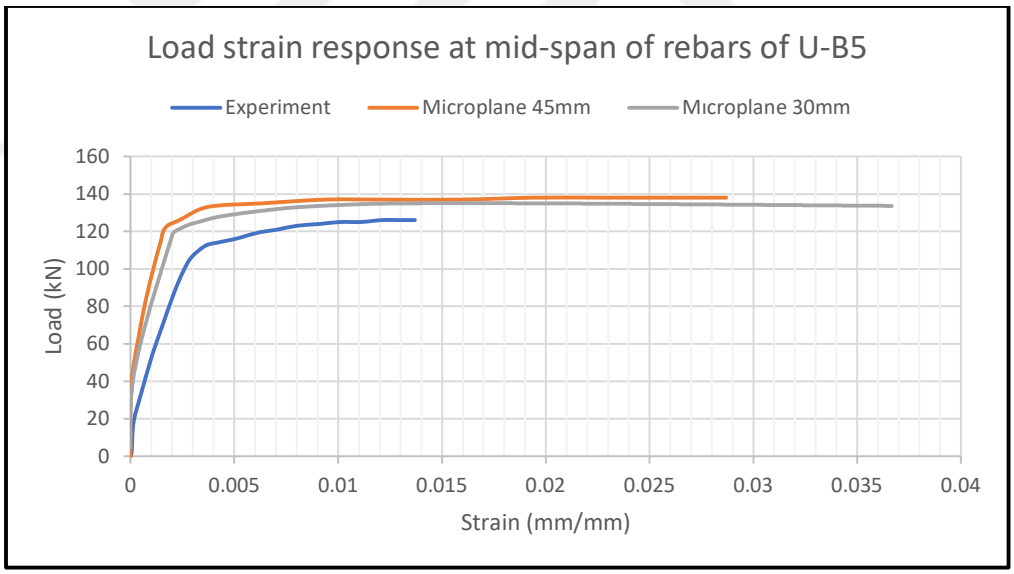
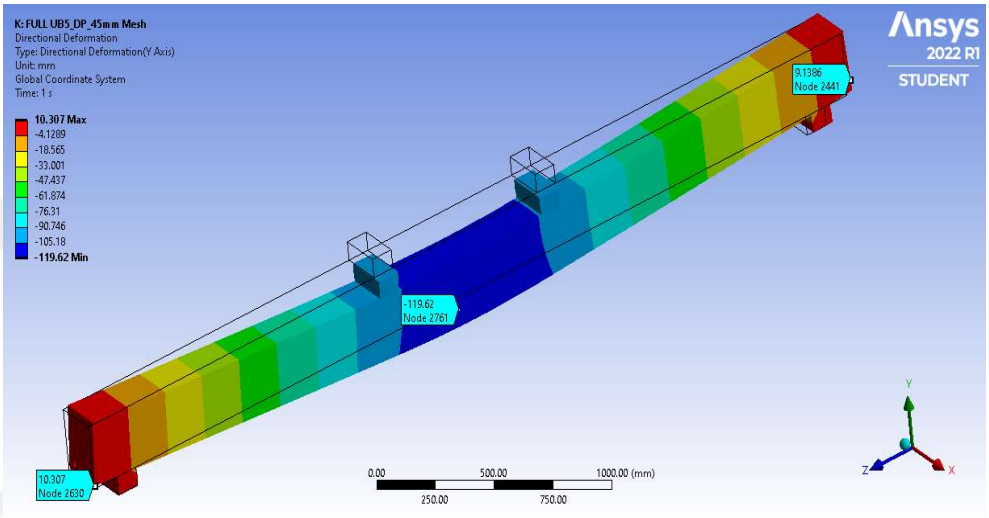


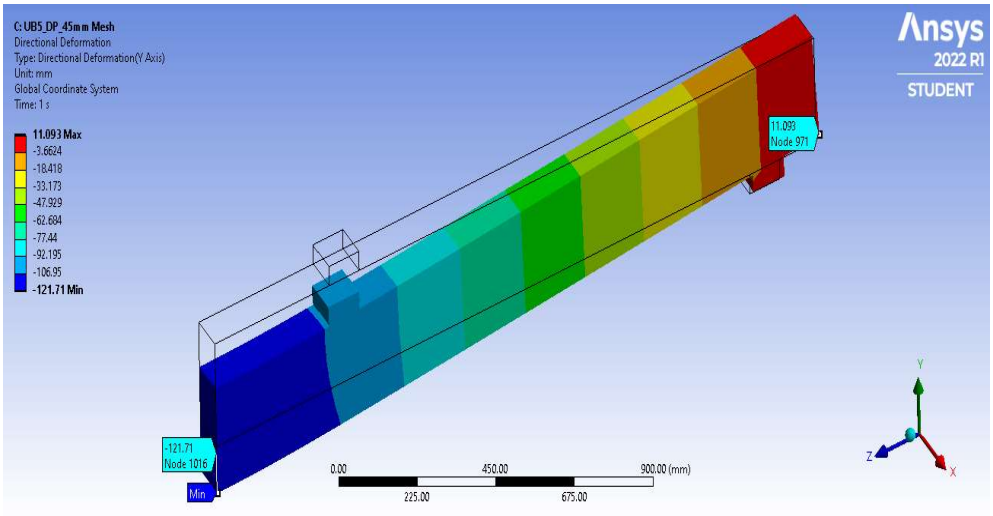
Figure 4.2 Load strain response at mid-span of rebars of U-B5, combined experimental plot and ANSYS microplane model plot

Figure 4.3 are three color plots of U-B5 results obtained by using full and quarter geometry structural analysis on ANSYS. The 45mm mesh result is discussed here. Figure 4.3a is the color plot using the full geometry model in ANSYS (microplane material model). This plot estimates a maximum midspan deflection of 119.62 mm. Figure 4.3b is a quarter geometry model analysis plot (microplane material model) and it predicts a maximum midspan deflection of 121.71 mm. Figure 4.3b is another

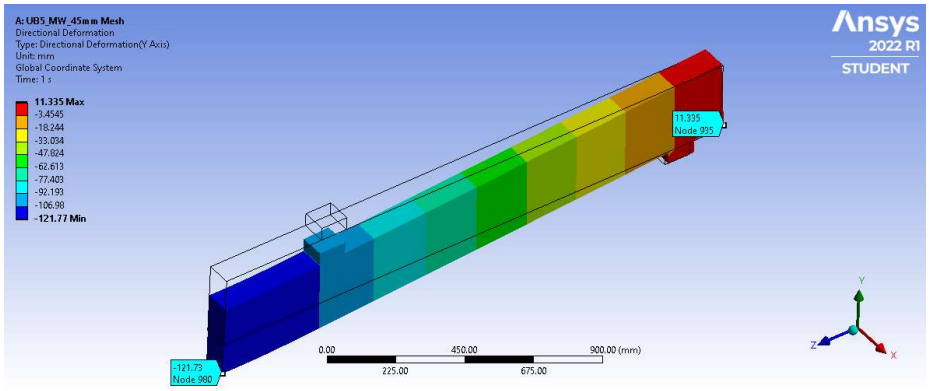
quarter geometry model analysis plot (Menetrey Willam) and it predicts a maximum midspan deflection of 121.73 mm. The experimental mid-span deflection is 122 mm. Since the midspan deflection results from the color plots are very close to the experimental data, it shows the Microplane and the Menetrey Willam material model can be used to predict the flexural behavior of reinforced UHPC beams.



(a)



(b)

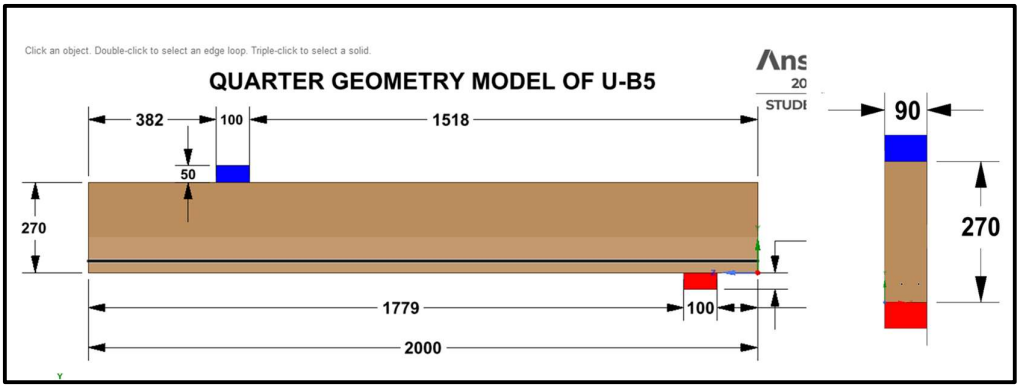


(c)

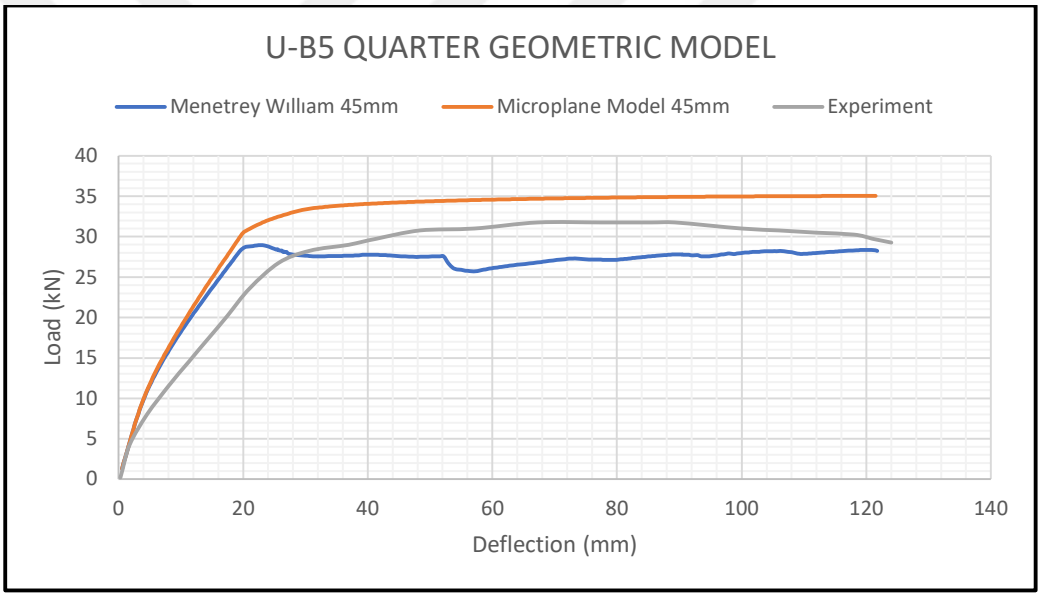
Figure 4.3 U-B5 deflection color plot at failure load. (a) full geometric microplane model plot, (b) quarter geometric microplane model plot, (c) quarter geometric Menetrey Willam model plot

Figure 4.4(b) are combined plots of the applied load (kN) at the top of the U-B5 beam vs the midspan deflection at the bottom of the beam by using a quarter geometry and it show plots of Microplane and Menetrey Willam model compared to experimental plot data. The discussed result is for 45mm mesh size. Under a 105 mm displacement loading at the top of the beam, a maximum applied load and midspan deflection of 35.038 kN and 121.51 mm is estimated for the microplane model. The total applied load on the beam is estimated as $35.038 \times 4 = 140.152$ kN.

Also, under a 105 mm displacement loading at the top of the beam, a maximum applied load and midspan deflection of 28.954 kN and 121.77 mm are estimated in Figure 4.4b. The total applied load on the beam is estimated as $28.954 \times 4 = 115.816$ kN. The shape of the load–deflection curve from ANSYS for the microplane model in Figure 4.4(b) is very similar to the plot from the experimental research work, Figure 4.1 (b). The microplane model overestimates the load capacity of U-B5, while the Menetrey Willam underestimate the capacity. Overall, these plots show the microplane model and Menetrey Willam material model in ANSYS can be used to predict the flexure behavior of reinforced UHPC beams. The difference in the post yield behavior between the 2 models in Figure 4.4b may be due to the assumptions made in the Menetray Willam and concrete damage microplane parameters in the calibration of the stress-strain curves of tension and compression behavior of the UHPC.



(a)

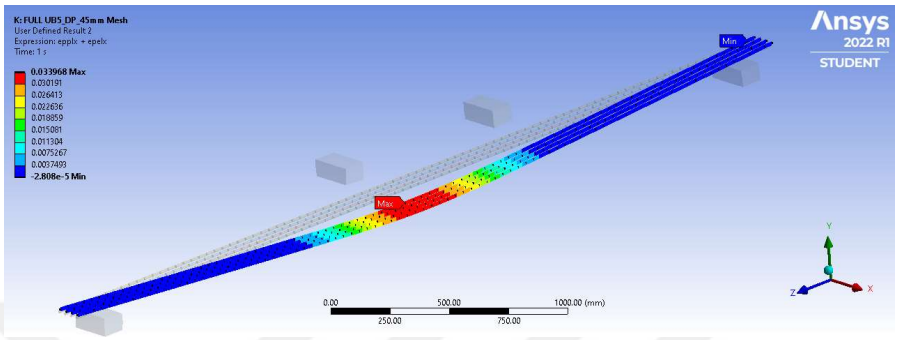


(b)

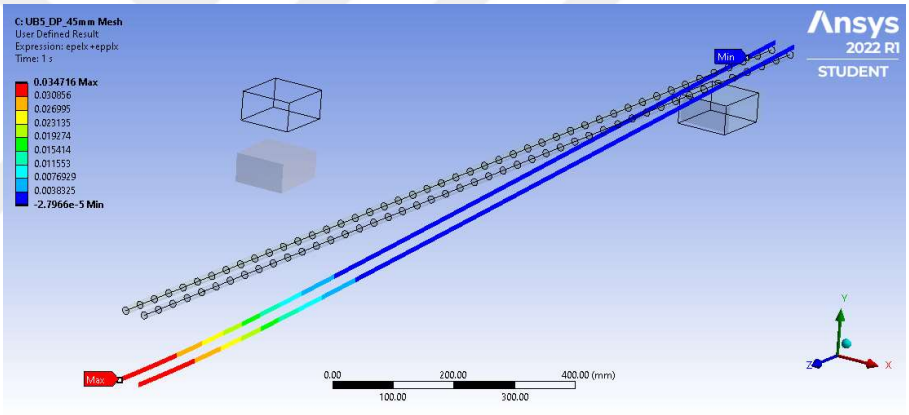
Figure 4.4 Total applied load vs midspan deflection of U-B5. (a) Quarter geometry, (b) Quarter geometric ANSYS microplane, and Mentray Willam model plot combined with experimental test data.

Figure 4.5 are the total strain color plots for the three methods mentioned above for the tensile reinforcements provided in the beam section. 45mm mesh results are discussed here. It predicts a maximum total strain of 0.033968, 0.034716, and 0.075498 mm/mm for the full geometry (microplane), quarter geometry (microplane and Menetrey Willam) models respectively. The Microplane material model plots in Figure 4.5(a) and (b) show that at least 30% of the length of the tensile reinforcements at the bottom section yielded. While just 10% of

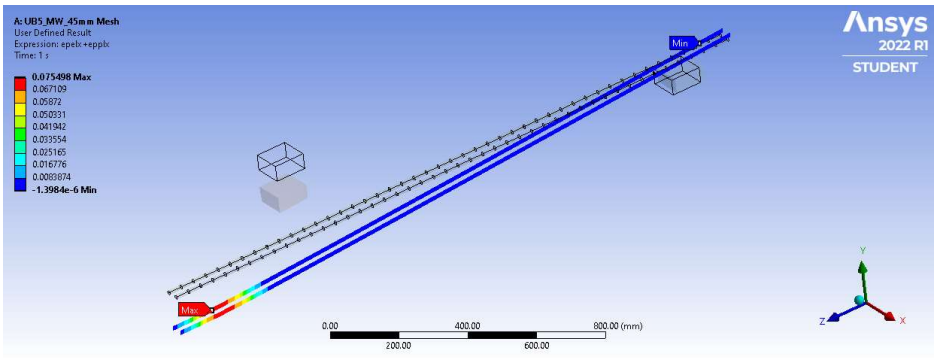
the length of the tensile reinforcements yielded in Figure 4.5(c) using the Menetrey Willam model.



(a)



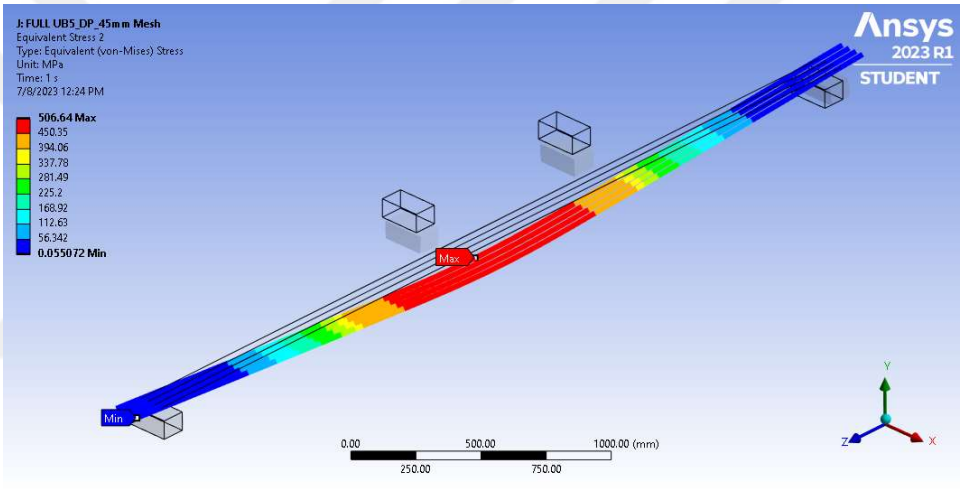
(b)



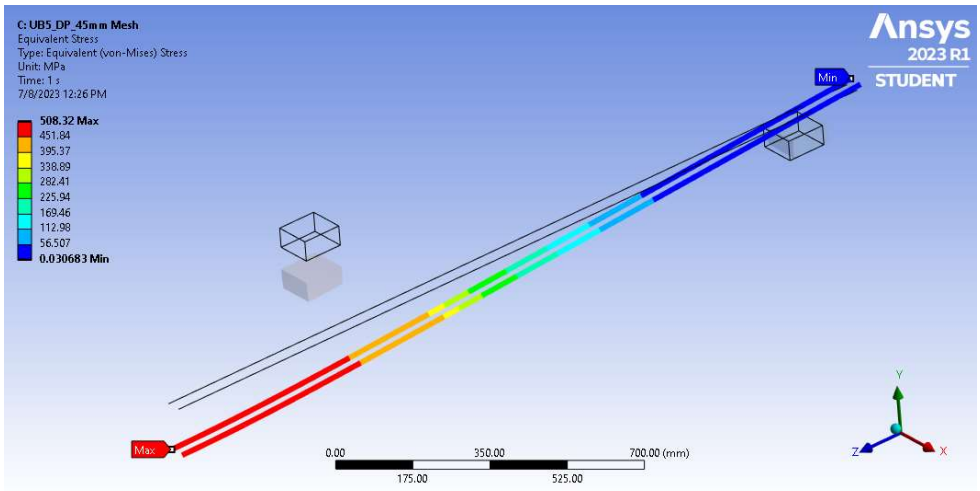
(c)

Figure 4.5 Total strain color plot for tensile reinforcements at load capacity in mm/mm. (a) Full geometric ANSYS microplane, (b) Quarter geometric ANSYS microplane, (b) Quarter geometric ANSYS Mentrey Willam.

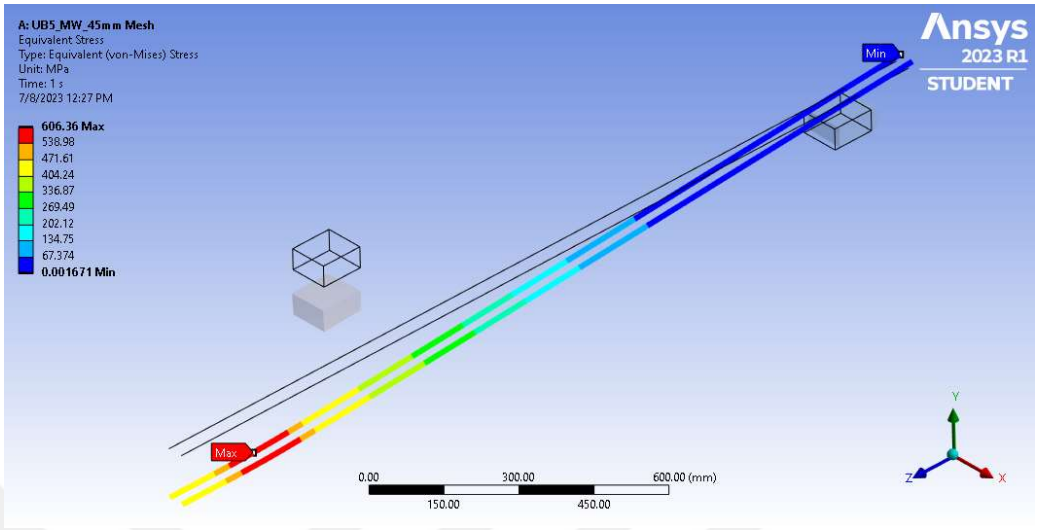
Figure 4.6 are the equivalent von-Mises stress color plots for the three methods mentioned above for the tensile reinforcements provided in the beam section. It predicts a maximum total stress of 506.64, 508.32, and 606.36 MPa for the full geometry (microplane), quarter geometry (microplane), and Menetrey Willam model respectively. The Microplane material model plots in Figure 4.6(a) and (b) show that at least 30% of the length of the tensile reinforcements at the bottom section is above the yield stress of the steel reinforcement (435 MPa). While just 10% of the length of the tensile reinforcements yielded in Figure 4.5(c) using the Menetrey Willam model.



(a)



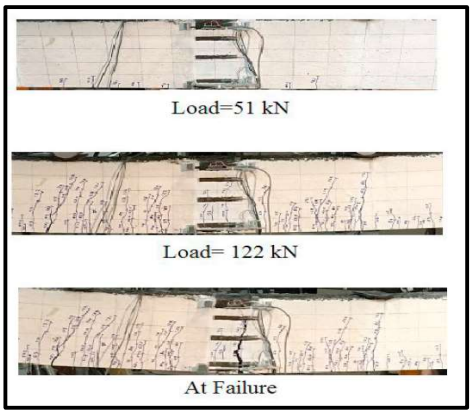
(b)



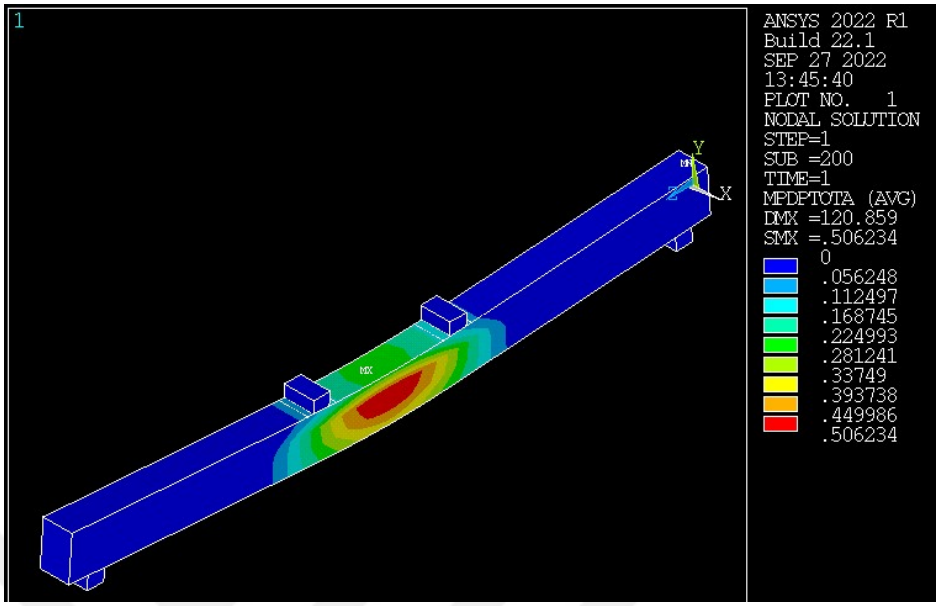
(c)

Figure 4.6 Equivalent von-Mises stress color plot for tensile reinforcements at failure load in MPa. (a) Full geometric ANSYS microplane, (b) Quarter geometric ANSYS microplane (b) Quarter geometric ANSYS Mentrey Willam

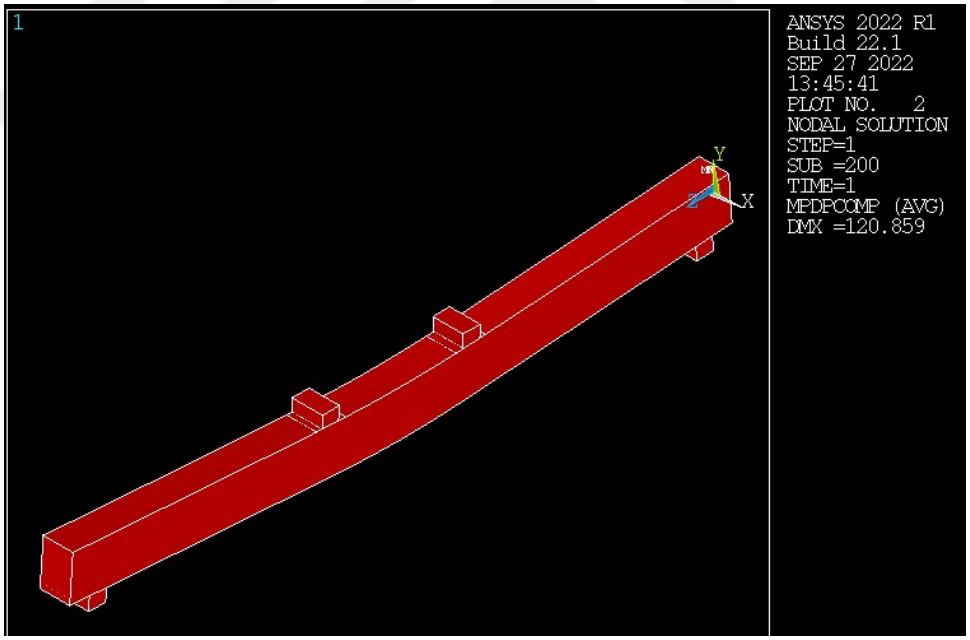
Figures 4.7 and 4.8 are color plot quantities used to denote damage in the UHPC material by using the microplane model. Also, the experimental crack patterns at different loading stages are shown in Figure 4.7(a). The full geometry of U-B5 was used for the color plot results. Figures 4.7(b), 4.7(c), 4.8(a), and 4.8(b) represent the transformed total damage TOTA, transformed tensile damage TENS, transformed compressive damage COMP, and the split weight factor (RW) respectively. Figure 4.7(b) shows that 100% of the beam section is already damaged in tension at the failure load. Figure 4.8(a) shows compression damage at the midspan section of the beam.



(a)

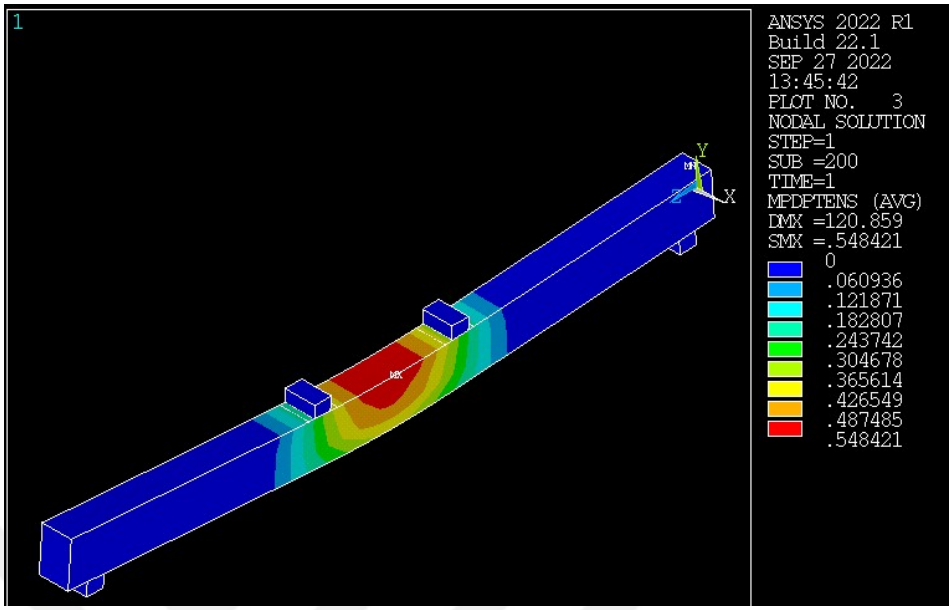


(b)

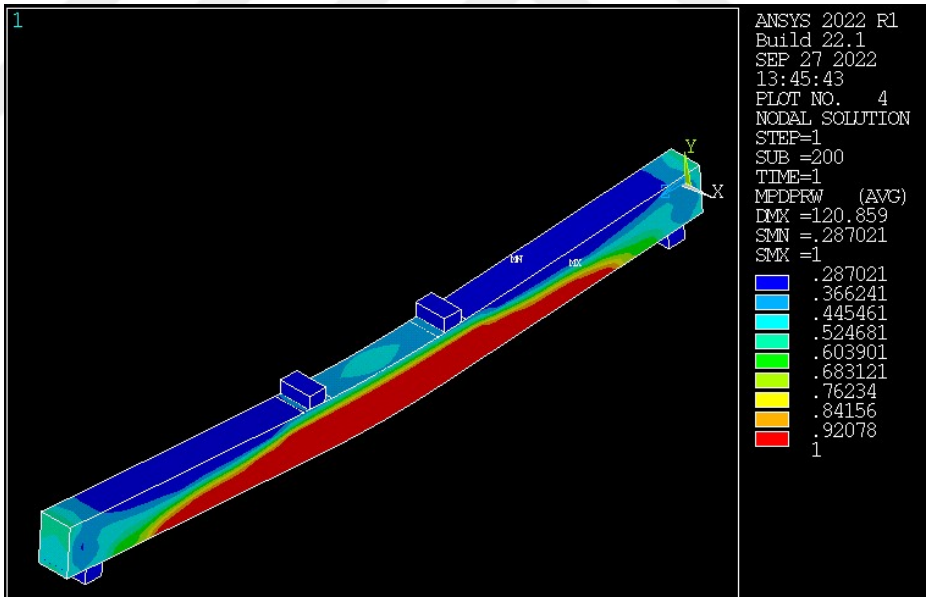


(c)

Figure 4.7 Coupled damage-plasticity microplane damage Output, (a) Experimental crack pattern, (Solhmirzaei & Kodur, 2017) (b) Total damage TOTA, (c) Tensile damage TENS.



(a)

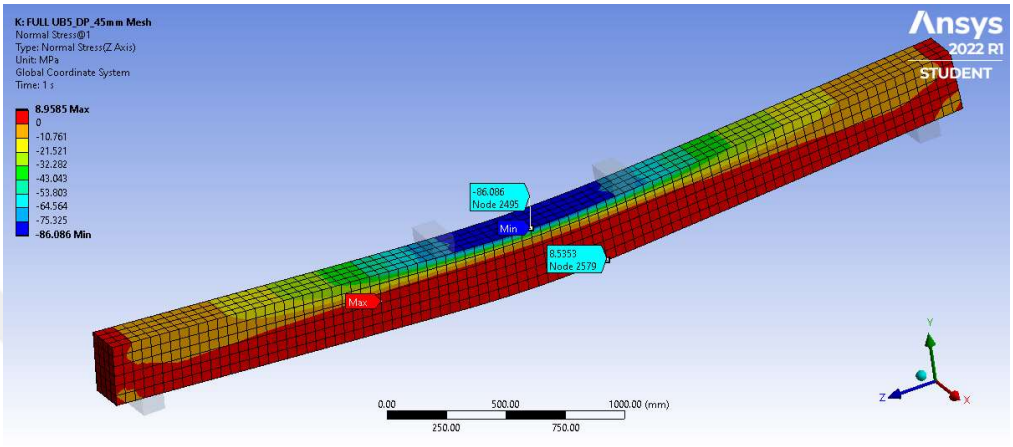


(b)

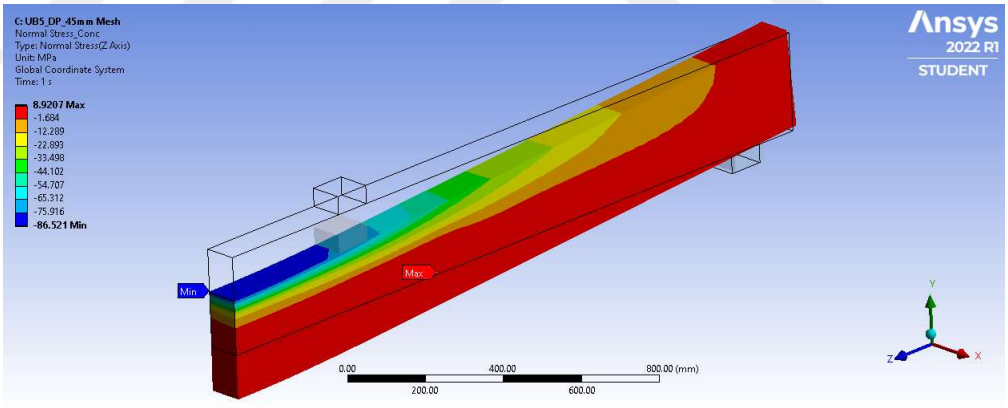
Figure 4.8 Coupled damage-plasticity microplane damage output, (a) Transformed compressive damage (COMP), (b) Split weight factor RW

Figure 4.9 are the normal stress color plots for the three methods mentioned above for the beam section at failure load. Figure 4.9(a) and 4.9(b) estimate identical results of maximum compression stress and maximum tensile stress of 8.9 MPa and 86 MPa

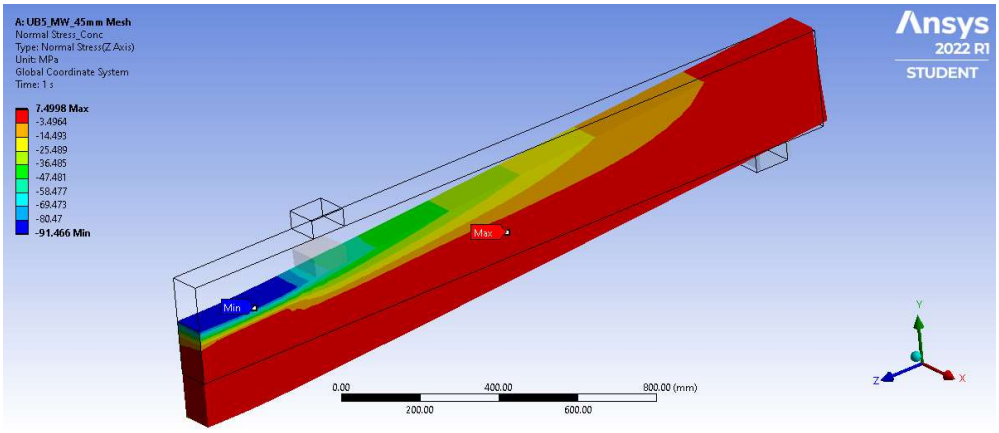
respectively. While the quarter color plot using the Menetrey Willam material model in Figure 4.9(c), shows maximum compression stress and maximum tensile stress of 7.5 MPa and 91.5 MPa respectively.



(a)



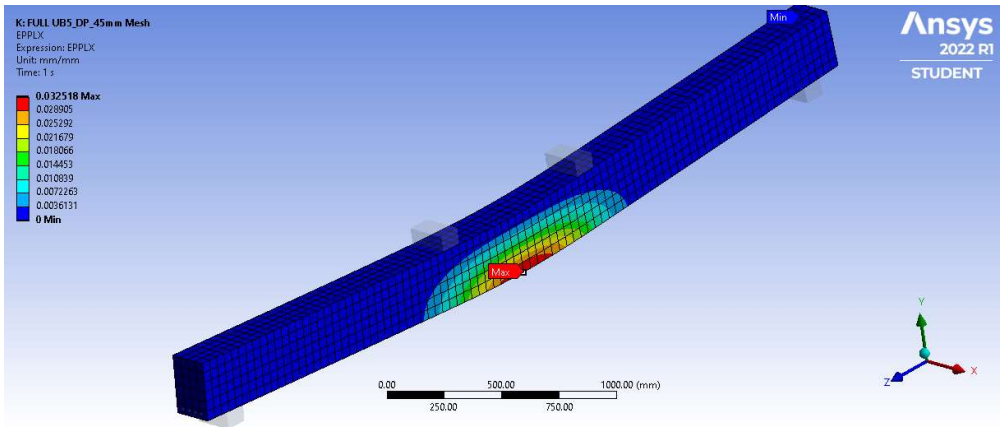
(b)



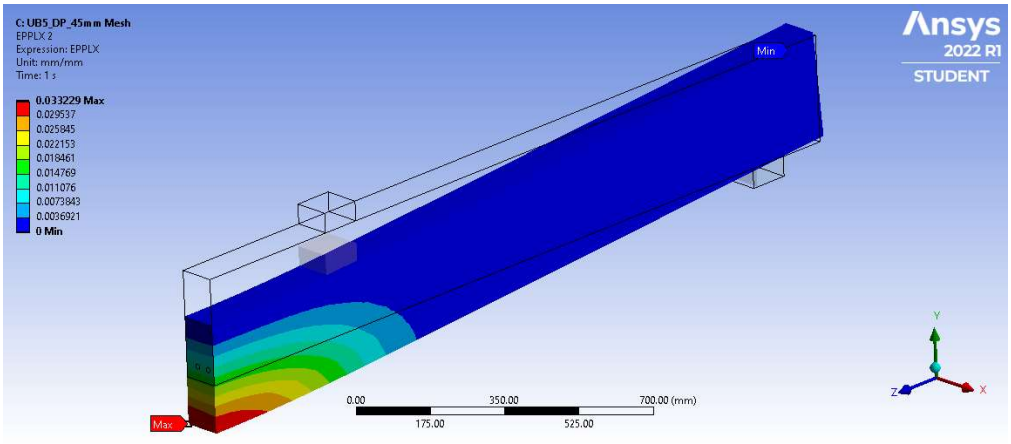
(c)

Figure 4.9 Normal stress color plot for U-B5 at failure load in MPa. (a) Full geometric ANSYS microplane, (b) Quarter geometric ANSYS microplane, (b) Quarter geometric ANSYS Mentrey Willam.

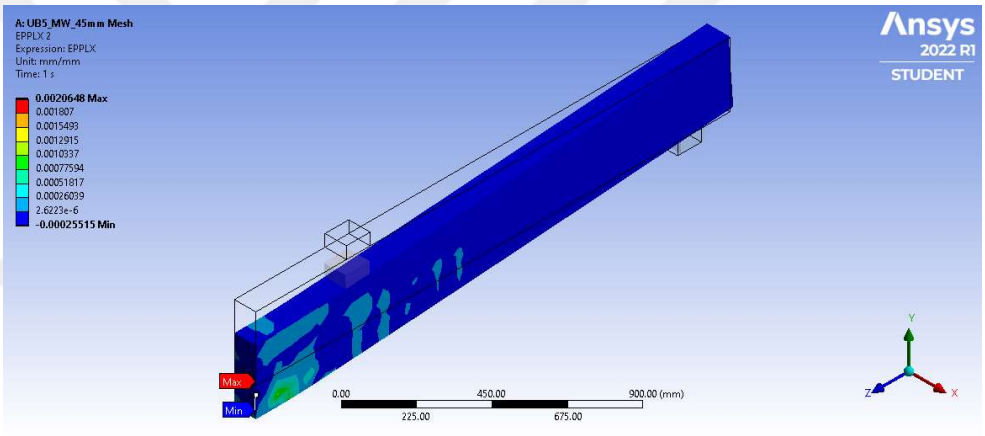
Figure 4.10 are the plastic strain color plots for the three methods mentioned above for the beam section at failure load. 45mm finite element mesh results are presented and discussed in this section. Figures 4.10(a) and 4.10(b) estimate similar results of an approximately maximum strain of 0.033. While the quarter color plot using the Menetrey Willam material model in Figure 4.10(c) shows a maximum strain of 0.00206. In this result, there is a big difference between the Microplane and Menetrey Willam results. Lastly, the color plot of Figure 4.10(a) and 4.10(b) can be compared to Figure 4.7(a), transformed total damage (TOTA). The color plot of Figures 4.10(a), 4.10(b), and 4.7(a) are very similar.



(a)



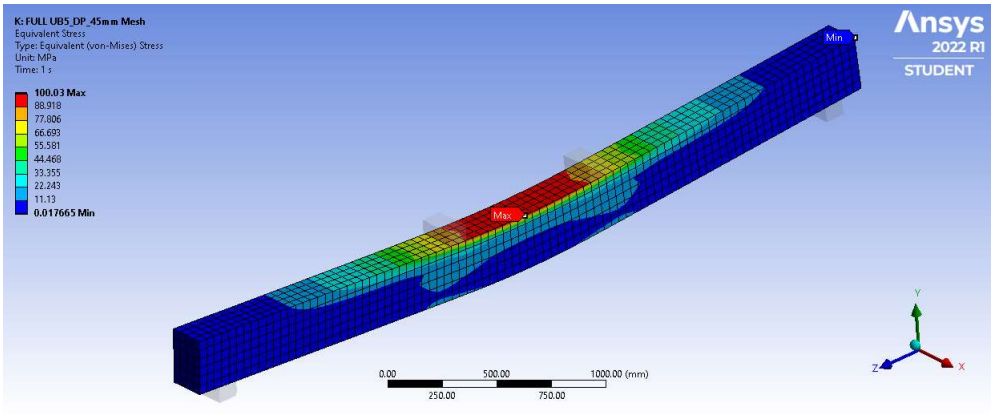
(b)



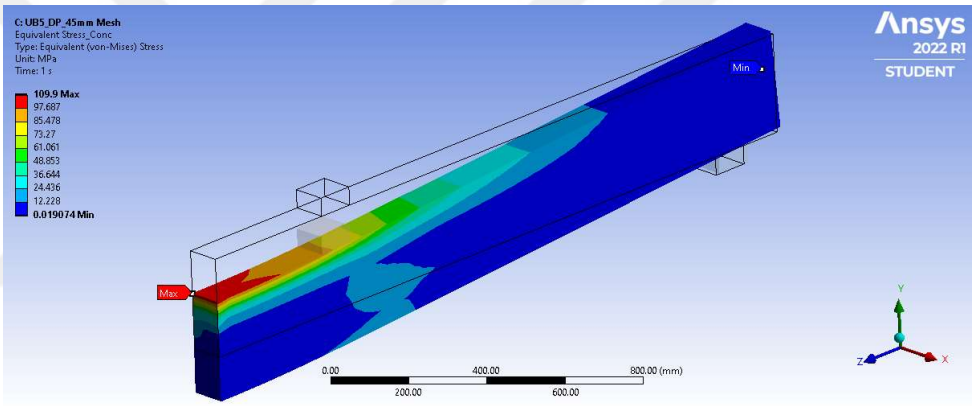
(c)

Figure 4.10 Plastic strain color plot for U-B5 at failure load in MPa. (a) full geometric ANSYS microplane, (b) quarter geometric ANSYS microplane (b) quarter geometric ANSYS Mentrey Willam

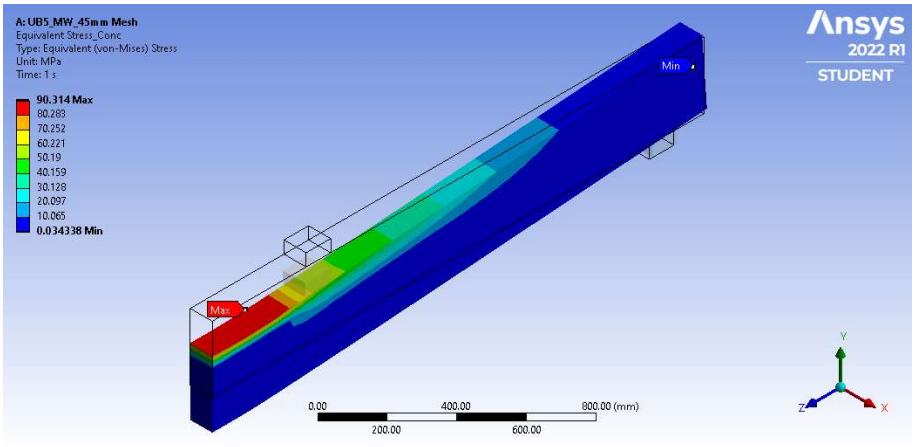
Figure 4.11 are the equivalent von-Mises stress color plots for the three methods mentioned above for the beam section at failure load. 45mm finite element mesh results are discussed and presented. here. Figures 4.10(a), 4.10(b), and 4.10(c) estimate a maximum of 100 MPa, 109.9 MPa and 90.314 MPa respectively at failure load. These results are a bit similar with a variance of a maximum of 8%. These results show that UHPC compressive strength is significantly underutilized because the peak compressive strength of the UHPC used in the study is 193MPa.



(a)



(b)



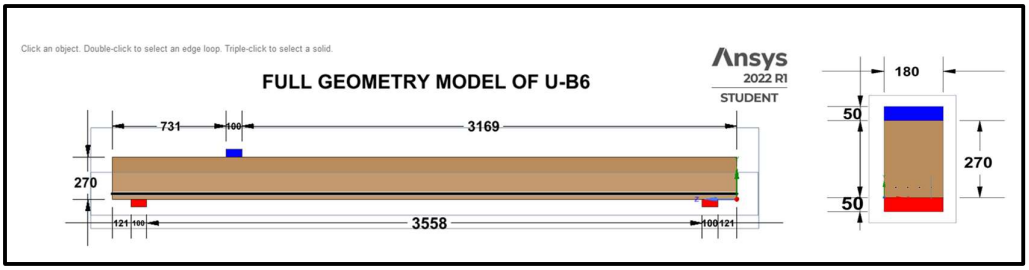
(c)

Figure 4.11 Equivalent (von-mises) Stress color plot for U-B5 at failure load in MPa. (a) full geometric ANSYS microplane, (b) quarter geometric ANSYS microplane (b) quarter geometric ANSYS Mentrey Willam.

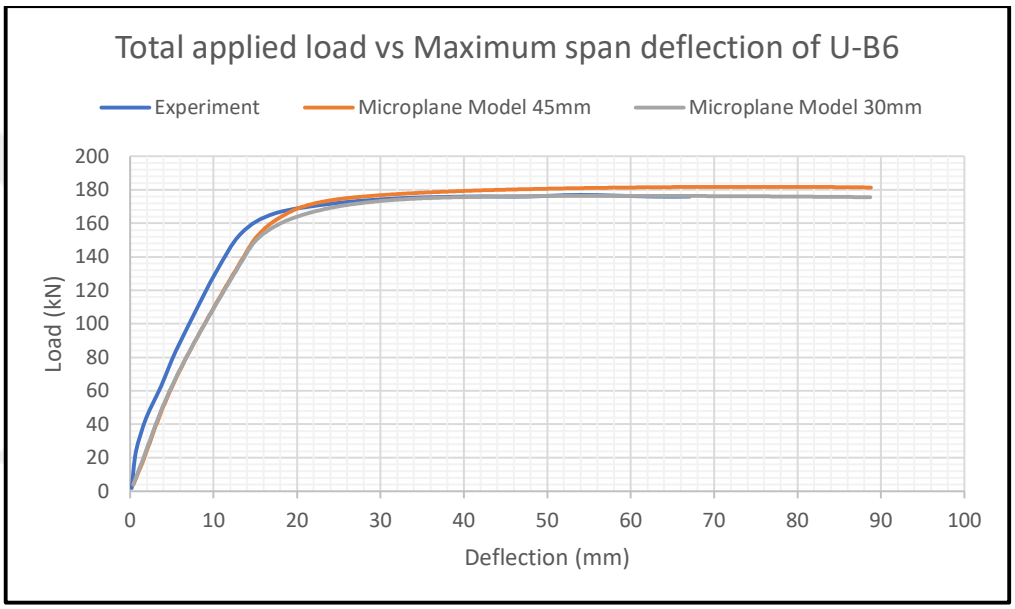
4.2 Presentation of beam U-B6 ANSYS results with experimental data

Figure 4.12(b) is a combined plot of the total applied load (kN) on the 2 steel plates at the top of the U-B6 beam vs the midspan deflection at the bottom of the beam. It contains result plots of U-B6 using the Microplane material model and the experimental plot data. U-B6 has a dimension of 180 mm x 270 mm x 4000 mm and consists of 4 tensile reinforcements at the bottom section of the beam. The microplane material model is used to analyze the full geometry section of U-B6. U-B6 is tested on ANSYS by discretization of the beam problem using (30 and 45) mm hexagonal finite element mesh. For the full and quarter geometry model structural analysis, the beam was tested using the 3-point load test to capture the shear behavior of the beam and it was evaluated by using 45mm and 30 mm finite element mesh sizes. Equal displacement loading of 72 mm was applied on the 2 steel plates at the top of the U-B6 beam. Displacement support specification of 0 mm in the x, y, and z direction was applied under one of the support steels plates to stimulate pinned support, while a displacement support specification of Free, 0 mm, and Free in the x, y, and z direction respectively was applied on the other steel plate support to stimulate roller support.

The experimental plot in Figure 4.12(b) recorded a maximum applied load and midspan deflection of 177 kN and 83 mm respectively. Under a 72 mm displacement loading at the top of the beam, a maximum applied load and maximum deflection of 181 kN and 88.81 mm are estimated by using the microplane material model for the 45mm finite element mesh size. While a maximum applied load and maximum deflection of 176.4 kN and 88.71 mm are estimated by using the microplane material model for the 30mm finite element mesh size. The load capacity of the beam reduced from 181 kN to 176 kN for the 45 mm and 30 mm finite element mesh size respectively. Overall, the shape of the load–deflection curves from ANSYS are very similar to the plot from the experimental research work. This shows the microplane model in ANSYS can be used to predict the shear behavior of reinforced UHPC beams.



(a)



(b)

Figure 4.12 Total applied load vs maximum span deflection of U-B6, (a) Full geometric U-B6 model, (b) Combined plot of experimental and full geometric ANSYS microplane model plot.

Figure 4.13 are combined plots of the total applied load (kN) on the 2 plates at the top of the U-B6 beam vs the total strain in the tensile reinforcement at the bottom section of the beam for 30 and 45mm finite element mesh. They are results plot of the full geometry structural analysis on ANSYS using the microplane model. Under a 72 mm displacement loading at the top of the beam a total strain of 0.049332 & 0.0527 is estimated for 45mm and 30mm finite element mesh size at the end of loading. However, this result could not be validated because of the absence of experimental data.

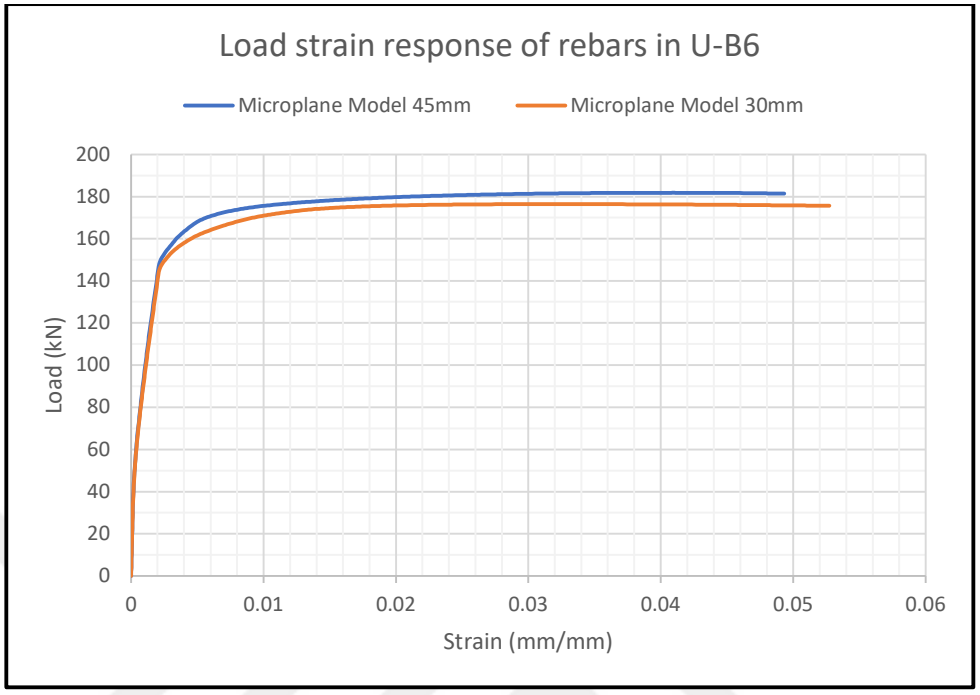


Figure 4.13 Load strain response of rebars in U-B6, ANSYS microplane model plot

Figure 4.14 is a load-deflection color plot of U-B6 result obtained by using full geometry structural analysis on ANSYS (microplane material model). 45 mm finite element mesh result is presented and discussed. This plot estimates a maximum midspan deflection of 88.81 mm.

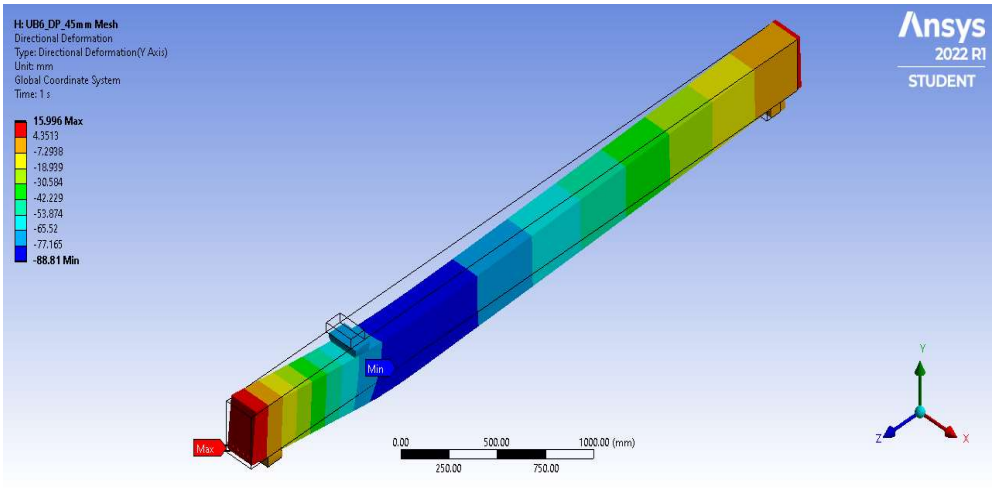


Figure 4.14 U-B6 deflection color plot at failure load, full geometric microplane model plot.

Figure 4.15 is the total strain color plot using full geometry structural analysis on ANSYS for the tensile reinforcements provided in the beam section. It predicts a maximum total strain of 0.049332 mm/mm. The Microplane material model plot shows that at least 20% of the length of the tensile reinforcements at the bottom section yielded.

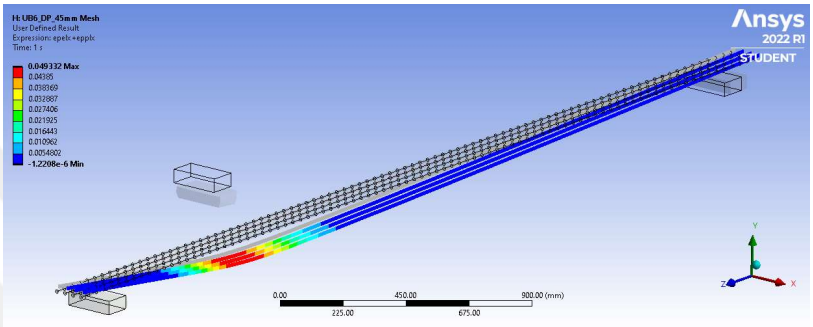


Figure 4.15 Total strain color plot for tensile reinforcements at failure load in mm/mm, full geometric ANSYS microplane

Figure 4.16 is the equivalent von-Mises stress color plot using full geometry structural analysis on ANSYS for the tensile reinforcements provided in the beam section. 45 mm finite element mesh result is presented here. It predicts a maximum total stress of 541.17 MPa for the full geometry (microplane). The Microplane material model plot also shows that at least 20% of the length of the tensile reinforcements at the bottom section is above the yield stress of the steel reinforcement (435 MPa).

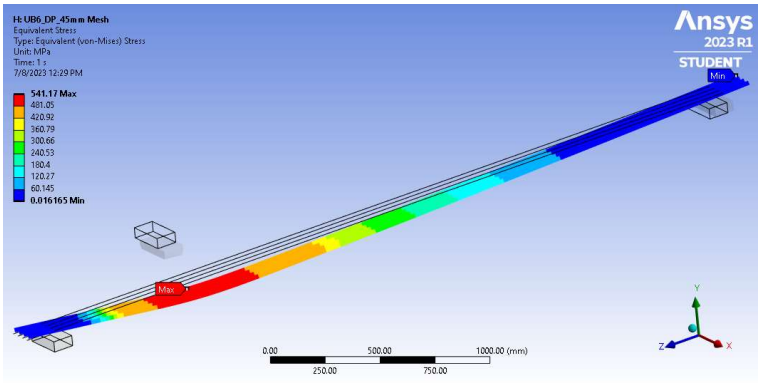
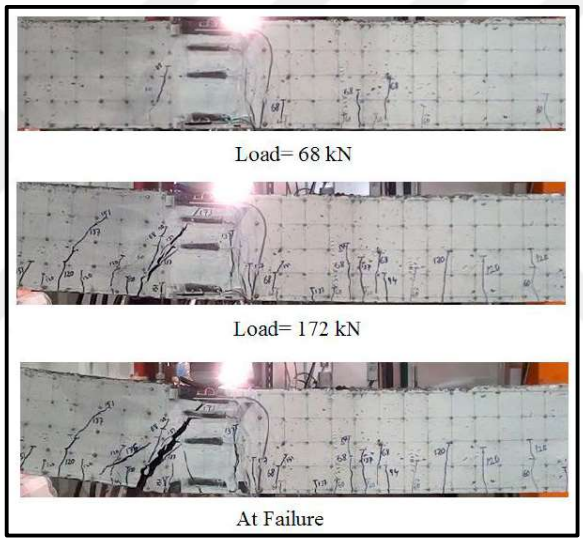
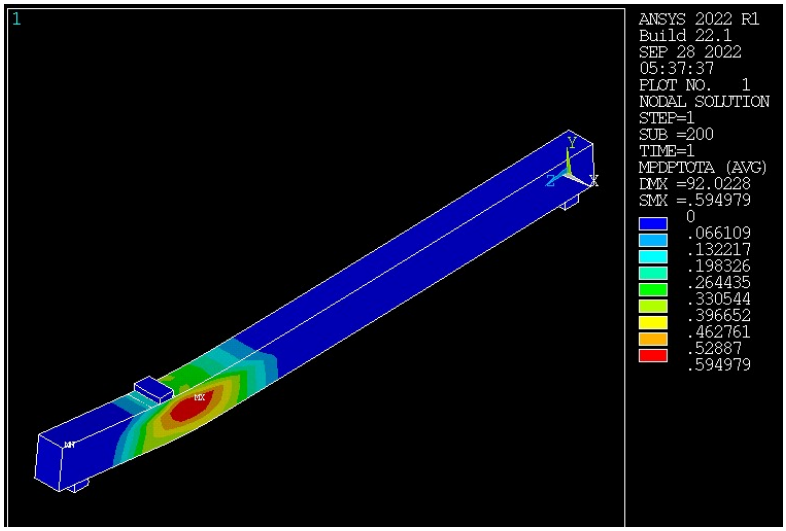


Figure 4.16 Equivalent von-Mises stress color plot for tensile reinforcements at failure load in MPa, full geometric ANSYS microplane (U-B6)

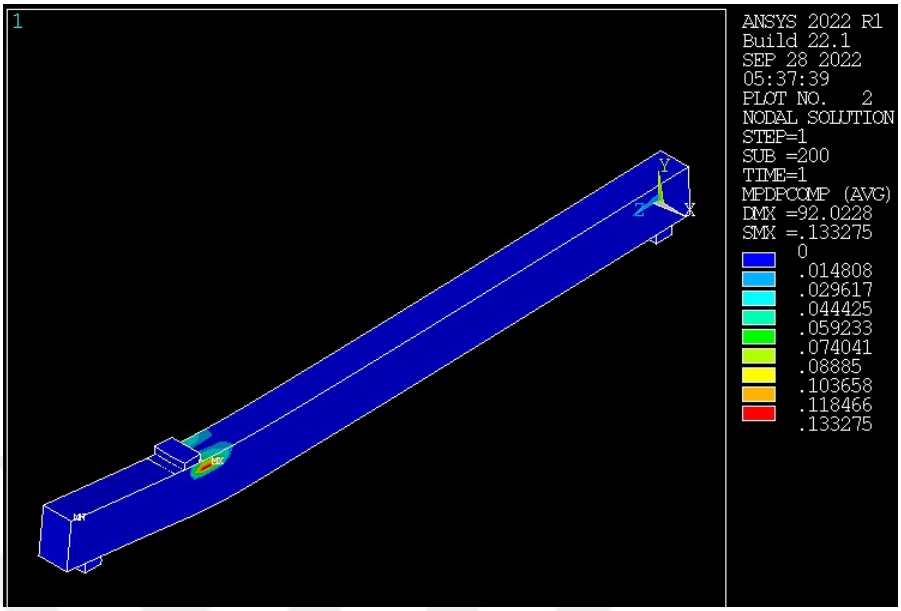
Figures 4.17 and 4.18 are color plot quantities used to show damage in the material by using the microplane model. Figures 4.17(a) shows the experimental diagonal shear crack pattern in the beam specimen at different loading stages. The full geometry of U-B6 was used for the color plot result. Figures 4.17(b), 4.17(c), 4.18(a), and 4.18(b) represent the transformed total damage TOTA, transformed tensile damage TENS, transformed compressive damage COMP, and the split weight factor RW respectively. Figure 4.17c shows no tension damage in the beam section overall. Figure 4.18a shows compression damage at the location of the applied load on the top of the beam.



(a)

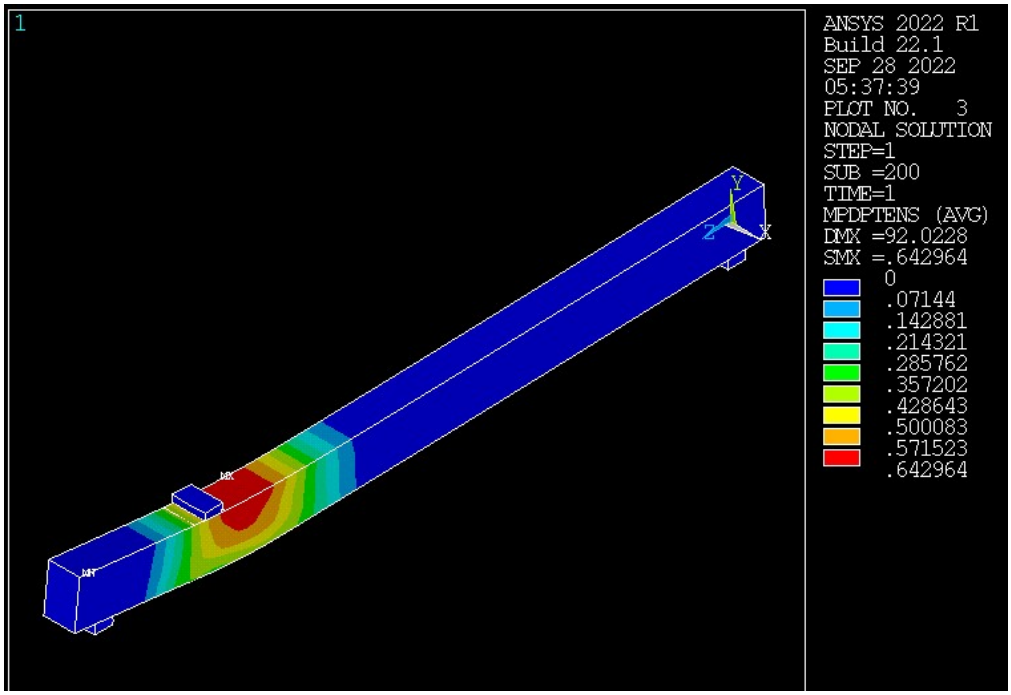


(b)

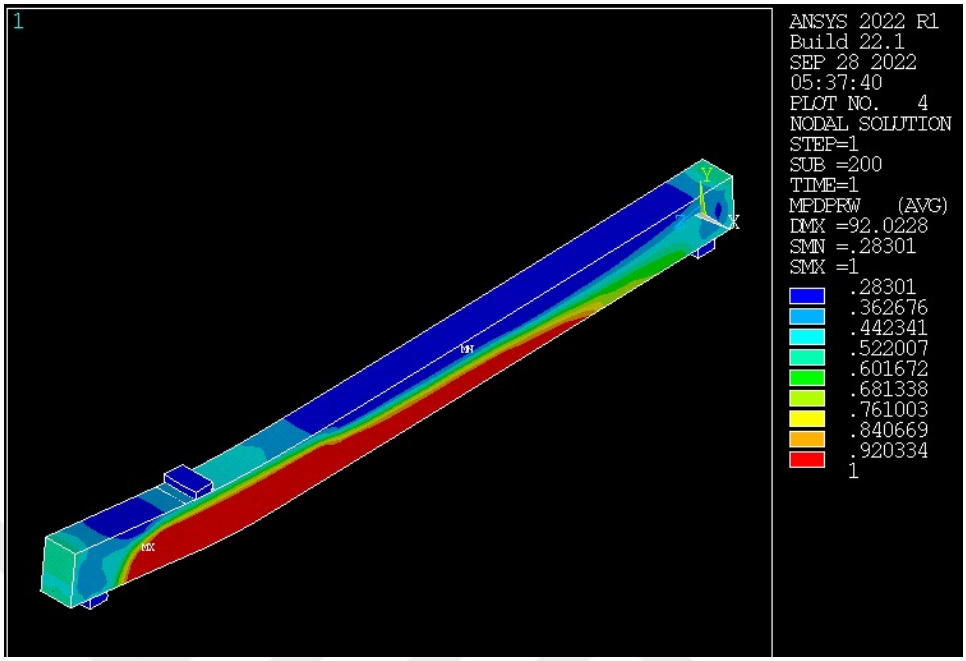


(c)

Figure 4.17 Coupled damage-plasticity microplane damage output – U-B6, (a) Experimental crack pattern, (Solhmirzaei & Kodur, 2017) (b) Transformed total damage TOTA, (c) Transformed tensile damage TENS.



(a)



(b)

Figure 4.18 Coupled damage-plasticity microplane damage output, (a) Transformed compressive damage COMP, (b) Split weight factor RW.

Figure 4.19 is the normal stress color plot for the full geometry microplane ANSYS analysis for the beam section at failure load. Figure 4.19 estimates the results of maximum tension stress and maximum compression stress of 10.029 MPa and 98.785 MPa respectively.

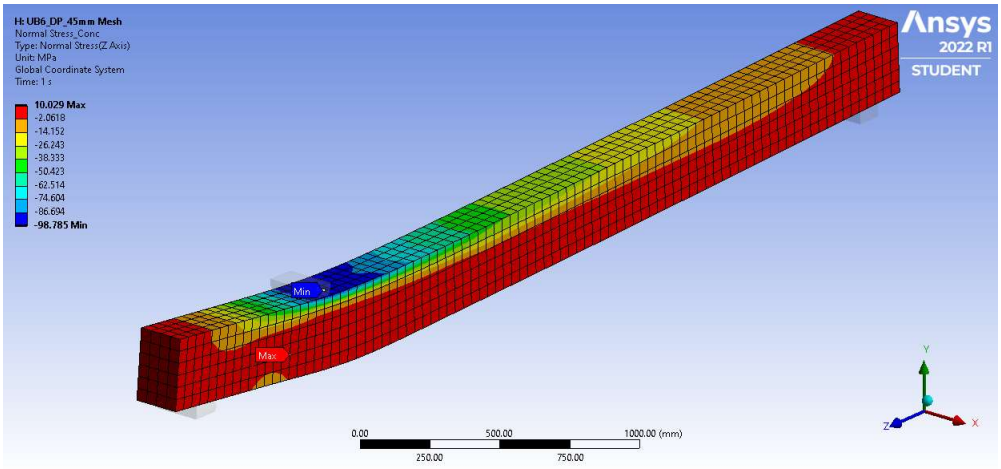


Figure 4.19 Normal stress color plot for U-B6 at failure load in MPa, full geometric ANSYS microplane

Figure 4.20 is the plastic strain color plots for the full geometry microplane ANSYS analysis for the beam section at failure load. 45mm finite element mesh is presented. Figure 4.20 estimates a maximum strain of 0.0469. This plastic strain color plot of Figure 4.20 can be compared to Figure 4.17b, transformed total damage (TOTA). Color plot Figure 4.20, and 4.17b are very similar.

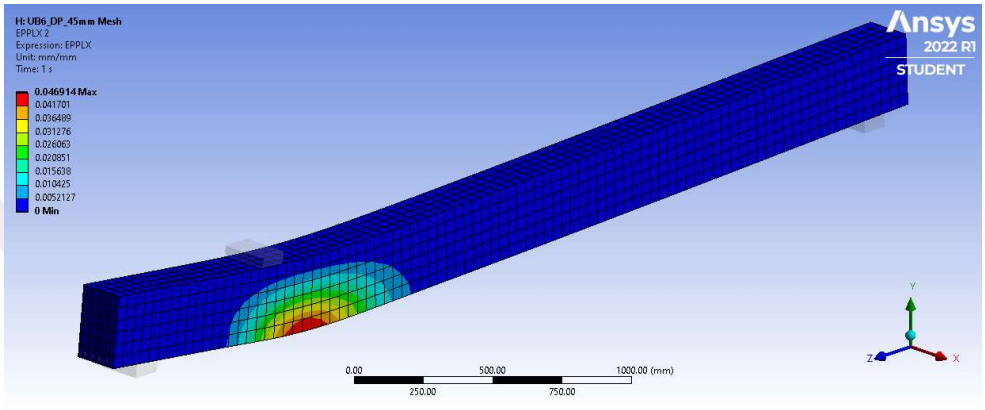


Figure 4.20 Plastic strain color plot for U-B6 at failure load in MPa, full geometric ANSYS microplane

Figure 4.21 is the equivalent von-Mises stress color plot for the full geometry microplane ANSYS analysis for the beam section at failure load. Figure 4.21 estimates a maximum of 109.47 MPa respectively at failure load. This estimate shows that failure of the beam sample was not from the top of the beam because 109.47 MPa is less than the experimental compressive strength of UHPC.

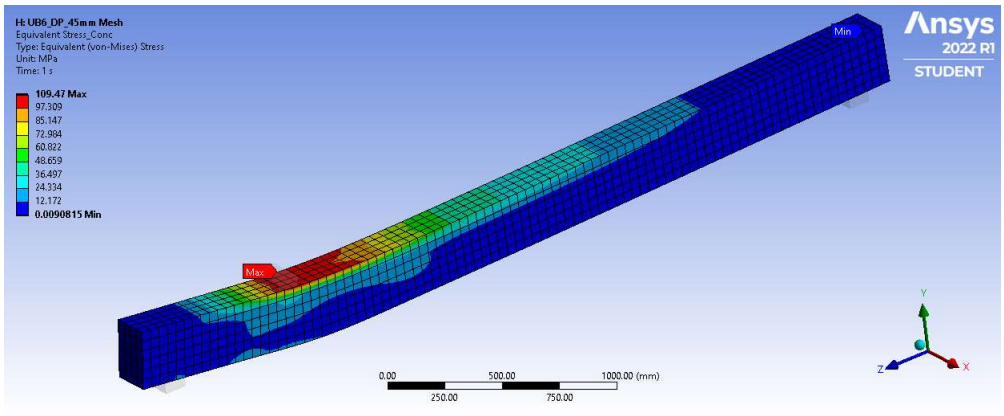


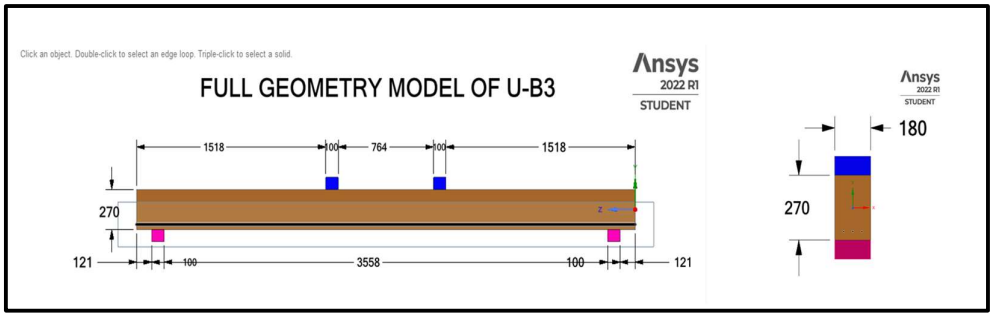
Figure 4.21 Equivalent von-Mises stress color plot for U-B6 at failure load in MPa, full geometric ANSYS microplane

4.3 Presentation of beam U-B3 ANSYS results with experimental data

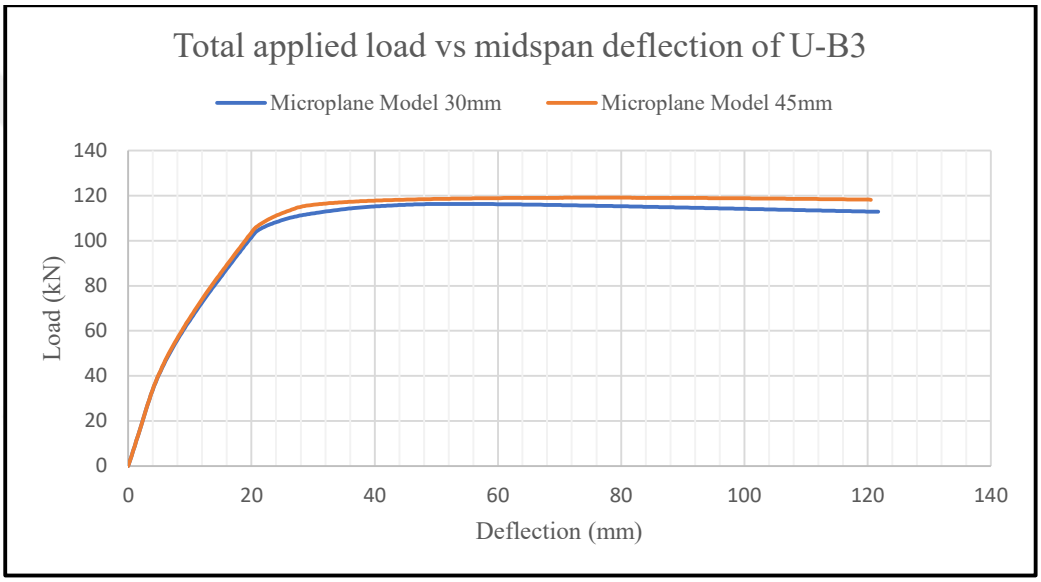
Figure 4.22(b) is a combined plot of the total applied load (kN) on the 2 steel plates at the top of the U-B3 beam vs the midspan deflection at the bottom of the beam by using 45 mm and 30 mm finite element mesh sizes. The reinforced UHPC beam U-B3 has a dimension of 180 mm x 270 mm x 4000 mm and consists of 3 tensile reinforcements at the bottom section of the beam as shown in Figure 4.22(a). The beam is analyzed using ANSYS by three methods. In the first method, the microplane material model is used to analyze the full geometry section of U-B3. A quarter geometry section is analyzed using the microplane material model and the Menetray Willam model in the second and third method respectively.

U-B3 is tested on ANSYS by discretization of the beam problem using 45 mm and 30 mm hexagonal finite element meshes. For the full and quarter geometry model structural analysis, the beam was tested using the 4-point load test to capture the flexural behavior of the beam. Equal displacement loading of 105 mm was applied on the 2 steel plates at the top of the U-B5 beam. A displacement support specification of 0 mm in the x, y, and z direction was applied under one of the support steel plates to stimulate pinned support, while a displacement support specification of Free, 0 mm, and Free in the x, y, and z direction was applied respectively on the other steel plate support to stimulate roller support.

Figure 4.22(b) are result plots of the full geometry structural analysis on ANSYS using the microplane model. Under a 105 mm displacement loading at the top of the beam, a maximum applied load and midspan deflection of 119.02 kN and 120.59 mm are estimated for the 45 mm finite element mesh size results. While 116.27 kN and 121.72 mm are estimated for the 30 mm finite element mesh size results.



(a)



(b)

Figure 4.22 Total applied load vs midspan deflection of U-B3, (a) U-B3 full geometry model, (b) Full geometric ANSYS microplane model plots.

Figure 4.23 is a combined plot of the total applied load (kN) on the 2 steel plates at the top of the U-B3 beam vs the total strain in the tensile reinforcement at the bottom section of the beam. It contains the resulting plots from the research work of Solhmirzaei & Kodur (2017) and finite element solution from the microplane material model. The microplane model is analyzed using 45 mm and 30 mm meshes. This finite element plot of the microplane model recorded a maximum total strain of 0.035273 and 0.038842 for the 45 mm and 30 mm finite element mesh sizes respectively. Under a 105 mm displacement loading at the top of the beam a total strain of 0.025 is estimated in experimental data plot. As already explained in previous section, the different in result may be due to the existence of microcracks and

imperfections of the beam specimen under investigation and from my assumptions used during the calibration of the parameters of the microplane material model. These results are similar to the experimental data. Overall, the ANSYS plot in Figure 4.23(b) matches well with the plot of the experimental data.

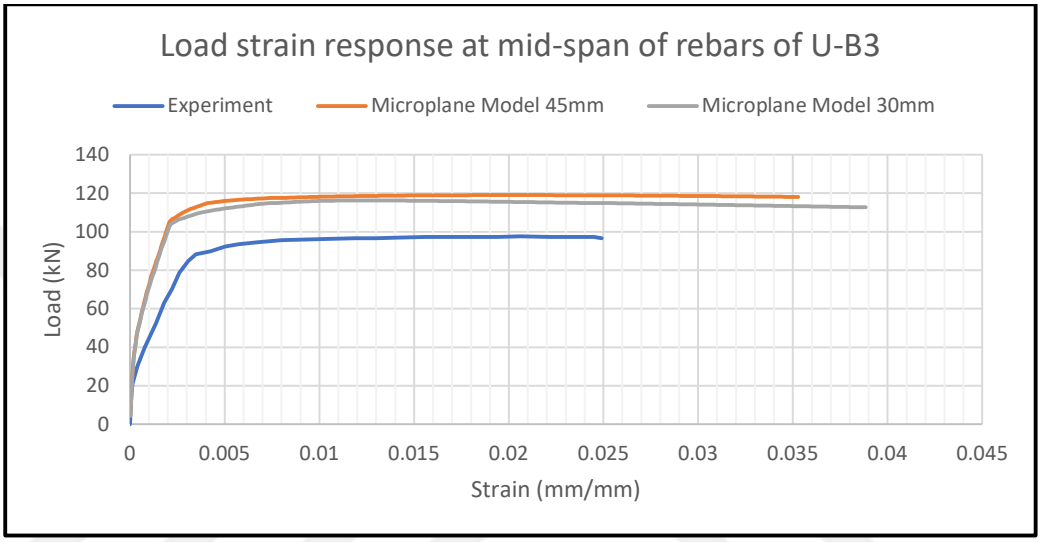
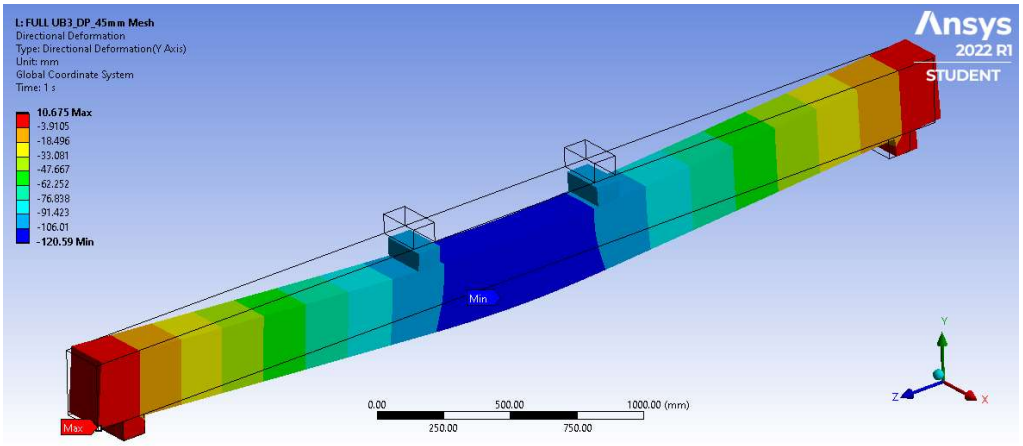
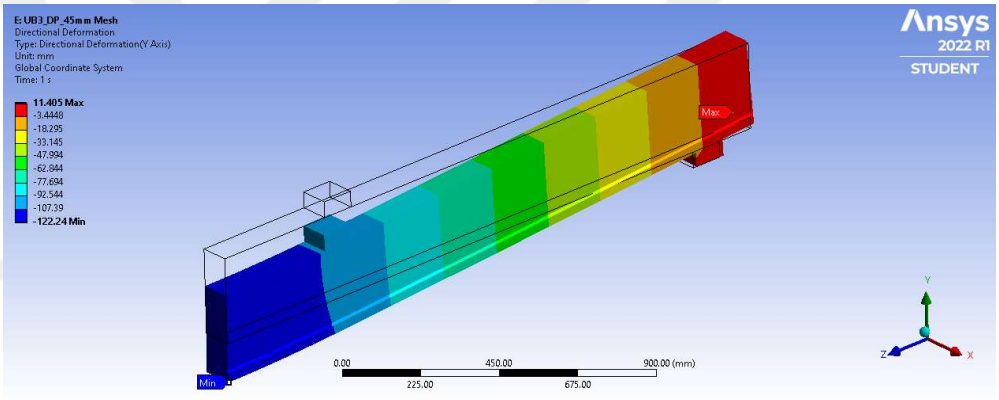


Figure 4.23 Load strain response at mid-span of rebars of U-B3, combined experimental and ANSYS microplane model plot.

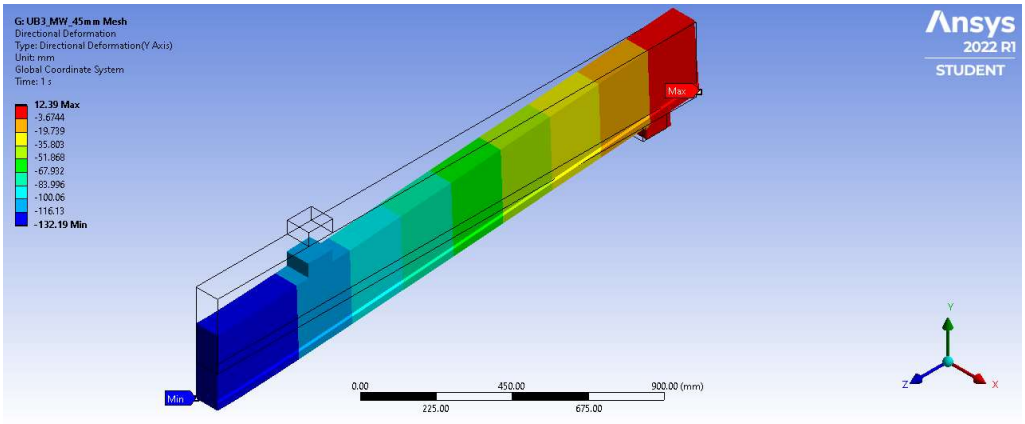
Figure 4.24 are three deflection color plots of U-B3 results obtained by using full and quarter geometry structural analysis on ANSYS with 45mm finite element mesh size. Figure 4.24(a) is the color plot using the full geometry model in ANSYS (microplane material model). This plot estimates a maximum midspan deflection of 120.59 mm. Figure 4.24(b) is a quarter geometry model analysis plot (microplane material model), and it predicts a maximum midspan deflection of 122.24 mm. Figure 4.24(c) is another quarter geometry model analysis plot (Menetrey Willam model) and it predicts a maximum midspan deflection of 132.19 mm. The Experimental mid-span deflection is 122 mm. Here the deflection estimates of both material models vary by about 15%.



(a)



(b)

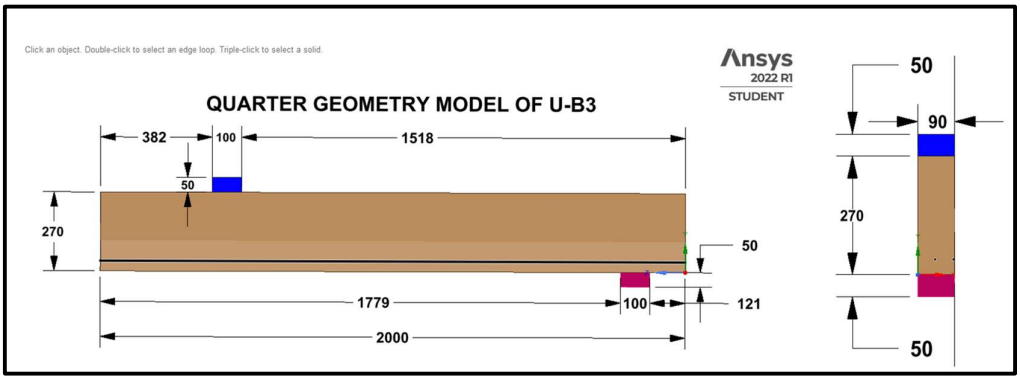


(c)

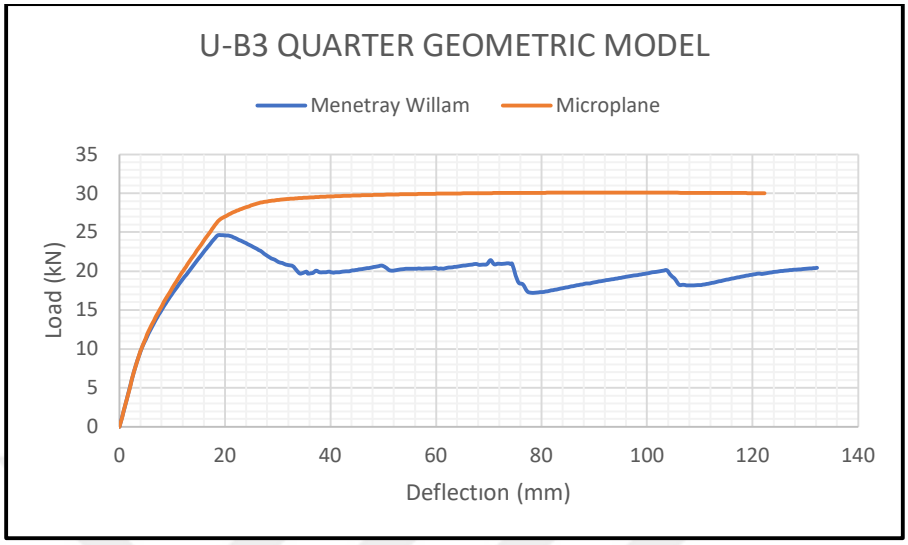
Figure 4.24 U-B3 deflection color plot at failure load. (a) Full geometric microplane model plot, (b) Quarter geometric microplane model plot, (c) Quarter geometric Menetrey Willam model plot.

Figure 4.25(b) are also plots of the applied load (kN) at the top of the U-B3 beam vs the midspan deflection at the bottom of the beam both for microplane and Menetrey-willam material models by using a quarter geometry model. 45 mm finite element result is presented and discussed for this geometric model. Under a 105mm displacement loading at the top of the beam, a maximum applied load and midspan deflection of 30.083 kN and 122.24 mm is estimated in Figure 4.25(b) for the microplane model. The total applied load on the beam is estimated as 30.083 x 4 = 120.332 kN. Under the same 105 mm displacement loading at the top of the beam, a maximum applied load and midspan deflection of 24.628 kN and 132.19 mm are estimated for the Menetrey-willam model. The total applied load on the beam is estimated as 24.628 x 4 = 98.512 kN.

Overall, the shapes of the load–deflection curve from ANSYS in Figure 4.25(b) are very similar to the plot from the experimental research work. However, as seen in Figure 4.25(b), the plot is irregular for the Mentray-willam model after the yielding point of the beam. The microplane performs better than the Menetrey-willam model because it gives a smooth curve. Overall, the microplane model and Menetrey Willam material model in ANSYS can be used to predict the flexure behavior of reinforced UHPC beams.



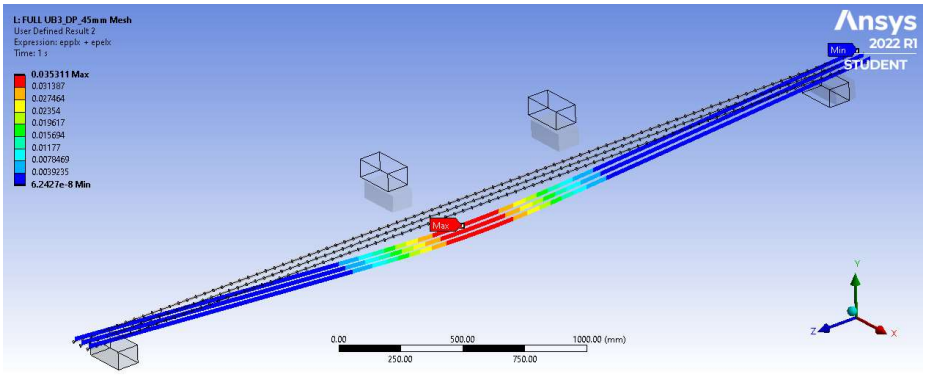
(a)



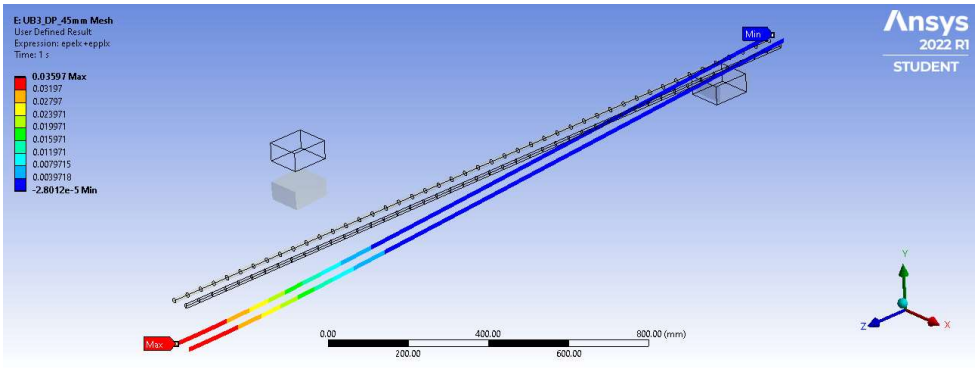
(b)

Figure 4.25 Total applied load vs midspan deflection of U-B3. (a) Quarter geometry on ANSYS (b) Quarter geometric ANSYS Microplane and Menetrey Willam model plot.

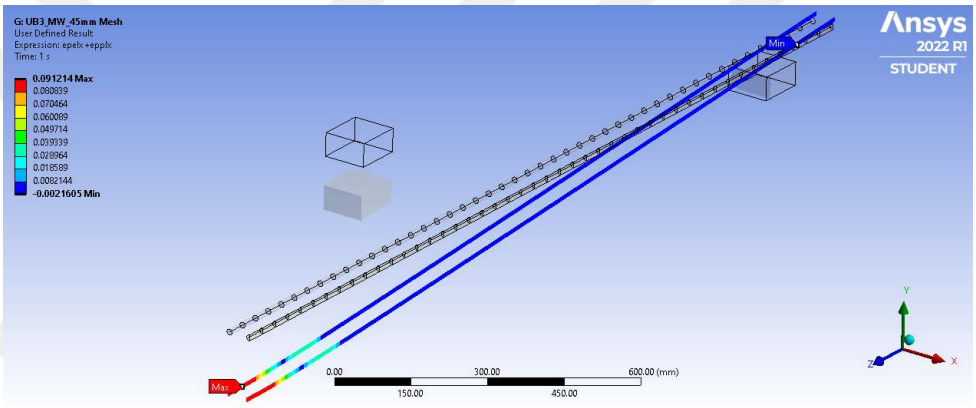
Figure 4.26 are the total strain color plots for the three methods mentioned above for the tensile reinforcements provided in the beam section by using the 45 mm finite element result. It predicts a maximum total strain of 0.035311, 0.03597, and 0.091214 mm/mm for the full geometry (microplane), and quarter geometry (microplane and Menetrey Willam) models respectively. The microplane material model plots in Figure 4.26(a) and (b) show that at least 35% of the length of the tensile reinforcements at the bottom section yielded. While just 12% of the length of the tensile reinforcements yielded in Figure 4.26(c) using the Menetrey Willam model.



(a)



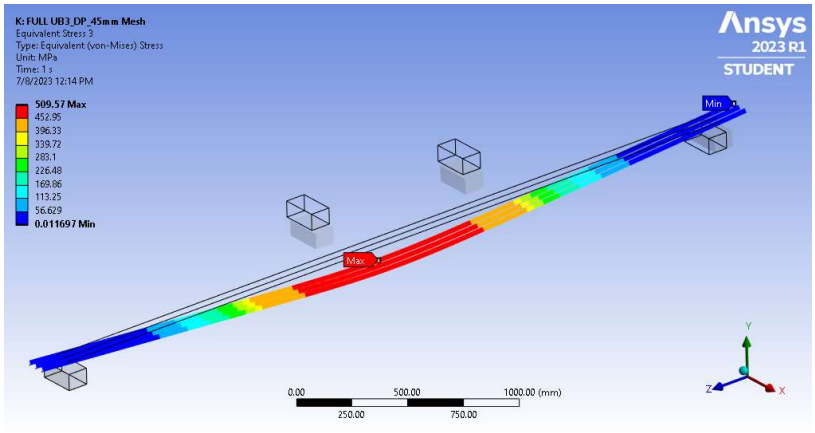
(b)



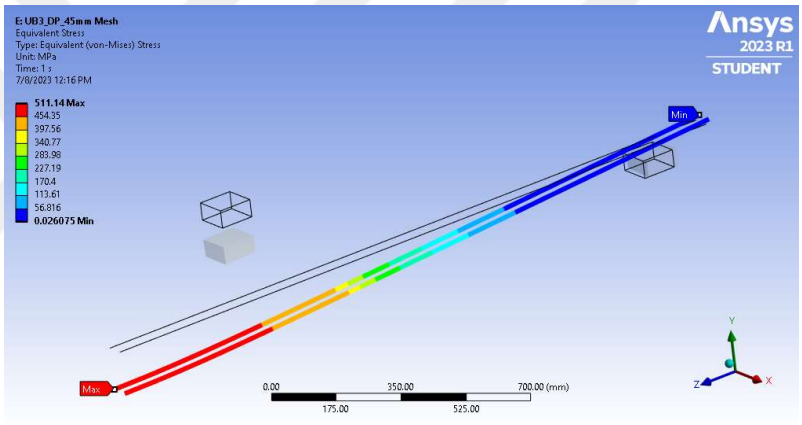
(c)

Figure 4.26 Total strain color plot for tensile reinforcements at failure load in mm/mm for U-B3. (a) full geometric ANSYS microplane, (b) Quarter geometric ANSYS microplane, (b) Quarter geometric ANSYS Mentrey Willam.

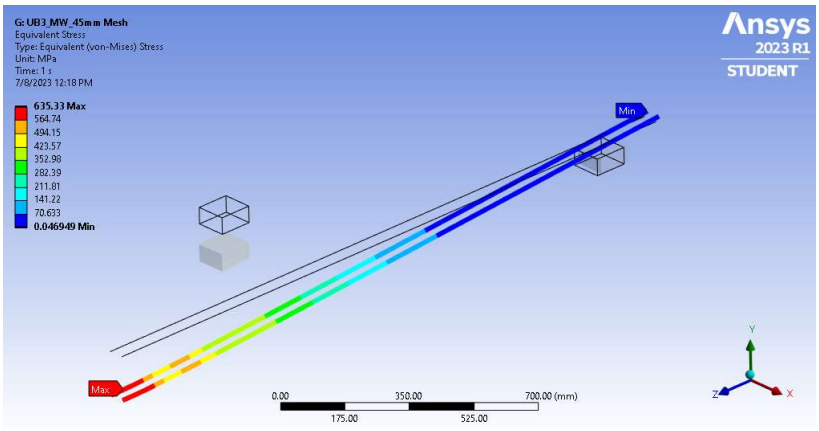
Figure 4.27 are the equivalent von-Mises stress color plots for the three methods mentioned above for the tensile reinforcements provided in the beam section by using the 45mm finite element result. It predicts a maximum total stress of 509.57, 511.14, and 635.33 MPa for the full geometry (microplane), quarter geometry (microplane), and Menetrey Willam model respectively. The Microplane material model plots in Figure 4.6(a) and (b) show that at least 35% of the length of the tensile reinforcements at the bottom section is above the yield stress of the steel reinforcement (435MPa). While just 12% of the length of the tensile reinforcements yielded in Figure 4.5(c) using the Menetrey Willam model.



(a)



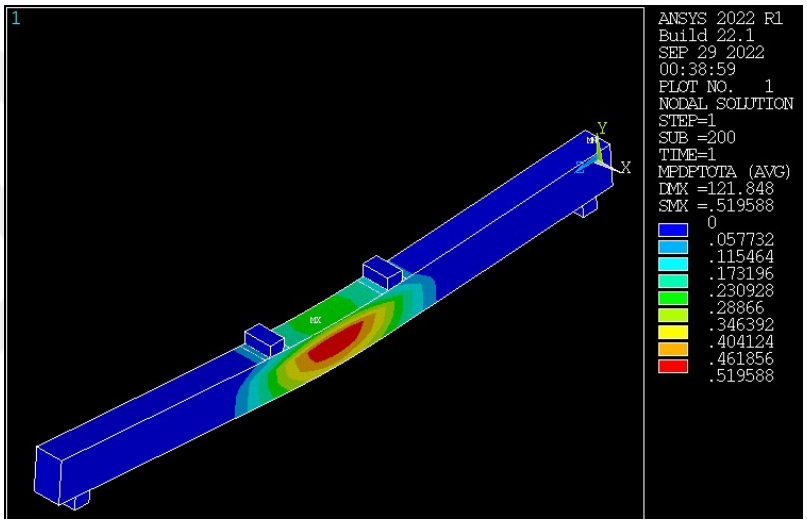
(b)



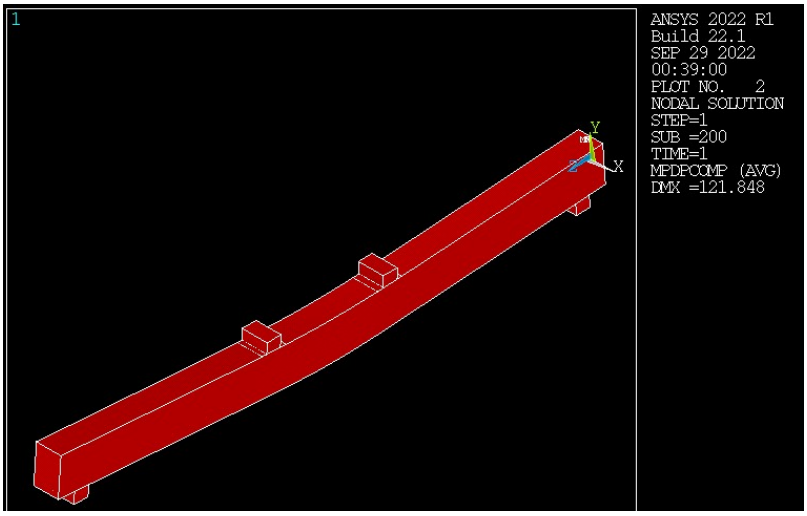
(c)

Figure 4.27 Equivalent (von-Mises) stress color plot for tensile reinforcements at failure load in MPa for U-B3. (a) Full geometric ANSYS microplane, (b) Quarter geometric ANSYS microplane (b) Quarter geometric ANSYS Mentrey Willam.

Figures 4.28 and 4.29 are color plot quantities used to denote damage in the material by using the microplane model. The full geometry of U-B3 was used for the color plot result. Figures 4.26(a), 4.28(b), 4.29(a), and 4.29(b) represent the transformed total damage TOTA, transformed tensile damage TENS, transformed compressive damage COMP, and the split weight factor RW respectively. Figure 4.28(b) shows that 100% of the beam section is already damaged in tension at the failure load. Figure 4.29a shows compression damage at the midspan section of the beam.

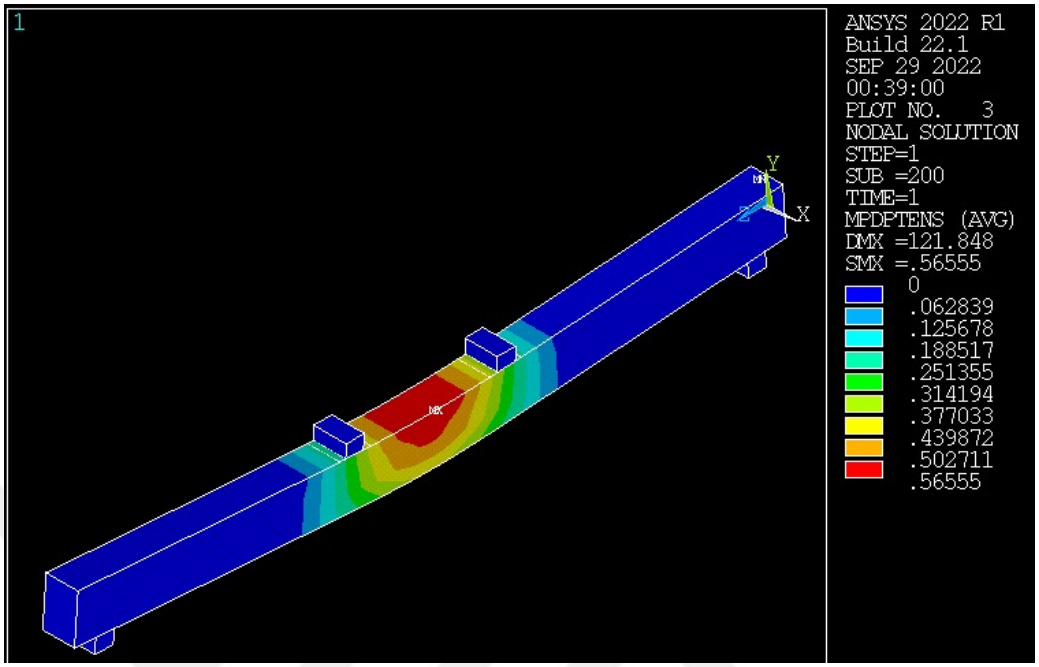


(a)

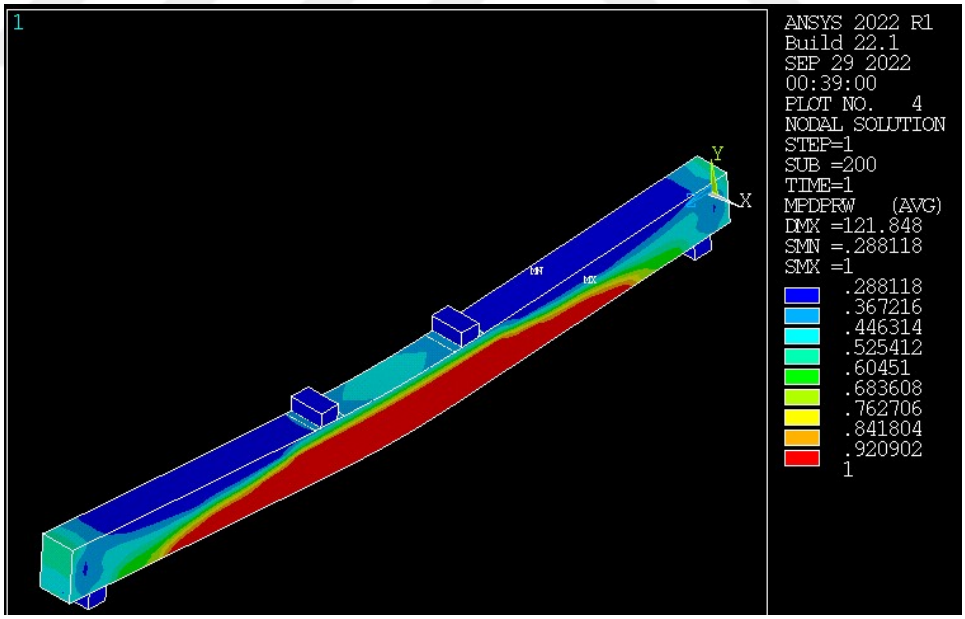


(b)

Figure 4.28 Coupled damage-plasticity microplane damage output for U-B3, (a) Transformed total damage TOTA, (b) Transformed tensile damage TENS.



(a)

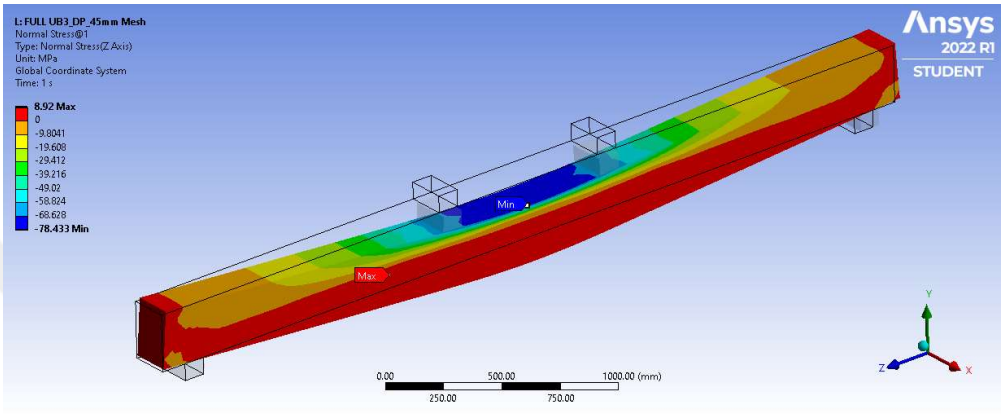


(b)

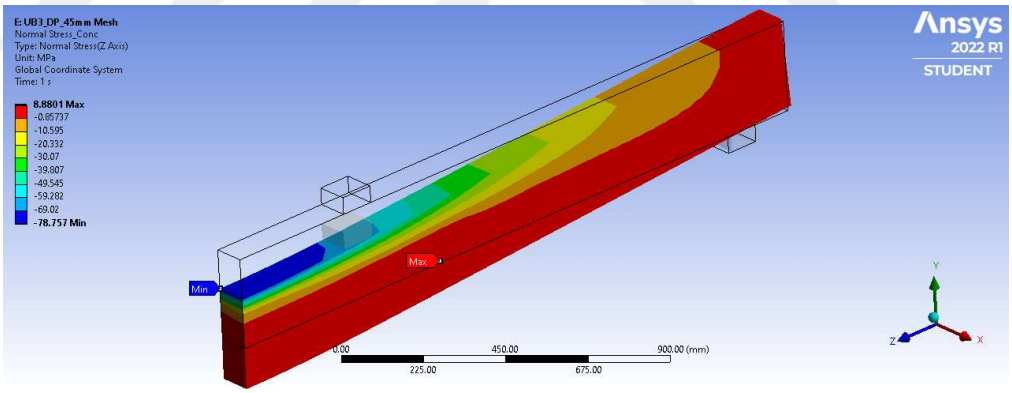
Figure 4.29 Coupled damage-plasticity microplane damage output for U-B3, (a) Transformed compressive damage COMP, (b) Split weight factor RW.

Figure 4.30 are the normal stress color plots for the three methods mentioned above for the beam section at failure load by using the 45mm finite element results. Figure

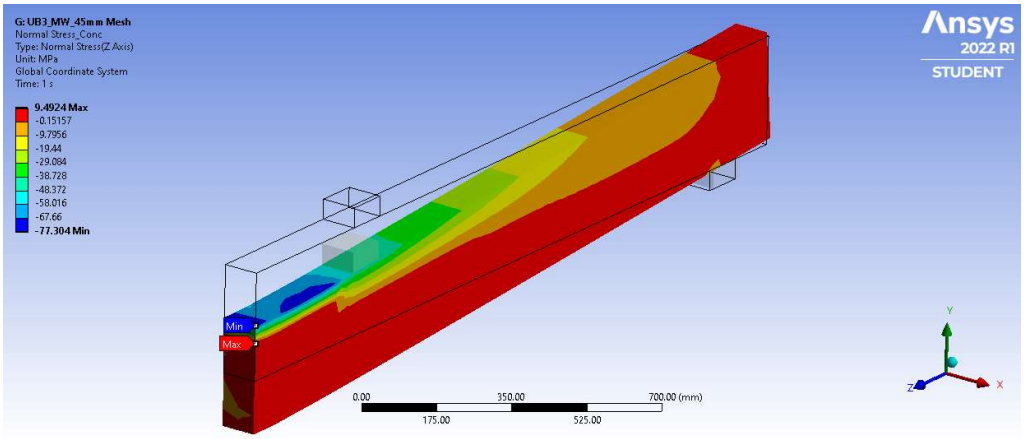
4.30(a) and 4.30(b) estimate identical results of maximum tension stress and maximum compressive stress of 8.9 MPa and 78.8 MPa respectively. While the Menetrey Willam material model in Figure 4.30c, the quarter color plot shows maximum tensile stress and maximum compressive stress of 9.4924 MPa and 77.304 MPa respectively.



(a)



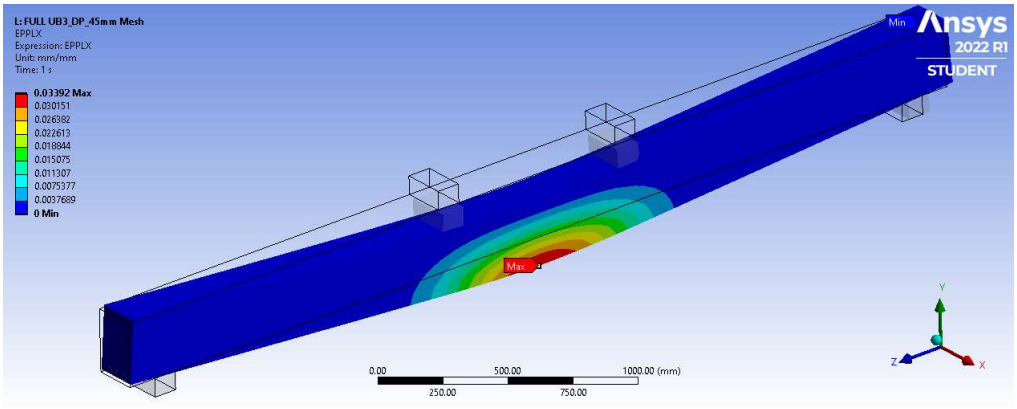
(b)



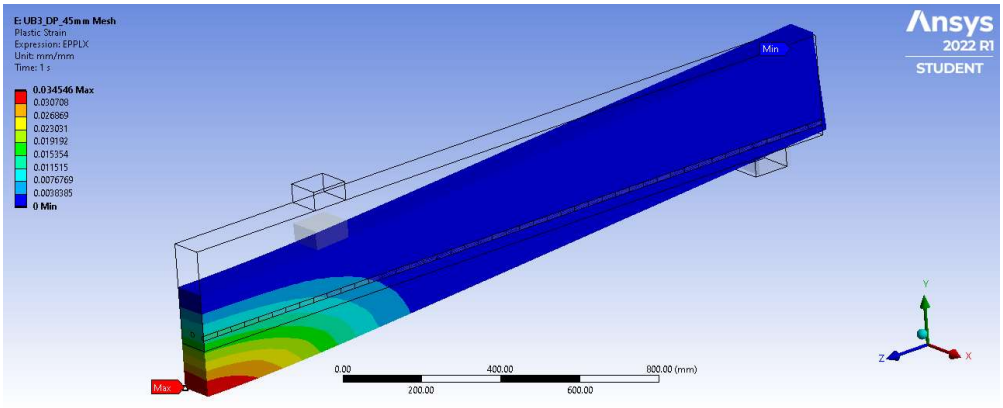
(c)

Figure 4.30 Equivalent (von-Mises) stress color plot for U-B3 at failure load in MPa. (a) Full geometric ANSYS microplane, (b) Quarter geometric ANSYS microplane (c) Quarter geometric ANSYS Menetrey Willam

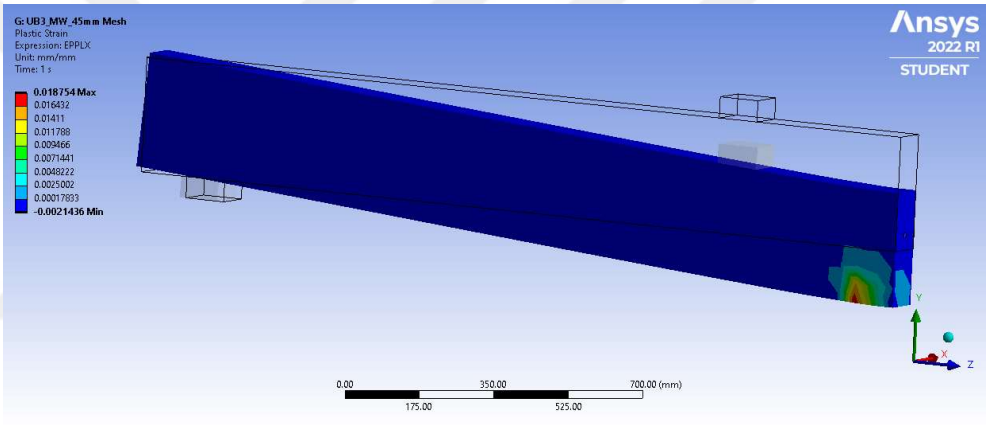
Figure 4.31 are the plastic strain color plots for the three methods mentioned above at failure load. Figures 4.31(a) and 4.31(b) estimate similar results of 0.03392 and 0.034546 maximum strains respectively. While the Menetrey Willam material model in Figure 4.31c, the quarter color plot shows a maximum strain of 0.0018754. In this result, there is a big difference between the Microplane and Menetrey Willam results. Lastly, the color plot of Figure 4.31(a) and 4.31(b) can be compared to Figure 4.28(a), transformed total damage (TOTA). The color plot in Figures 4.31(a) and 4.31(b) are very similar to Figure 4.28(a).



(a)



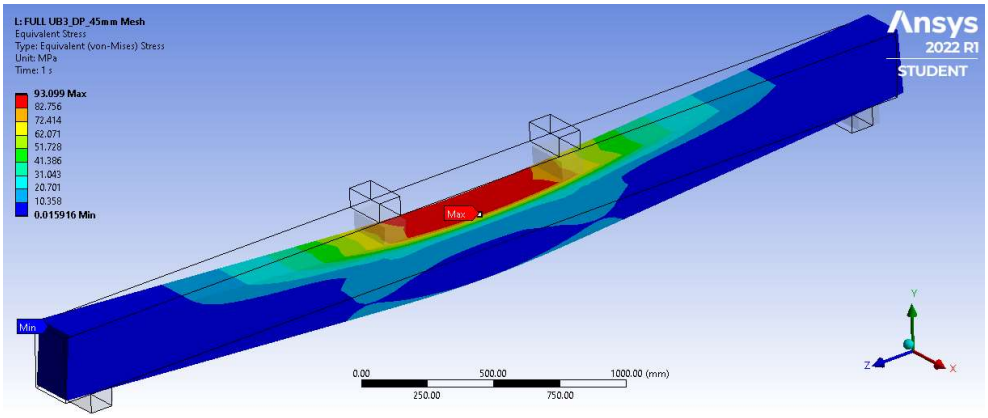
(b)



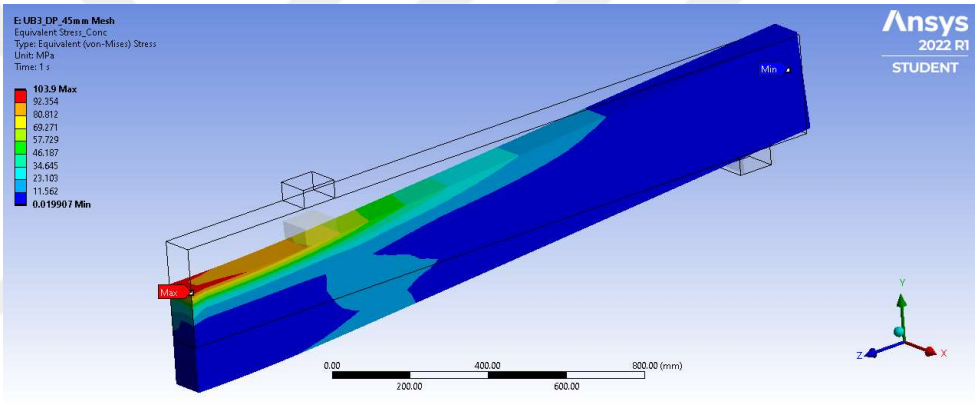
(c)

Figure 4.31 Plastic strain color plot for U-B3 at failure load in MPa. (a) Full geometric ANSYS microplane, (b) Quarter geometric ANSYS microplane (b) Quarter geometric ANSYS Mentrey Willam

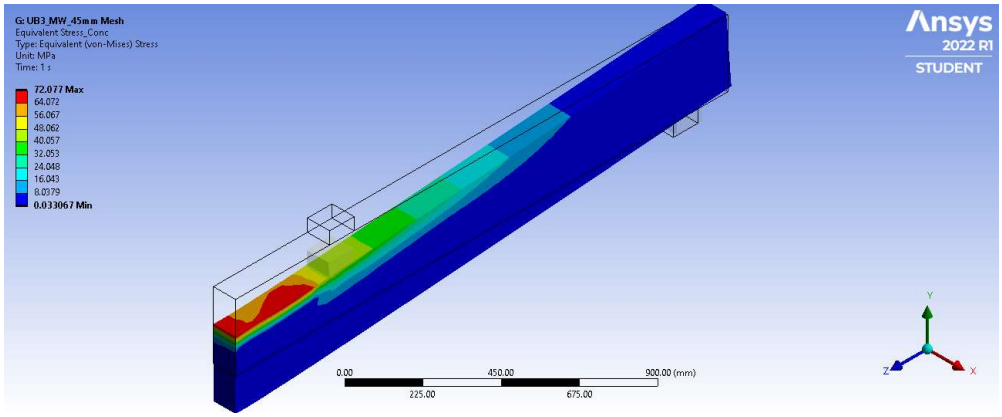
Figure 4.32 are the equivalent von-Mises stress color plots for the three methods mentioned above at failure load. Figures 4.32(a), 4.32(b), and 4.32(c) estimate a maximum stress of 93.099 MPa, 103.9 MPa and 72.077 MPa respectively at failure load. These results are a bit similar with a variance of a maximum of 25%.



(a)



(b)



(c)

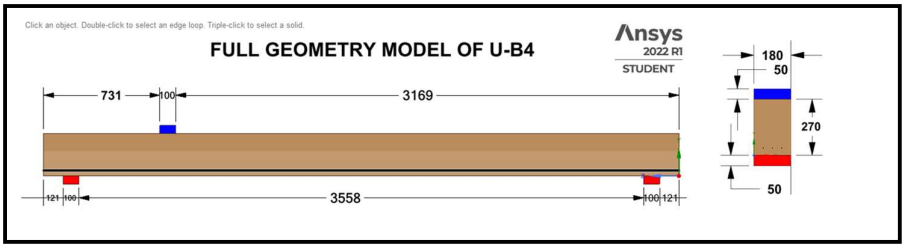
Figure 4.32 Equivalent (von-mises) stress color plot for U-B3 at failure load in MPa. (a) Full geometric ANSYS microplane, (b) Quarter geometric ANSYS microplane (b) Quarter geometric ANSYS Menetrey Willam

4.4 Presentation of beam U-B4 ANSYS results with experimental data

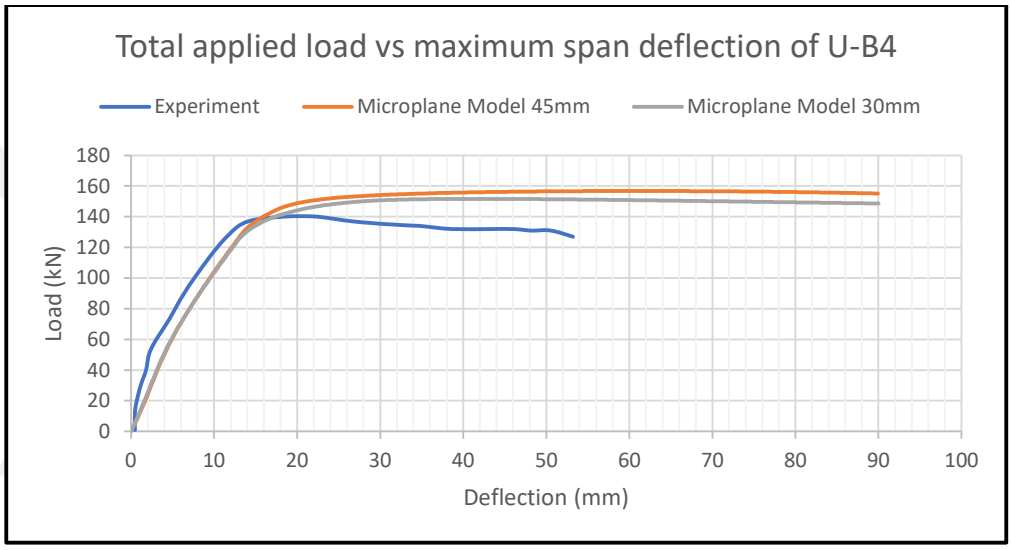
Figure 4.33(b) is a combined plot of the total applied load (kN) on the 2 steel plates at top of the U-B4 beam vs the maximum span deflection at the bottom of the beam. It contains data for both the experiment and finite element results by using the microplane model (30mm and 45mm finite element meshes). U-B4 has a dimension of 180 mm x 270 mm x 4000 mm and consists of 3 tensile reinforcements at the bottom section of the beam as shown in figure 4.33(a). The microplane material model is used to analyze the full geometry section of U-B4.

U-B4 is tested on ANSYS by discretization of the beam problem using 45mm and 30mm hexagonal finite element meshes. For the full and quarter geometry model structural analysis, the beam was tested using the 3-point load test to capture the shear behavior of the beam. Equal displacement loading of 72 mm was applied on the 2 steel plates at the top of the U-B6 beam. The displacement support specification of 0 mm in the x, y, and z direction was applied under one of the support steel plates to stimulate pinned support, while a displacement support specification of Free, 0 mm, and Free in the x, y, and z direction respectively was applied on the other steel plate support to stimulate roller support.

The experimental plot recorded a maximum applied load and maximum span deflection of 140 kN and 53 mm respectively. Under a 72 mm displacement loading at the top of the beam, a maximum applied load and midspan deflection of 156.76 kN and 89.927 mm are estimated for the 45mm mesh result in Figure 4.33(b). While a maximum applied load and midspan deflection of 151.64 kN and 89.999 mm are estimated for the 30 mm mesh result in Figure 4.33(b). Overall, the shapes of the load–deflection curve from ANSYS is very similar to the plot from the experimental research work. This shows the microplane model in ANSYS can be used to predict the shear behavior of reinforced UHPC beams.



(a)



(b)

Figure 4.33 Total applied load vs maximum span deflection of U-B4, (a) U-B4 full geometry model, (b) Combined experimental and full geometric ANSYS microplane model plots.

Figure 4.34 are plots of the total applied load (kN) on the 2 plates at top of the U-B4 beam vs the total strain in the tensile reinforcement at the bottom section of the beam. It shows the result plots of the full geometry structural analysis on ANSYS using the microplane material model. Under a 72 mm displacement loading at the top of the beam a total strain of 0.050354 is estimated for the 45 mm mesh result and 0.05481 total strain for the 30 mm mesh result respectively. However, this result could not be validated because of the absence of experiment data.

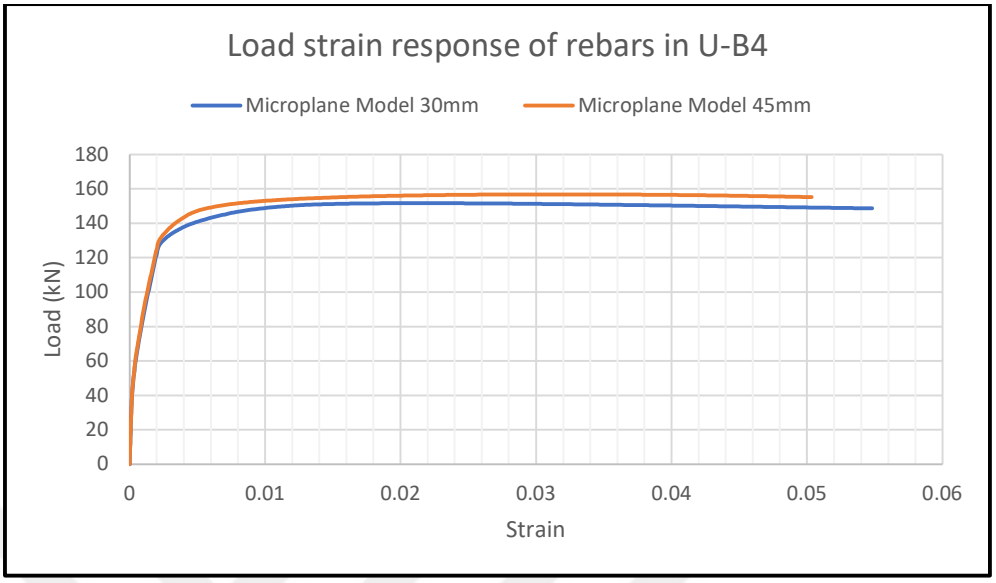


Figure 4.34 Load strain response of rebars in U-B4, ANSYS microplane model plot.

Figure 4.35 is a load-deflection color plot of U-B4 results obtained by using full geometry structural analysis on ANSYS (microplane material model). This plot estimates a maximum midspan deflection of 89.927 mm by using 45 mm finite element mesh size.

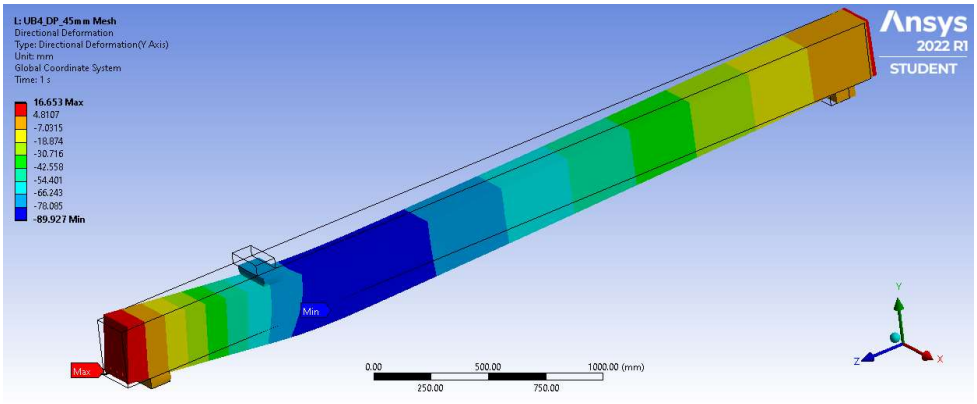


Figure 4.35 U-B4 deflection color plot at failure load. full geometric microplane model plot.

Figure 4.36 is the total strain color plot using full geometry structural analysis on ANSYS for the tensile reinforcements provided in the beam section. It predicts a maximum total strain of 0.050354 mm/mm using 45 mm finite element mesh size. The

microplane material model plot shows that at least 20% of the length of the tensile reinforcements at the bottom section yielded.

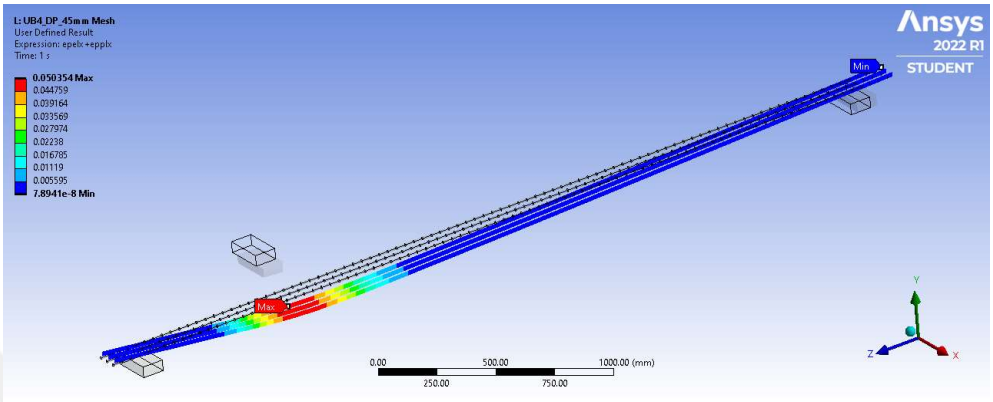


Figure 4.36 Total strain color plot for tensile reinforcements at failure load in mm/mm, full geometric ANSYS microplane.

Figure 4.37 is the equivalent von-Mises stress color plot using full geometry structural analysis on ANSYS for the tensile reinforcements provided in the beam section. It predicts a maximum total stress of 543.47 MPa for the full geometry (microplane). The microplane material model plot also shows that at least 20 % of the length of the tensile reinforcements at the bottom section is above the yield stress of the steel reinforcement (435 MPa).

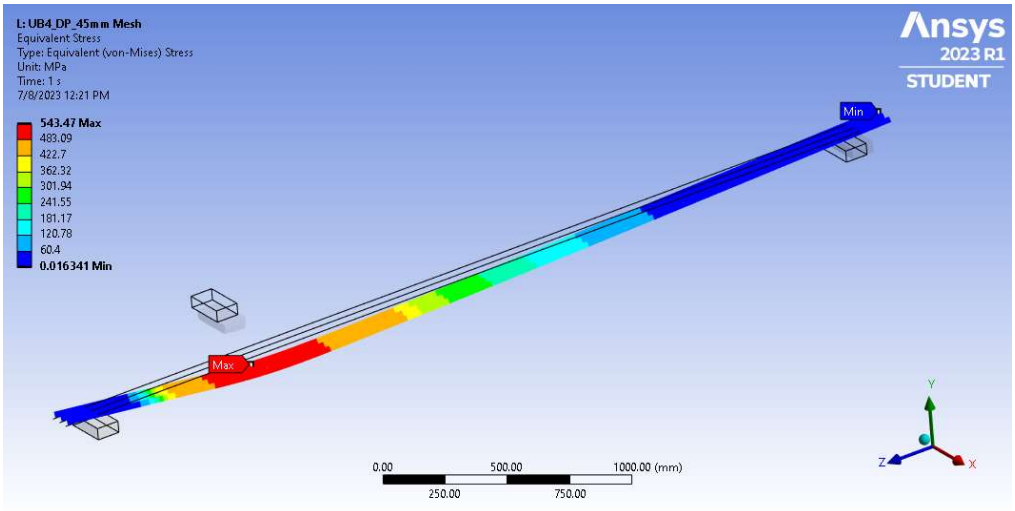
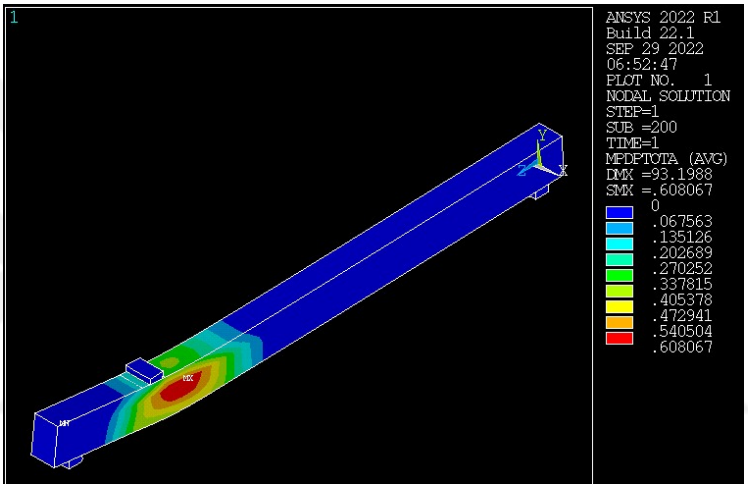
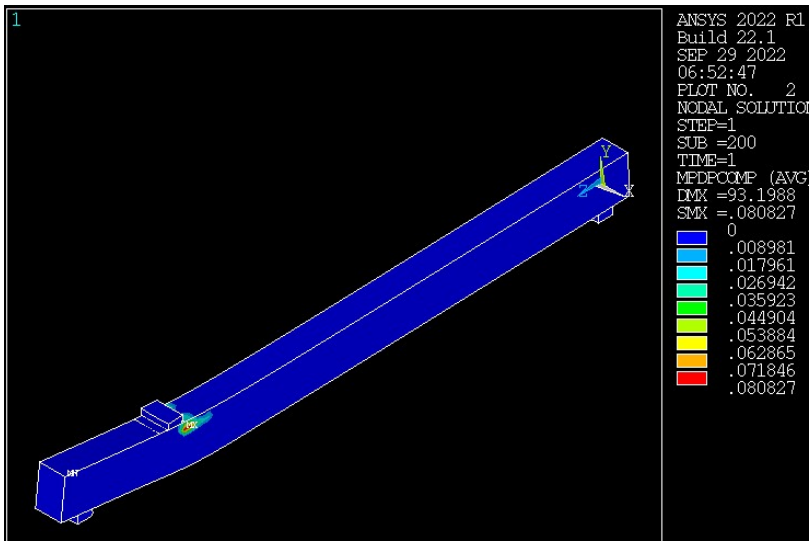


Figure 4.37 Equivalent von-Mises stress color plot for tensile reinforcements at failure load in MPa, full geometric ANSYS microplane (U-B4).

Figures 4.38 and 4.39 are color plot quantities used to denote damage in the material by using the microplane model. The full geometry of U-B4 was used for these color plot result. Figures 4.38(a), 4.38(b), 4.39(a), and 4.39(b) represent the transformed total damage TOTA, transformed tensile damage TENS, transformed compressive damage COMP, and the split weight factor RW respectively. Figure 4.38(b) shows no tension damage in the beam section overall. Figure 4.39(a) shows compression damage at the location of the applied load on the top of the beam.

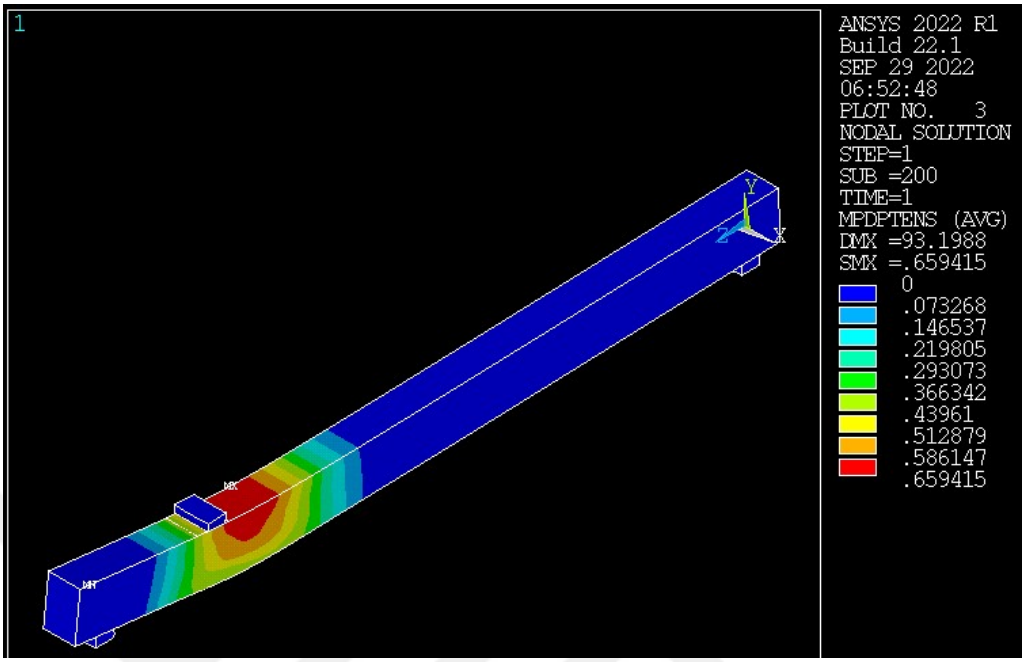


(a)

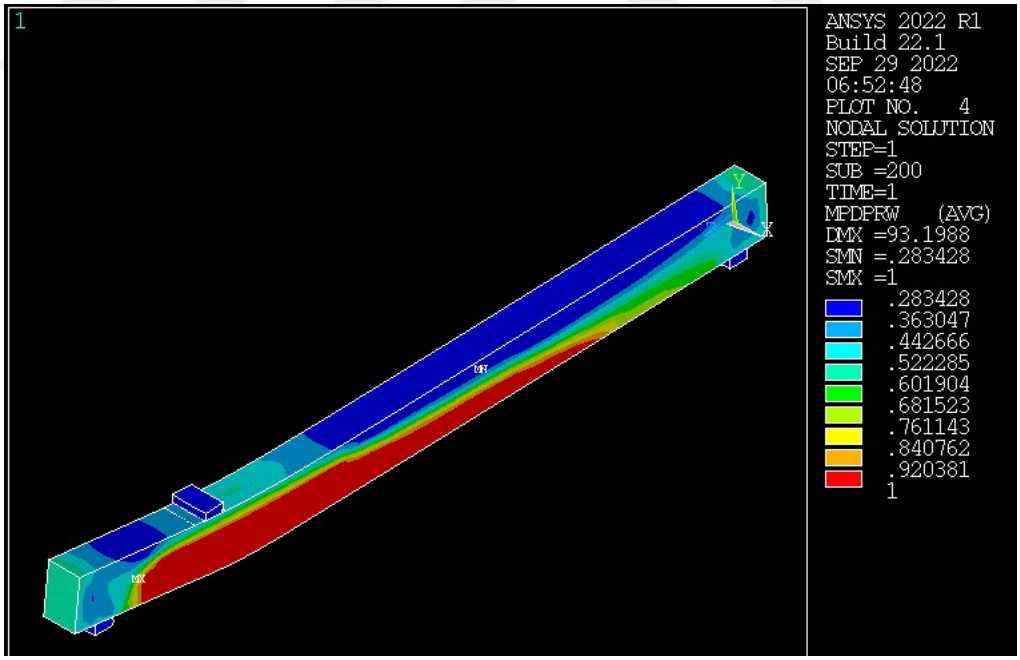


(b)

Figure 4.38 Coupled damage-plasticity microplane damage output – U-B4, (a) Transformed total damage TOTA, (b) Transformed tension damage TENS.



(a)



(b)

Figure 4.39 Coupled damage-plasticity microplane damage output, (a) Transformed compression damage COMP, (b) Split weight factor RW.

Figure 4.40 is the normal stress color plot for the full geometry microplane ANSYS analysis at failure load. Figure 4.40 estimates the results of maximum tensile stress and maximum compressive stress of 9.7011 MPa and 88.246 MPa respectively.

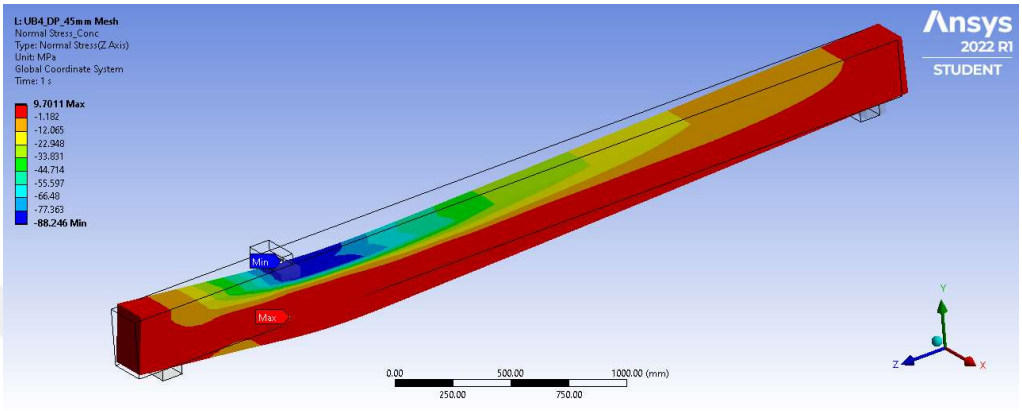


Figure 4.40 Normal stress color plot for U-B4 at failure load in MPa, full geometric ANSYS microplane

Figure 4.41 is the plastic strain color plots for the full geometry microplane ANSYS analysis for the beam section at failure load. Figure 4.41 estimates a maximum strain of 0.048337. The color plot of Figure 4.41 can be compared to Figure 4.38(a), transformed total damage (TOTA). The color plot of Figures 4.41 and 4.38(a) are very similar.

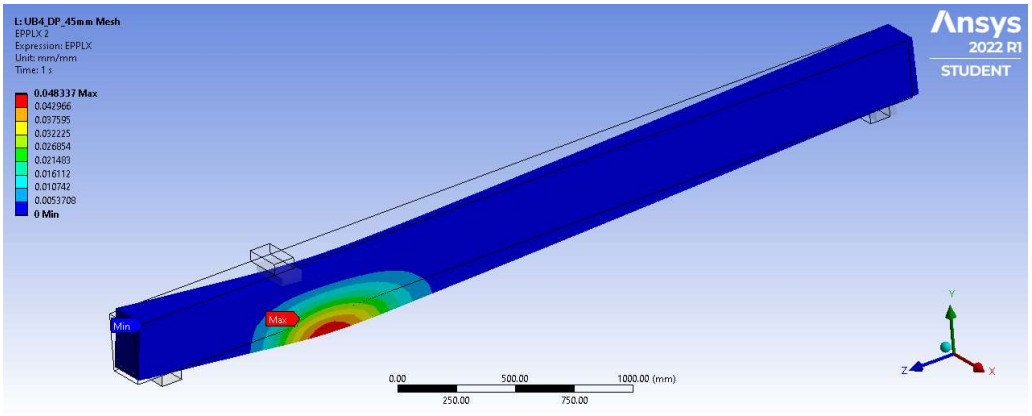


Figure 4.41 Plastic strain color plot for U-B4 at failure load in MPa, full geometric ANSYS microplane

Figure 4.42 is the equivalent von-Mises stress color plot for the full geometry microplane ANSYS analysis for the beam section at failure load. Figure 4.42 estimates a maximum stress of 101.99 MPa respectively at failure load.

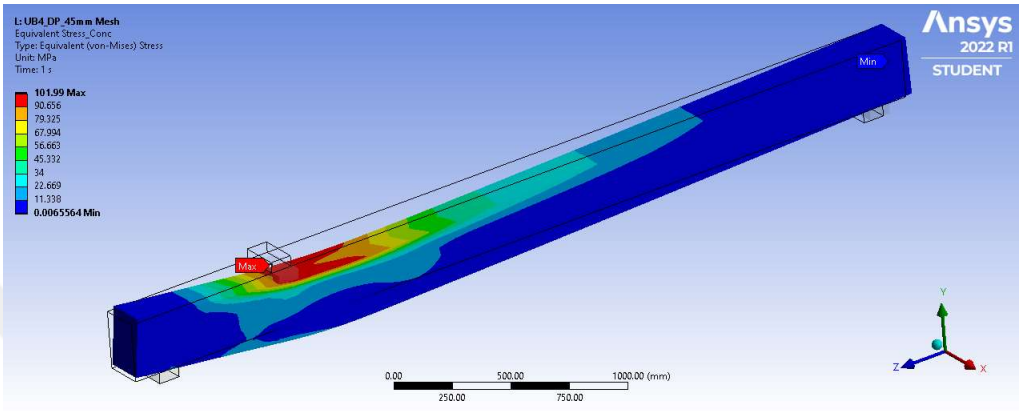


Figure 4.42 Equivalent (von-Mises) Stress color plot for U-B4 at failure load in MPa, full geometric ANSYS microplane.

CHAPTER FIVE
SUMMARY AND CONCLUSIONS

5.1 Conclusions

In this thesis, 4 UHPC reinforced beams were studied using ANSYS finite element program to investigate their flexural and shear behavior. Two material models were used to characterize UHPC structural material for the UHPC reinforced beams. The finite element results from ANSYS were compared to experimental data. It was discovered that the microplane material model of ANSYS gives a more accurate result than the Menetray Willam material model. The load-deflection curve from the microplane model is very smooth and closely resembles the experimental plot data of Solhmirzaei & Kodur (2017).

The general conclusions obtainable from this project are highlighted below:

1. ANSYS finite element software can be used to analyze and design UHPC reinforced beams accurately when the CDP microplane material model is used.
2. ANSYS finite element software captures the behavior of UHPC beams under flexural and shear load when the concrete damage plasticity microplane material model is applied.
3. The failure pattern of reinforced UHPC beams can be defined by using the coupled damage plasticity microplane damage output, such as the transformed total damage TOTA, transformed tensile damage TENS, Transformed compressive damage COMP, and the split weight factor RW color plots. In this research work all the beams failed by either flexural or shear crack localization.
4. Since the load midspan deflection curve and load strain response of tension rebars from the experiment were accurately predicted, it is assumed that the other results such as deformation, normal stress, von-Mises stress, elastic strain, plastic strain, total strain, etc. are also valid.
5. The Menetrey Willam model was able to predict the flexural behavior of reinforced UHPC beams by either using the full or quarter geometry model.

6. The menetrey Willam model was unable to predict the shear behavior of reinforced UHPC beams under 3-point load experimental test.

REFERENCES

Ahmad, S., Sharif, A. M., Al-Osta, M. A., Al-Zahrani, M. M., Sharif, A. M., & Al-Huri, M. A. (2023, February). Flexural performance of pre-damaged RC beams strengthened with different configurations of UHPFRC layer–experimental and analytical investigation. In *Structures* (Vol. 48, pp. 1772-1787). Elsevier.

ANSYS, I. (2022, July). Material Reference. ANSYS Mechanical APDL Material Reference.https://ansyshelp.ansys.com/Views/Secured/corp/v222/en/pdf/ANSYS_Mechanical_APDL_Material_Reference.pdf

Argyris, J. H. (1969). ASKA—Automatic System for Kinematic Analysis: A universal system for structural analysis based on the matrix displacement (finite element) method. *Nuclear Engineering and Design*, *10*(4), 441-455.

Bazant, Z. P., & Byung, H. O. (1985, April). Microplane model for progressive fracture of concrete and rock. ASCE.

Bazant, Z. P., & Gambarova, P. G. (1984). Crack shear in concrete: crack band microplane model. *Journal of structural engineering*, *110*(9), 2015-2035.

Bazoant, Z. P., & Pijaudier-Cabot, G. (1989). Measurement of characteristic length of nonlocal continuum. Journal of Engineering Mechanics, 115(4), 755-767.

Binnur, G. K. (2022). Course note. FEM_2_Basic_Steps_in_FEM_Shape_Functions

Chen, W. F., & Saleeb, A. F. (2013). *Constitutive equations for engineering materials: Elasticity and modeling*. Elsevier.

Dahish, H. A., & Bakri, M. (2022). Flexural behavior of RC composite beams with ultrahigh performance fiber reinforced concrete layer using finite element modeling. Geomate Journal, 22(93), 75-82.

El-Helou, R. G., & Graybeal, B. A. (2022). Flexural Behavior and Design of Ultrahigh-Performance Concrete Beams. Journal of Structural Engineering, 148(4), 04022013.

Grøstad, Ø., & Sandberg, E. (2018). Analysing UHPFRC beams with the help of ANSYS (Master's thesis, Universitetet i Agder; University of Agder).

Implicit and Explicit Time Integration Methods — Lesson 2 - ANSYS Innovation Courses, n.d.

Jiang, H., & Zhao, J. (2015). Calibration of the continuous surface cap model for concrete. *Finite Elements in Analysis and Design*, *97*, 1-19.

Jirásek, M. (1999). Numerical modeling of deformation and failure of materials. *Lecture notes*.

Le Bellégo, C., Dubé, J. F., Pijaudier-Cabot, G., & Gérard, B. (2003). Calibration of nonlocal damage model from size effect tests. *European Journal of Mechanics-A/Solids*, *22*(1), 33-46.

Leukart, M., & Ramm, E. (2003). A comparison of damage models formulated on different material scales. Computational Materials Science, 28(3-4), 749-762.

Menetrey, P. (1994). *Numerical analysis of punching failure in reinforced concrete structures* (No. THESIS). EPFL.

Rajesh B. (2021). A Hands-on Introduction to Engineering Simulations. Edx course. https://learning.edx.org/course/course-v1:CornellX+ENGR2000X+1T2018/home

Russell, H. G., Graybeal, B. A., & Russell, H. G. (2013). *Ultra-high performance concrete: A state-of-the-art report for the bridge community* (No. FHWA-HRT-13-060). United States. Federal Highway Administration. Office of Infrastructure Research and Development.

Solhmirzaei, R., & Kodur, V. K. R. (2017). Modeling the response of ultra high performance fiber reinforced concrete beams. *Procedia engineering*, *210*, 211-219.

Solhmirzaei, R., & Kodur, V. (2021). A numerical model for tracing structural response of ultra-high performance concrete beams. *Modelling*, *2*(4), 448-466.

Valente, R., Alves, G., & Pacheco, P. Design of a pre-stressed bridge deck with ultra-high performance concrete (UHPC).

Willam, K. J. (1975). Constitutive model for the triaxial behaviour of concrete. *Proc. Intl. Assoc. Bridge Structl. Engrs*, *19*, 1-30.

Xenos, D., Grégoire, D., Morel, S., & Grassl, P. (2015). Calibration of nonlocal models for tensile fracture in quasi-brittle heterogeneous materials. *Journal of the Mechanics and Physics of Solids*, *82*, 48-60.

Yoo, D. Y., Banthia, N., & Yoon, Y. S. (2017). Experimental and numerical study on flexural behavior of ultra-high-performance fiber-reinforced concrete beams with low reinforcement ratios. *Canadian Journal of Civil Engineering*, *44*(1), 18-28.

Zreid, I., & Kaliske, M. (2014). Regularization of microplane damage models using an implicit gradient enhancement. *International Journal of Solids and Structures*, *51*(19-20), 3480-3489.

Zreid, I., & Kaliske, M. (2016). An implicit gradient formulation for microplane Drucker-Prager plasticity. *International Journal of Plasticity*, *83*, 252-272.

Zreid, I., & Kaliske, M. (2018). A gradient enhanced plasticity–damage microplane model for concrete. Computational Mechanics, 62(5), 1239-1257.